Nuclear Science
NEA/NSC/R(2021)1
January 2023
www.oecd-nea.org

Role of Integral Experiment Covariance Data for Criticality Safety Validation

EG UACSA Benchmark Phase IV

OECD
BETTER POLICIES FOR BETTER LIVES

NEA
NUCLEAR ENERGY AGENCY

Nuclear Energy Agency

NEA/NSC/R(2021)1

Unclassified **English text only**

17 January 2023

NUCLEAR ENERGY AGENCY
NUCLEAR SCIENCE COMMITTEE

Role of Integral Experiment Covariance Data for Criticality Safety Validation

EG UACSA Benchmark Phase IV

This document is available in PDF format only.

JT03510848

ORGANISATION FOR ECONOMIC CO-OPERATION AND DEVELOPMENT

The OECD is a unique forum where the governments of 38 democracies work together to address the economic, social and environmental challenges of globalisation. The OECD is also at the forefront of efforts to understand and to help governments respond to new developments and concerns, such as corporate governance, the information economy and the challenges of an ageing population. The Organisation provides a setting where governments can compare policy experiences, seek answers to common problems, identify good practice and work to co-ordinate domestic and international policies.

The OECD member countries are: Australia, Austria, Belgium, Canada, Chile, Colombia, Costa Rica, the Czech Republic, Denmark, Estonia, Finland, France, Germany, Greece, Hungary, Iceland, Ireland, Israel, Italy, Japan, Korea, Latvia, Lithuania, Luxembourg, Mexico, the Netherlands, New Zealand, Norway, Poland, Portugal, the Slovak Republic, Slovenia, Spain, Sweden, Switzerland, Türkiye, the United Kingdom and the United States. The European Commission takes part in the work of the OECD.

OECD Publishing disseminates widely the results of the Organisation's statistics gathering and research on economic, social and environmental issues, as well as the conventions, guidelines and standards agreed by its members.

NUCLEAR ENERGY AGENCY

The OECD Nuclear Energy Agency (NEA) was established on 1 February 1958. Current NEA membership consists of 34 countries: Argentina, Australia, Austria, Belgium, Bulgaria, Canada, the Czech Republic, Denmark, Finland, France, Germany, Greece, Hungary, Iceland, Ireland, Italy, Japan, Korea, Luxembourg, Mexico, the Netherlands, Norway, Poland, Portugal, Romania, Russia (suspended), the Slovak Republic, Slovenia, Spain, Sweden, Switzerland, Türkiye, the United Kingdom and the United States. The European Commission and the International Atomic Energy Agency also take part in the work of the Agency.

The mission of the NEA is:

– to assist its member countries in maintaining and further developing, through international co-operation, the scientific, technological and legal bases required for a safe, environmentally sound and economical use of nuclear energy for peaceful purposes;

– to provide authoritative assessments and to forge common understandings on key issues as input to government decisions on nuclear energy policy and to broader OECD analyses in areas such as energy and the sustainable development of low-carbon economies.

Specific areas of competence of the NEA include the safety and regulation of nuclear activities, radioactive waste management and decommissioning, radiological protection, nuclear science, economic and technical analyses of the nuclear fuel cycle, nuclear law and liability, and public information. The NEA Data Bank provides nuclear data and computer program services for participating countries.

Foreword

This benchmark report has been compiled under the guidance of the NEA Working Party on Nuclear Criticality Safety (WPNCS) in the Subgroup on the Role of Integral Experiment Uncertainties and Covariance Data in Criticality Safety Validation. One of the objectives of this Subgroup is to complete the open tasks of its predecessor, the NEA Expert Group on Uncertainty Analysis for Criticality Safety Assessment (EG UACSA).

The UACSA was established in 2008 to address issues related to sensitivity and uncertainty (S/U) studies for criticality safety calculations. In the first years, the group's activity focused on two principal topics: estimation of the bias and its uncertainty for criticality safety calculations and the assessment of manufacturing/operational (including depletion when applicable) uncertainties.

The expert group performed specific tasks associated with the study of uncertainty analysis methods and their use by criticality safety practitioners. The following areas have been the focus of the expert group's work:

- k_{eff} uncertainty due to technological or manufacturing parameters;
- k_{eff} sensitivities to nuclear data;
- parameter correlations between benchmarks and k_{eff} sensitivities to parameters, related to repeatability and reproducibility;
- correlations in k_{eff} biases and uncertainties and their origins in benchmark parameter biases and uncertainties.

The objectives of the expert group were to:

- survey the techniques for the establishment of best-estimate results (as opposed to nominal or design-basis results) together with biases and uncertainties due to technological parameters;
- survey the techniques and software tools for computation of k_{eff} sensitivities to nuclear data and draft recommendations to practitioners for using those techniques;
- draft recommendations to the International Criticality Safety Benchmark Evaluation Project (ICSBEP) on methods to identify, estimate and document parameter correlations between different experiments and to identify, estimate and document k_{eff} correlations between benchmark experiments due to those parameters.

The report consists of a main part and two appendices. The main part summarises and concludes the UACSA Phase IV Benchmark. After the introduction, Chapter 1 contains some general explanations and definitions, while Chapters 2 and 3 discuss the analytic toy model exercise. Chapter 4 describes and discusses the more realistic application cases and Chapter 5 concludes the main part with some remarks and an outlook on further activities.

The UACSA Phase IV Benchmark has a long history and numerous experts have contributed to it with suggestions, remarks and discussions. Appendix A lists all attendees of the UACSA meetings since the benchmark was proposed for the first time in 2012.

For comparison of the individual correlation matrices, the results of all evaluations were transformed using a unique colour scheme. Appendix B shows the correlation matrices in higher resolution to present more details.

All individual contributions, which were sent by the participants, are published as *Complementary material to "Role of Integral Experiment Covariance Data for Criticality Safety Validation: EG UACSA Benchmark Phase IV" (NEA/NSC/R(2021)1)*[1] to account for the variety of approaches and efforts made during the process of generating the results.

1. www.oecd-nea.org/nsc-compl-doc

Acknowledgements

The authors wish to express their sincere gratitude to all contributors to the UACSA Phase IV Benchmark, especially to the members of the former EG UACSA and the WPNCS Subgroup 1. We are also grateful to Brad Rearden for monitoring the activities and to the responsible WPNCS secretaries Franco Michel-Sendis, Shuichi Tsuda and Julie-Fiona Martin.

The NEA wishes to express its sincere gratitude to the authors, Maik Stuke and Axel Hoefer (Germany), for writing this report and for their dedication in co-ordinating the WPNCS Subgroup activities and to the members of the Subgroup.

Lead authors

Maik Stuke (GRS Gesellshaft für Reaktor Sicherheit, Germany[2])

Axel Hoefer (Framatome GmbH, Germany)

2. Current affiliation BGZ Company for Interim Storage, Germany.

Table of contents

List of abbreviations and acronyms **8**

Executive summary **9**

1. Introduction **10**

2. Covariances and correlations between calculated benchmark neutron multiplication factors **11**

3. Analytic toy model exercise **15**

3.1 Definition of the toy model 15
3.2 Definition of tasks 16
3.3 True values 17
3.4 Summary of toy model results 17
3.5 Summary of results 21

4. Realistic case: Experiments with water-reflected UO_2 fuel rod arrays **22**

4.1 Differences to previous benchmark definition 29
4.2 Phase IV-a: Generation of the integral experiment covariance data 30
4.3 Phase IV-b: Study on importance of accounting for the integral experiment correlations in the criticality safety validation 34

5. Conclusions and outlook **40**

References **42**

Appendix A. List of participants **43**

Appendix B. Correlation matrices **44**

List of figures

Figure 2.1. Two benchmark experiments A and B with common system parameters 11
Figure 3.1. Results for Toy Model Task 1a: Assuming no stochastic dependence for x1 18
Figure 3.2. Results for Toy Model Task 1a: Assuming no stochastic dependence for x1 19
Figure 3.3. Results for Toy Model Task 1b: Assuming stochastic dependence for x_1 19
Figure 3.4. Results for Toy Model Task 1b: Assuming stochastic dependence for x1 20
Figure 3.5. Graphic presentation of results listed in Table 3.3 21
Figure 4.1. Schematic overview of the experimental set-up for LCT-007 and LCT-039 cases 22
Figure 4.2. Cases 1 – 3 from LCT-007 23
Figure 4.3. Cases 1-6 from LCT-039 24
Figure 4.4. Cases 7-10 from LCT-039 25
Figure 4.5. Cases 11-17 from LCT-039 25
Figure 4.6. Positioning of fuel rod within its grid hole 26
Figure 4.7. Overview of received results for Scenario A 31
Figure 4.8. Overview of received results for Scenario E 32
Figure 4.9. Received results for Scenarios B, C, and D (from left to right) 33
Figure 4.10. Received result for Option 1 33
Figure 4.11. Received result for Option 2 34
Figure 4.12. Received result for Option 3 34
Figure 4.13. Geometry for 16x16 fuel rod lattice of Application Case 1 35
Figure 4.14. LEU-COMP-THERM-079 Case 1 with 2.0-cm pitch 36
Figure 4.15. LEU-COMP-THERM-079 Case 6 with 2.8-cm pitch 36
Figure 4.16. Results for Application Case 1 38
Figure 4.17. Received results for the Application Case LCT-079 Case 1 38

List of tables

Table 3.1. Benchmark system parameters and corresponding 1-σ errors of nine different benchmark experiments 16
Table 3.2. True values for the benchmark system parameters 17
Table 3.3. Results for Tasks 2a and 2b and the true value 20
Table 4.1. Options for correlations of benchmark uncertainties and for modelling of the rod position uncertainty 28
Table 4.2. System parameters and their uncertainties 29
Table 4.3. Additional parameters, distributions and model parameters defined in an earlier version of the benchmark description 30
Table 4.4. Options for quantification of benchmark uncertainties and correlations taken from an earlier version of benchmark description 30
Table 4.5. Parameters defining Application Case 1 35
Table 4.6. Received results for Application Case 1 37
Table 4.7. Received results for Application Case LCT-079-001 38

List of abbreviations and acronyms

BGZ	Gesellschaft für Zwischenlagerung (Germany)
EG	Expert group
GRS	Gesellschaft für Anlagen- und Reaktorsicherheit (Germany)
ICSBEP	International Criticality Safety Benchmark Evaluation Project (NEA)
LCT-007	LEU-COMP-THERM-007
LCT-039	LEU-COMP-THERM-039
LCT-079	LEU-COMP-THERM-079
NEA	Nuclear Energy Agency
pdf	Probability density function
PWR	Pressurised water reactor
S/U	Sensitivity and uncertainty
UACSA	Uncertainty Analysis for Criticality Safety Assessment (NEA)
WPNCS	Working Party on Nuclear Criticality Safety (NEA)

Executive summary

The NEA Uncertainty Analysis for Criticality Safety Assessment (UACSA) Benchmark Phase IV deals with the quantification of covariances between neutron multiplication factors k_{eff} of criticality safety benchmark experiments and their impact on criticality safety validation. Generally, these covariances have an impact on the computation of the k_{eff} bias and its uncertainty and, hence, on the best estimate plus uncertainty k_{eff} prediction for a given application case.

Covariances between neutron multiplication factors k_{eff} of benchmark experiments are caused by uncertainties in shared system parameters for experiments belonging to the same experimental series. For example, in a series of fuel lattice experiments the same fuel rods are generally used in different experimental arrangements, and all experiments belonging to this series are impacted by the same manufacturing tolerances of the fuel rods. This leads to non-vanishing covariances between the benchmark k_{eff} values.

The UACSA Benchmark Phase IV included two exercises: a simple analytic toy model exercise and a more realistic exercise involving fuel lattice experiments from the LEU-COMP-THERM-007/039 experimental series documented in the ICSBEP Handbook. For both exercises, the objective was to calculate for a series of benchmark experiments the covariance matrix of neutron multiplication factors due to system parameter uncertainties and to quantify the impact of these covariances on the k_{eff} prediction (best estimate and uncertainty) of an application case.

The motivation for including an analytic toy model exercise was that it constitutes a simple and well-defined problem to apply the same computational steps that must be performed for a realistic application case. This gives the opportunity for a clean comparison between different computational approaches.

For the realistic exercise, the calculations should be performed using computational tools typically used for licensing cases. Three different application cases were considered: a water-moderated pressurised water reactor (PWR) fuel assembly, and two experiments from the LEU-COMP-THERM-079 benchmark series. Using these benchmark experiments as application cases allows for a test of the applied methodology by comparing the predicted k_{eff} values to the experimental k_{eff} values given in the ICSBEP Handbook.

The benchmark and surrounding discussions in and outside the WPNCS led to an awareness of the challenges and the development of various methodologies to account for shared uncertainties and covariances between benchmark experiments. Further research has to be conducted to draw generalised statements on the methodologies to express the joint variability between benchmark neutron multiplication factors in terms of covariances and on the evaluation of the impact of these covariances on the predictions of the bias-corrected neutron multiplication factors.

1. Introduction

The NEA Handbook of the International Criticality Safety Benchmark Evaluation Project (ICSBEP) (NEA, 2015) is the primary reference of criticality safety benchmark specifications, which is used by criticality safety practitioners all over the world to validate and calibrate their calculations.

The criticality benchmarks in the ICSBEP Handbook are derived from critical experiments, which are defined by parameters determining the material composition, spatial dimensions and spatial arrangement of their components, as well as by physical state variables, such as temperature, and by the measured neutron multiplication factor.

Because of manufacturing tolerances and measurement uncertainties, the parameters defining the actual experimental configurations are only known with limited precision. Therefore, the benchmark experiment specifications in the ICSBEP Handbook do not only include best-estimate values of the benchmark experiment parameters but also their uncertainties. This allows to propagate parameter uncertainties to uncertainties of benchmark experiment neutron multiplication factors. Expressing the benchmark experiment parameters as the components of a random vector $\boldsymbol{x}$, defined by a probability density function (pdf) $p(\boldsymbol{x})$, the corresponding benchmark experiment neutron multiplication factor can be viewed as a function $k(\boldsymbol{x})$, whose pdf $p(k)$ is defined by $p(\boldsymbol{x})$.

Often, a critical experiment belongs to a series of similar experimental configurations that share certain experimental components. Therefore, the benchmark experiment parameter vectors $\boldsymbol{x}_A$ and $\boldsymbol{x}_B$ of two benchmark experiments A and B belonging to the same experimental series generally share certain vector components, and, consequently, the benchmark experiment neutron multiplication factors $k_A(\boldsymbol{x}_A)$ and $k_B(\boldsymbol{x}_B)$ are not independent. Mathematically, this means that the joint pdf $p(k_A, k_B)$ of k_A and k_B does not factorise into the marginal pdfs $p(k_A)$ and $p(k_B)$. This has an impact on criticality safety validation, since the dependence between evaluated benchmark neutron multiplication factors determines, inter alia, the information that is provided by a set of criticality benchmark experiments.

The objective of Benchmark Phase IV is to test methodologies to express the joint variability between benchmark neutron multiplication factors in terms of covariances and to evaluate the impact of these covariances on the predictions of the bias-corrected neutron multiplication factors. Two different benchmark exercises are included:

1. an analytic toy model exercise;
2. a realistic case involving experiments with water-reflected UO_2 fuel rod arrays.

The report is structured as follows: Chapter 2 describes a summary of some basic mathematical relationships related to covariances and presents correlations. Chapter 3 describes the toy model exercise and summarises the benchmark results obtained by the different participants. Chapter 4 describes the exercise related to the realistic case. Finally, Chapter 5 concludes the main part with an outlook on further activities. Appendix A contains the list of participants in this benchmark and Appendix B summarises the correlation matrices obtained for the two exercises. All individual contributions, which were submitted by the participants, are published as complementary material[3].

3. Complementary material to "Role of Integral Experiment Covariance Data for Criticality Safety Validation: EG UACSA Benchmark Phase IV" (NEA/NSC/R(2021)1), www.oecd-nea.org/nsc-compl-doc.

2. Covariances and correlations between calculated benchmark neutron multiplication factors

In Figure 2.1, the simple case of two benchmark experiments A and B is illustrated. Their respective material compositions and geometric dimensions are assumed to be completely defined by the system parameter sets $X_A := \{x_{A,1}, \dots, x_{A,n_A}\}$ and $X_B := \{x_{B,1}, \dots, x_{B,n_B}\}$, respectively. Experiments A and B generally share certain system parameters, i.e. the intersection $X_A \cap X_B$ of the two parameter sets X_A and X_B is generally not empty ($X_A \cap X_B \neq \emptyset$).

Figure 2.1. Two benchmark experiments A and B with common system parameters

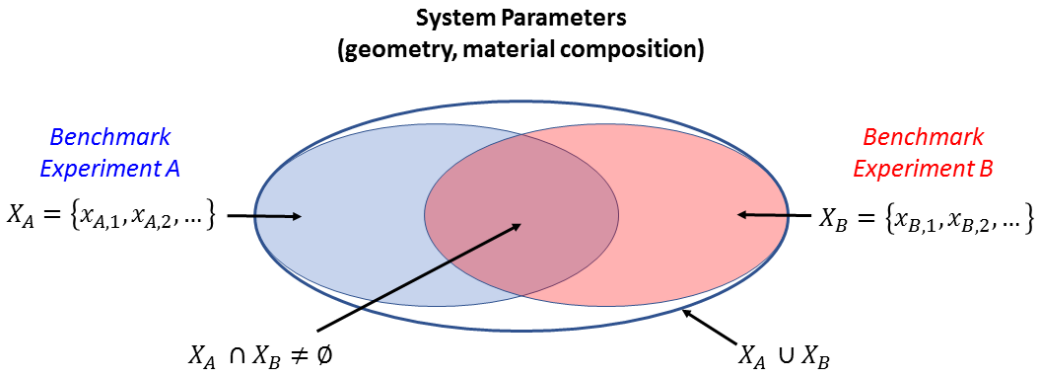

Source: NEA, 2020.

Let $\boldsymbol{x}_A := (x_{A,1}, \dots, x_{A,n_A})^T$ and $\boldsymbol{x}_B := (x_{B,1}, \dots, x_{B,n_B})^T$ be the vectors whose components are given by the elements of X_A and X_B, respectively. To account for the fact that $\boldsymbol{x}_A$ and $\boldsymbol{x}_B$ are known with limited precision, these vectors are treated as random vectors. Hence, the system parameter uncertainties are expressed in terms of the respective probability density functions (pdfs) $p(\boldsymbol{x}_A)$ and $p(\boldsymbol{x}_B)$. The calculated neutron multiplication factors $k_A(\boldsymbol{x}_A)$ and $k_B(\boldsymbol{x}_B)$ of experiment A and experiment B are functions of the random vectors $\boldsymbol{x}_A$ and $\boldsymbol{x}_B$, respectively. Hence, $k_A(\boldsymbol{x}_A)$ and $k_B(\boldsymbol{x}_B)$ are random variables whose respective pdfs $p\big(k_A(\boldsymbol{x}_A)\big)$ and $p\big(k_B(\boldsymbol{x}_B)\big)$ reflect the uncertainties of the calculated neutron multiplication factors due to the uncertainties in $\boldsymbol{x}_A$ and $\boldsymbol{x}_B$. If $\boldsymbol{x}_A$ and $\boldsymbol{x}_B$ have shared components, $k_A(\boldsymbol{x}_A)$ and $k_B(\boldsymbol{x}_B)$ are stochastically dependent, i.e. their joint pdf does not factorise into the product of their marginal pdf (Brandt, 1999):

$$p\big(k_A(\boldsymbol{x}_A), k_B(\boldsymbol{x}_B)\big) \neq p\big(k_A(\boldsymbol{x}_A)\big) \cdot p\big(k_B(\boldsymbol{x}_B)\big)\,. \tag{2.1}$$

The generalisation to an arbitrary number of benchmark experiments is straightforward. Let $X_1, \dots, X_n$ be the system parameter sets belonging to the benchmark experiments $1, \dots, n$. These sets are generally not disjoint since experiments may share certain components. Hence, defining $\boldsymbol{x}_1, \dots, \boldsymbol{x}_n$ as the parameter vectors whose components are given by the elements of $X_1, \dots, X_n$, respectively, the calculated benchmark neutron multiplication factors $k_1(\boldsymbol{x}_1), \dots, k_n(\boldsymbol{x}_n)$ are not mutually independent, i.e.

$$p\big(k_1(\boldsymbol{x}_1), \dots, k_n(\boldsymbol{x}_n)\big) \neq \prod_{i=1}^{n} p\big(k_i(\boldsymbol{x}_i)\big)\,. \tag{2.2}$$

It is convenient to view $k_1(\boldsymbol{x}_1), \ldots, k_n(\boldsymbol{x}_n)$ as the components of a vector $\boldsymbol{k}$ of dimension n:

$$\boldsymbol{k}(\boldsymbol{x}) \coloneqq \big(k_1(\boldsymbol{x}), \ldots, k_n(\boldsymbol{x})\big)^T = \big(k_1(\boldsymbol{x}_1), \ldots, k_n(\boldsymbol{x}_n)\big)^T. \tag{2.3}$$

Here $\boldsymbol{x} = (x_1, \ldots, x_s)^T$ is the system parameter vector whose components are given by the elements of the union X of the system parameter sets $X_1, \ldots, X_n$ of all n benchmark experiments:

$$X = \{x_1, \ldots, x_s\} = X_1 \cup X_2 \cup \ldots \cup X_n \,. \tag{2.4}$$

According to its definition, X is an irreducible parameter set characterising all n benchmark experiments. Here the parameters $x_1, \ldots, x_s$ may usually be chosen independently. For example, the uncertainty in the fuel rod outer diameter is independent from the uncertainty in the fuel density and both are independent from the uncertainty in the moderator temperature. The joint pdf of $\boldsymbol{x}$ then factorises into the product of the marginal pdfs of $x_1, \ldots, x_s$:

$$p(\boldsymbol{x}) = \prod_{i=1}^{s} p(x_i) \,. \tag{2.5}$$

The covariance matrix $\boldsymbol{\Sigma_k}$ of $\boldsymbol{k}(\boldsymbol{x})$ is defined as:

$$\begin{aligned} \boldsymbol{\Sigma_k} &= \boldsymbol{E}[(\boldsymbol{k}(\boldsymbol{x}) - \boldsymbol{E}[\boldsymbol{k}(\boldsymbol{x})])(\boldsymbol{k}(\boldsymbol{x}) - \boldsymbol{E}[\boldsymbol{k}(\boldsymbol{x})])^T] \\ &= \int (\boldsymbol{k}(\boldsymbol{x}) - \boldsymbol{E}[\boldsymbol{k}(\boldsymbol{x})])(\boldsymbol{k}(\boldsymbol{x}) - \boldsymbol{E}[\boldsymbol{k}(\boldsymbol{x})])^T \, p(\boldsymbol{x}) \, d^s x \,, \end{aligned} \tag{2.6}$$

where $\boldsymbol{E}[\boldsymbol{k}(\boldsymbol{x})]$ denotes the expectation vector of $\boldsymbol{k}(\boldsymbol{x})$:

$$\boldsymbol{E}[\boldsymbol{k}(\boldsymbol{x})] = \int \boldsymbol{k}(\boldsymbol{x}) \, p(\boldsymbol{x}) \, d^s x. \tag{2.7}$$

The Pearson correlation matrix $\boldsymbol{P_k}$ is derived from the covariance matrix $\boldsymbol{\Sigma_k}$ according to:

$$\begin{aligned} \boldsymbol{P_k} &= \begin{pmatrix} 1 & \rho_{12} & \cdots & \rho_{1n} \\ \rho_{12} & 1 & \ddots & \vdots \\ \vdots & \ddots & \ddots & \rho_{n-1,n} \\ \rho_{1n} & \cdots & \rho_{n-1,n} & 1 \end{pmatrix}, \\ \rho_{ij} &= \frac{(\boldsymbol{\Sigma_k})_{ij}}{\sqrt{(\boldsymbol{\Sigma_k})_{ii}(\boldsymbol{\Sigma_k})_{jj}}}. \end{aligned} \tag{2.8}$$

$\boldsymbol{\Sigma_k}$ and $\boldsymbol{P_k}$ would be diagonal if the parameter vectors $\boldsymbol{x}_1, \ldots, \boldsymbol{x}_n$ were mutually independent, i.e. if $X_1, \ldots, X_n$ were disjoint. This may be verified by inserting $p(\boldsymbol{x}) = p(\boldsymbol{x}_1) \cdot \ldots \cdot p(\boldsymbol{x}_n)$ into Equations (2.6) and (2.7). If the different benchmark experiments have common system parameters, $\boldsymbol{\Sigma_k}$ is generally non-diagonal.

Since the neutron multiplication factors $k_i(\boldsymbol{x})$ $(i = 1, \ldots, n)$ are usually obtained numerically, e.g. by means of a Monte Carlo transport code, $\boldsymbol{\Sigma_k}$ can hardly ever be evaluated by explicitly solving the integral in Equation (2.6). Hence, what is needed is some numerical procedure or some mathematical approximation.

A straightforward numerical procedure for evaluating $\boldsymbol{\Sigma_k}$ involves the Monte Carlo sampling of the system parameter vector $\boldsymbol{x}$ from its pdf $p(\boldsymbol{x})$ (Buss et al., 2010). Each random draw $\tilde{\boldsymbol{x}}_{i_{MC}}$ of $\boldsymbol{x}$ is then used as a separate input to the criticality calculations of the n benchmark neutron multiplication factors:

$$\boldsymbol{k}_{i_{MC}} = \boldsymbol{k}(\tilde{\boldsymbol{x}}_{i_{MC}}) = \left(k_1(\tilde{\boldsymbol{x}}_{i_{MC}}), \dots, k_n(\tilde{\boldsymbol{x}}_{i_{MC}})\right)^T, \quad i_{MC} = 1, \dots, n_{MC}\,. \tag{2.9}$$

Finally, after a sufficient number n_{MC} of Monte Carlo cycles $\boldsymbol{\Sigma_k}$ may be approximated by the sample covariance matrix:

$$\widehat{\boldsymbol{\Sigma}}_{\boldsymbol{k}} = \frac{1}{n_{MC}-1}\sum_{i_{MC}=1}^{n_{MC}} \left(\boldsymbol{k}_{i_{MC}} - \overline{\boldsymbol{k}}\right)\left(\boldsymbol{k}_{i_{MC}} - \overline{\boldsymbol{k}}\right)^T, \quad \overline{\boldsymbol{k}}_{MC} = \frac{1}{n_{MC}}\sum_{i_{MC}=1}^{n_{MC}} \boldsymbol{k}_{i_{MC}}\,. \tag{2.10}$$

Another possibility to evaluate $\boldsymbol{\Sigma_k}$ is based on the linear expansion approximation of $\boldsymbol{k}(\boldsymbol{x})$,

$$\boldsymbol{k}(\boldsymbol{x}) \approx \boldsymbol{k}(\boldsymbol{x}_0) + \boldsymbol{S}(\boldsymbol{x} - \boldsymbol{x}_0)\,, \tag{2.11}$$

which is a good approximation if the system parameter uncertainties represented by $p(\boldsymbol{x})$ are sufficiently small. $\boldsymbol{x}_0$ in Equation (2.11) denotes the nominal vector of $\boldsymbol{x}$ (e.g. the mean, median, or mode of $p(\boldsymbol{x})$), and $\boldsymbol{S}$ denotes the matrix of sensitivities of the benchmark neutron multiplication factors with respect to the system parameters $\boldsymbol{x}$ at $\boldsymbol{x} = \boldsymbol{x}_0$:

$$\boldsymbol{S} \approx \begin{pmatrix} \frac{\partial k_1}{\partial x_1} & \cdots & \frac{\partial k_1}{\partial x_s} \\ \vdots & & \vdots \\ \frac{\partial k_n}{\partial x_1} & \cdots & \frac{\partial k_n}{\partial x_s} \end{pmatrix}_{\boldsymbol{x}=\boldsymbol{x}_0}\,. \tag{2.12}$$

Since $\boldsymbol{k}(\boldsymbol{x})$ in Equation (2.11) is approximated by a linear transformation of $\boldsymbol{x}$ involving the transformation matrix $\boldsymbol{S}$, the covariance matrix $\boldsymbol{\Sigma_k}$ of $\boldsymbol{k}(\boldsymbol{x})$ is approximated by a linear transformation of the covariance matrix $\boldsymbol{\Sigma_x}$ of $\boldsymbol{x}$ defined by the same transformation matrix:

$$\boldsymbol{\Sigma_k} \approx \boldsymbol{S}\,\boldsymbol{\Sigma_x}\,\boldsymbol{S}^{\boldsymbol{T}}\,, \tag{2.13}$$

with:

$$\boldsymbol{\Sigma_x} = \int (\boldsymbol{x} - \boldsymbol{E}[\boldsymbol{x}])(\boldsymbol{x} - \boldsymbol{E}[\boldsymbol{x}])^T\, p(\boldsymbol{x})\, d^s x\,. \tag{2.14}$$

Usually, one is dealing with a diagonal covariance matrix $\boldsymbol{\Sigma_x}$ since $x_1, \dots, x_s$ may usually be chosen independently; see Equation (2.5):

$$\boldsymbol{\Sigma_x} = diag(\sigma_1^2, \sigma_2^2, \dots, \sigma_s^2)\,. \tag{2.15}$$

The linear transformation in Equation (2.13) then transforms a diagonal covariance matrix $\boldsymbol{\Sigma_x}$ of benchmark system parameters into a generally non-diagonal covariance matrix $\boldsymbol{\Sigma_k}$ of calculated benchmark neutron multiplication factors. $\boldsymbol{\Sigma_k}$ would be diagonal only under the condition that each column vector $\boldsymbol{s}_i = (s_{1i}, \dots, s_{ni})^T$ of $\boldsymbol{S} = (\boldsymbol{s}_1, \dots, \boldsymbol{s}_s)^T$ had just one non-vanishing component, i.e. if $\boldsymbol{s}_i = \left(0, \dots, 0, s_{ji}, 0 \dots, 0\right)^T$. This is just the special case of disjoint system parameter sets $X_1, \dots, X_n$, i.e. the special case that none of the benchmark experiments has any common system parameter with any other benchmark experiment.

3. Analytic toy model exercise

The first part of the UACSA Phase IV Benchmark discusses a simple toy model. The motivation for an analytic toy model exercise is that it constitutes a simple and well-defined problem to apply the same computational steps that must be performed for a realistic application case. This gives the opportunity for a clean comparison between different computational approaches. The tasks of Phase IV-a are envisaged to not require development of sophisticated mathematical tools but to be solved by a simple approach, e.g. by using a spreadsheet application.

3.1 Definition of the toy model

For this exercise, it is assumed that any nuclear fuel system is completely defined by a three-dimensional system parameter vector[4]:

$$\boldsymbol{x} = (x_1, x_2, x_3)^T . \tag{3.1}$$

For given system parameters $\boldsymbol{x}$ the calculated k_{eff} value k_C is given by:

$$k_C(\boldsymbol{x}, \hat{\boldsymbol{\alpha}}) = \frac{\hat{\alpha}_1 \hat{\alpha}_4 x_1}{\hat{\alpha}_1 x_1 + \hat{\alpha}_2 x_2 + \hat{\alpha}_3 x_3}, \tag{3.2}$$

with:

$$\hat{\boldsymbol{\alpha}} = (\hat{\alpha}_1, \hat{\alpha}_2, \hat{\alpha}_3, \hat{\alpha}_4)^T = (9.9968, 1.0066, 1.0225, 1.2198)^T \tag{3.3}$$

The parameter vector $\hat{\boldsymbol{\alpha}}$ is assumed to be derived from some nuclear data evaluation. $\hat{\boldsymbol{\alpha}}$ is supposed to be the best estimate of the unknown vector $\boldsymbol{\alpha} = (\alpha_1, \alpha_2, \alpha_3, \alpha_4)^T$ corresponding to the true nuclear data. The uncertainties and correlations related to the estimation of $\boldsymbol{\alpha}$ are expressed by the covariance matrix:

$$\boldsymbol{\Sigma}_{\boldsymbol{\alpha}} = \begin{pmatrix} \sigma_{\alpha_1}^2 & 0 & 0 & 0 \\ 0 & \sigma_{\alpha_2}^2 & 0 & 0 \\ 0 & 0 & \sigma_{\alpha_3}^2 & 0 \\ 0 & 0 & 0 & \sigma_{\alpha_4}^2 \end{pmatrix} = 10^{-4} \begin{pmatrix} 1 & 0 & 0 & 0 \\ 0 & 1 & 0 & 0 \\ 0 & 0 & 1 & 0 \\ 0 & 0 & 0 & 1 \end{pmatrix}. \tag{3.4}$$

Since $\boldsymbol{\Sigma}_{\boldsymbol{\alpha}}$ is diagonal, the estimates of α_1 through α_4 are uncorrelated. The parameters $\sigma_{\alpha_1}^2$ through $\sigma_{\alpha_4}^2$ may be interpreted as variances of normal distribution models reflecting the uncertainties in the estimation of α_1 through α_4, respectively.

Table 3.1 contains the best-estimate values of the system parameters x_1, x_2 and x_3 of nine different benchmark experiments and their corresponding standard deviations σ_1, σ_2 and σ_3. These best estimates and standard deviations may be interpreted as mean values and standard deviations of normal distribution models, respectively.

4. Please note that the considered toy model does not represent an actual fuel system.

Table 3.1. Benchmark system parameters and corresponding 1-σ errors of nine different benchmark experiments

ID	x_1	σ_1	x_2	σ_2	x_3	σ_3	$k_c(\boldsymbol{x}, \hat{\boldsymbol{\alpha}})$	k
Benchmark 1	2.0072	0.05	4.0424	0.05	-0.0746	0.05	1.0174	1.0
Benchmark 2	2.0072	0.05	1.9601	0.05	1.9292	0.05	1.0194	1.0
Benchmark 3	2.0072	0.05	-0.0506	0.05	3.9477	0.05	1.0177	1.0
Benchmark 4	2.0072	0.05	-2.0458	0.05	6.0650	0.05	1.0111	1.0
Benchmark 5	2.0072	0.05	-3.9905	0.05	8.0370	0.05	1.0086	1.0
Benchmark 6	2.0072	0.05	-6.0613	0.05	9.8448	0.05	1.0185	1.0
Benchmark 7	2.0072	0.05	-12.0059	0.05	15.9819	0.05	1.0063	1.0
Benchmark 8	2.0072	0.05	-16.0923	0.05	19.9995	0.05	1.0066	1.0
Benchmark 9	2.0072	0.05	-20.0440	0.05	23.9692	0.05	1.0032	1.0

Source: NEA, 2020.

The second-to-last column contains the calculated k_{eff} values according to Equation (3.2), and the last column contains the experimental k_{eff} values k. Here the errors related to the k_{eff} measurements are assumed to be negligible. Hence, the k values may be regarded as the true neutron multiplication factors of the respective benchmark experiments.

3.2 Definition of tasks

1) Evaluate the 9×9 covariance matrix $\boldsymbol{\Sigma_k}$ and the 9×9 correlation matrix of the nine calculated benchmark k_{eff} values:
    a. assuming that there is no stochastic dependence between the system parameter vectors $\boldsymbol{x} = (x_1, x_2, x_3)^T$ of different benchmark experiments (e.g. because of independent production processes);
    b. assuming that system parameter x_1 is identical for all nine benchmark experiments (all nine experiments have a common component).
2) Estimate the bias-corrected k_{eff} value and quantify the uncertainty of this estimation for the application case defined by the system parameter vector $\boldsymbol{x} = (1.5, -6{,}10)^T$:
    a. assuming that there is no stochastic dependence between the system parameter vectors $\boldsymbol{x} = (x_1, x_2, x_3)^T$ of different benchmark experiments (e.g. because of independent production processes);
    b. assuming that system parameter x_1 is identical for all nine benchmark experiments (all nine experiments have a common component).

For Task 2, it may be assumed that the computational bias of k_{eff} is predominantly due to errors in the nuclear data. Furthermore, to facilitate matters, it shall be assumed for this toy model exercise that the system parameter uncertainties of the application case are so small that their contribution to the uncertainty of the application case's bias-corrected k_{eff} value may be neglected.

3.3 True values

One can never exactly know the true values of the nuclear data and the system describing parameters. The parameters used in the toy model were random draws from normal distributions using predefined true values as mean values. These true values were not given in the benchmark specifications and thus were unknown to the participants.

The nuclear data vector $\widehat{\boldsymbol{\alpha}}$ used in the benchmark specification is a random draw from the normal distribution $N(\boldsymbol{\alpha}, \boldsymbol{\Sigma}_{\boldsymbol{\alpha}})$, where $\boldsymbol{\alpha}$ denotes the true nuclear data vector $\boldsymbol{\alpha} = (10,1,1,1.2)^T$.

Similarly, the benchmark system parameters x_i used in the benchmark specification are random draws from the normal distributions $N(\mu_i, \sigma_i^2)$, where μ_i denotes the true system parameters, as shown in the table below.

Table 3.2. True values for the benchmark system parameters

ID	μ_1	μ_2	μ_3
Benchmark 1	2	4	0
Benchmark 2	2	2	2
Benchmark 3	2	0	4
Benchmark 4	2	-2	6
Benchmark 5	2	-4	8
Benchmark 6	2	-6	10
Benchmark 7	2	-12	16
Benchmark 8	2	-16	20
Benchmark 9	2	-20	24

Source: NEA, 2020.

Using the true values of the nuclear data to calculate the application case k_{eff} value yields $k_{eff} = 0.9474$. The resulting benchmark predictions will be compared against this value.

3.4 Summary of toy model results

In the following, the submitted results for the toy model will be reviewed. To ensure better comparability, all solutions were transferred into the same colour-coded representation of correlation matrices. The original matrices sent by the different participants can be found in the complementary material of this report[5]. Note that only the representation was changed and not the received numerical values. The original intention of the toy model Task 1a and b was to evaluate $\boldsymbol{\Sigma}_{\boldsymbol{k}}$ as defined in Equation (2.6), i.e. the covariance matrix due to system parameter uncertainties only. However, results were received which also included the covariances due to uncertainties of $\boldsymbol{\alpha}$. A total six numerical results were submitted for Task 1a (four also including covariances due to nuclear data uncertainties)

5. www.oecd-nea.org/nsc-compl-doc

and eight for Task 1b (four also including covariances due to nuclear data uncertainties). A further nine results for Tasks 2a and b were evaluated, respectively.

3.4.1 Task 1

Task 1a: Assuming no stochastic dependence for x_1

Per definition, the correlation matrix of an uncorrelated case is defined by the off-diagonal elements being zero. The diagonal elements are identical to the ones from the correlated case in Task 1b. However, some participants sent numerical results with values different from zero due to statistical uncertainties. These results could be used, e.g. to estimate statistical errors of the applied method.

Figure 3.1. Results for Toy Model Task 1a: Assuming no stochastic dependence for x_1 (correlation matrix due to system parameter uncertainties)

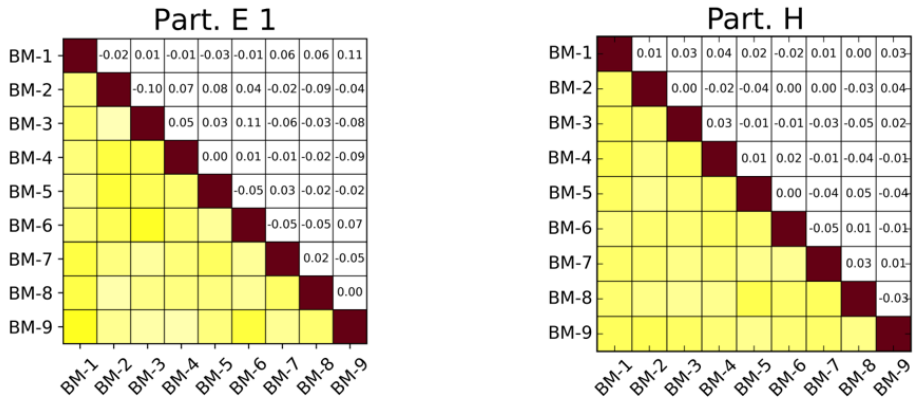

Source: NEA, 2020.

Figure 3.2. Results for Toy Model Task 1a: Assuming no stochastic dependence for x_1 (correlation matrix due to system parameter and nuclear data uncertainties)

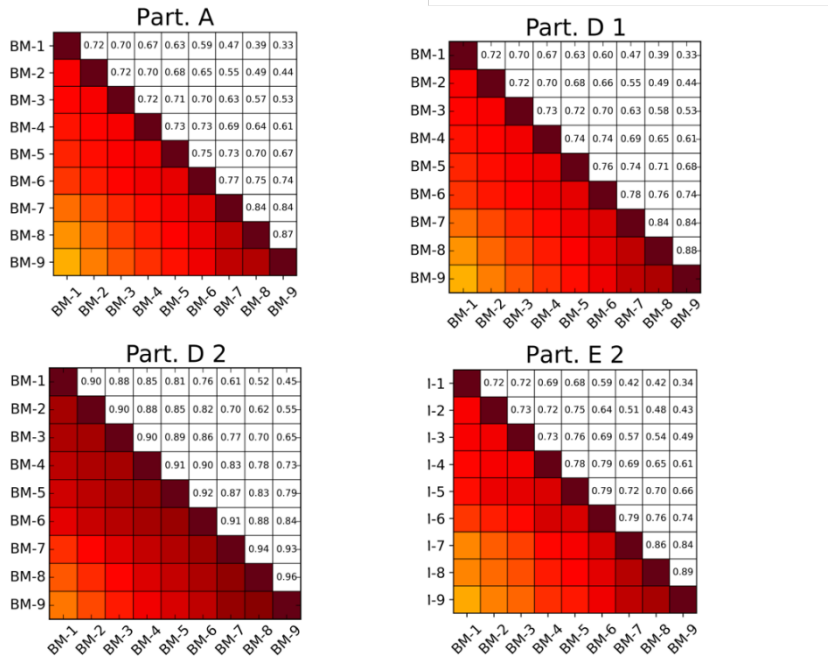

Source: NEA, 2020.

Task 1b: Assuming stochastic dependence for x_1

In Task 1b stochastic dependence for x_1 was assumed and the following results were received:

Figure 3.3. Results for Toy Model Task 1b: Assuming stochastic dependence for x_1 (correlation matrix due to system parameter uncertainties)

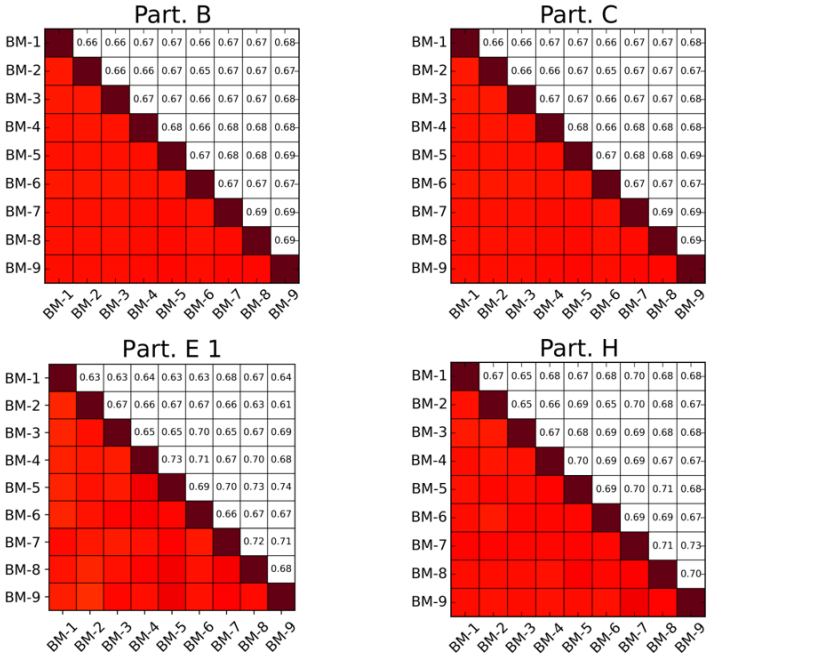

Source: NEA, 2020.

Figure 3.4. Results for Toy Model Task 1b: Assuming stochastic dependence for x_1 (correlation matrix due to system parameter and nuclear data uncertainties)

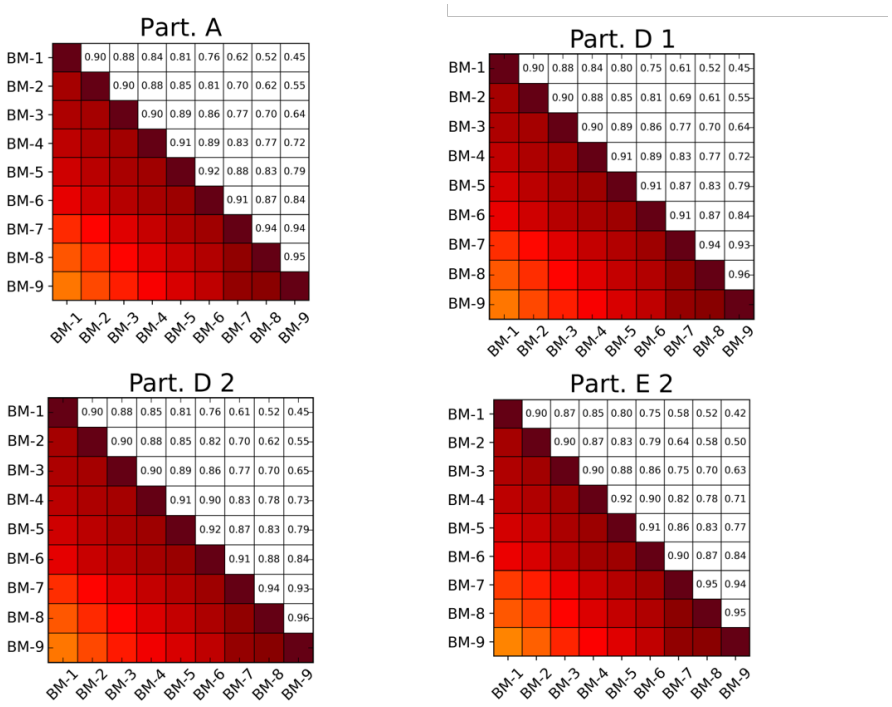

Source: NEA, 2020.

3.4.2 Task 2

The following results were sent:

Table 3.3. Results for Tasks 2a and 2b and the true value

Evaluation	Task 2a		Task 2b	
	k_{eff}	1-σ uncertainty	k_{eff}	1-σ uncertainty
A1	0.9416	0.00175	0.9416	0.00442
A2	0.9415	0.00175	0.9393	0.0044
A3	0.9437	0.00173	0.9460	0.00378
B	0.9437	0.0019	0.9462	0.0039
C	0.9433	0.0019	0.9450	0.0041
D	0.9413	0.004	0.9465	0.004
E1	0.9476	0.0106	0.9495	0.0108
E2	0.9419	0.0082	0.9450	0.0089
H	0.9536	0.0120	0.9536	0.0121
True value	0.9474			

Source: NEA, 2020.

Figure 3.5. Graphic presentation of results listed in Table 3.3

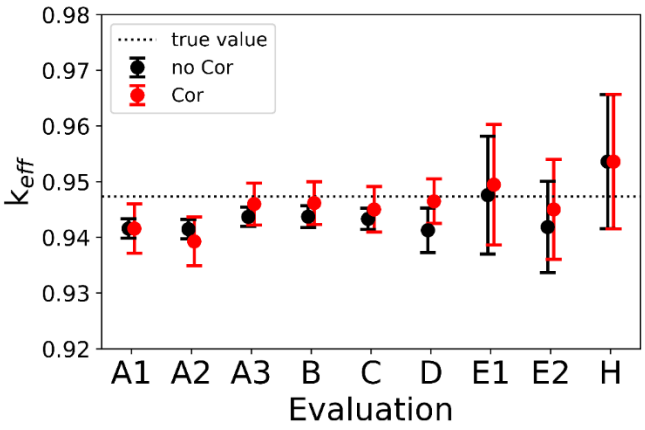

Source: NEA, 2020.

Note: The dotted line represents the (unknown) true value of k_{eff} = 0.9474. The black values represent the uncorrelated case, and the red values the correlated case. The error bars indicate the 1-σ uncertainties.

3.5 Summary of results

The objective of the toy model was to analyse the impact of different methods to evaluate covariance/correlation data and to predict the bias-corrected k_{eff} values.

The results E1 and H for the toy model Task 1a show no statistically significant correlation coefficients. The second group of results for Task 1a, namely participants A, D1 and E2, show significantly larger correlation coefficients ranging from 0.33 to 0.88. The results of E2 show even larger coefficients. The reason for the differences between the solutions of both groups is that the solutions of the second group include the correlation coefficients due to uncertainties of the nuclear data $\hat{\boldsymbol{\alpha}}$, while solutions E1 and H show the correlation coefficients solely due to uncertainties of the system parameters $\boldsymbol{x}$.

The results for Task 1b of evaluations B, C, E1 and H are in excellent agreement. All correlation coefficients have values around 0.7. The same agreement can be found for the solutions of the second group A, D and E2. The correlation coefficients cover a range of values between 0.45 and 0.96. The differences between the solutions of group 1 and 2 can again be explained by the different treatment of correlation coefficients due to nuclear data.

The results for the bias-corrected k_{eff} values for Task 2 show generally a good agreement. Most results reproduce the true k_{eff} value within 1-σ uncertainty. Only the results A1 and A2 and the uncorrelated results of B, C, and D show a larger than 1-σ deviation. Further, it can be observed that the mean values of the updated results for the correlated case of B, C, D, E1 and E2 are larger compared to the non-correlated case. The results of H show no difference between the assumption of correlation and non-correlation. The mean values and 1-σ uncertainties seem to be statistically identical. It is notable that the solutions B, C, and D have significantly smaller 1-σ uncertainties compared to the results E and H. The larger 1-σ uncertainties for solutions E and H might be because frameworks were used, in which only the mean value but not the standard deviation is updated. The results A3 and B are statistically identical and are obtained with the same method.

4. Realistic case: Experiments with water-reflected UO_2 fuel rod arrays

This exercise is based on 21 criticality safety benchmark experiments described in the ICSBEP Handbook (NEA, 2015). Four experiments are taken from the series LEU-COMP-THERM-007 (LCT-007) (Poullot and Hanlon, 2015a), namely Cases 1, 2, 3 and 4. The remaining 17 experiments are taken from LEU-COMP-THERM-039 (LCT-039) (Poullot and Hanlon, 2015b). All experiments of LCT-007 and LCT-039 were carried out in the "Apparatus B" facility at the Criticality Laboratory of Valduc in 1978 (Manaranche et al., 1979; Barbry et al., 2003).

Each of these 21 experimental configurations was defined by a single water-moderated array of fuel rods in a square pitch arrangement. The fuel rods contained low-enriched (4.738 wt.% of ^{235}U) UO_2 fuel. For each experiment, the fuel rod array was placed in a tank and the water level was raised close to the critical level (see Figure 4.1). The critical water height was then obtained by extrapolation from the subcritical water height measurements to the critical water height.

Figure 4.1. Schematic overview of the experimental set-up for LCT-007 and LCT-039 cases

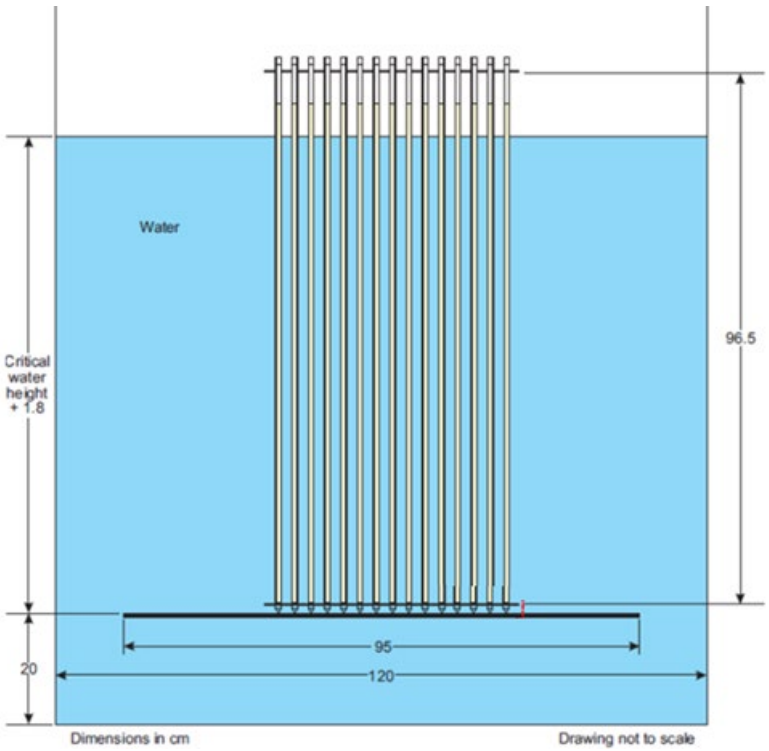

Source: Poullot and Hanlon, 2015a.

The square lattice configurations corresponding to the experimental Cases 1 through 3 from LCT-007 are shown in Figure 4.2, and the 17 configurations from LCT-039 are shown in Figure 4.3 through Figure 4.5. Case 4 from LCT-007 is based on the same grid as Case 1 but with only every second hole filled, resulting in a pitch of 2.52 cm. The details of the experimental set-up are given in Sections 1 and 2 while the benchmark specifications are given in Section 3 of the respective evaluations (NEA, 2015).

Figure 4.2. Cases 1 – 3 from LCT-007

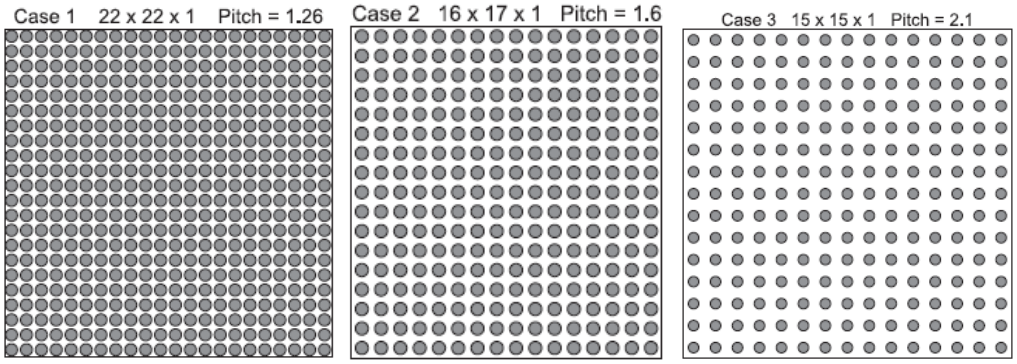

Source: Poullot and Hanlon, 2015b.

Figure 4.3. Cases 1-6 from LCT-039

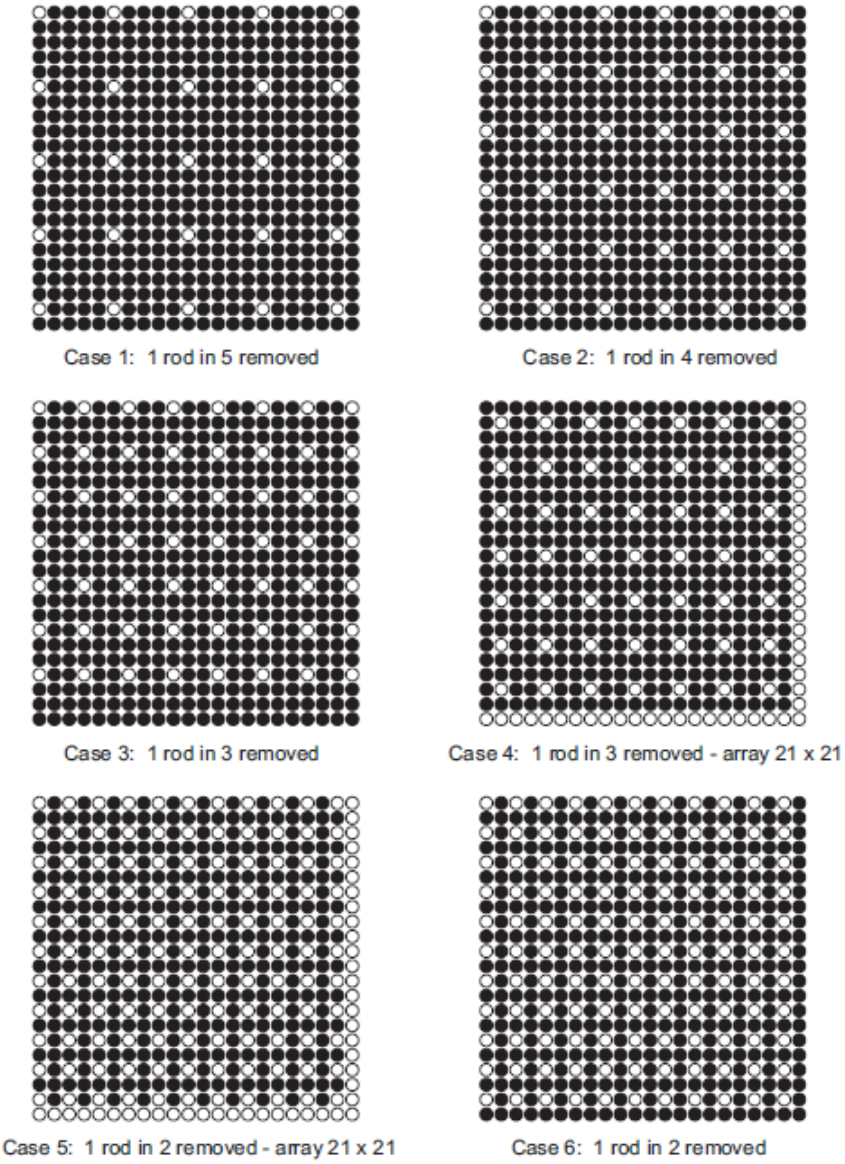

Source: Poullot and Hanlon, 2015b.

Figure 4.4. Cases 7-10 from LCT-039

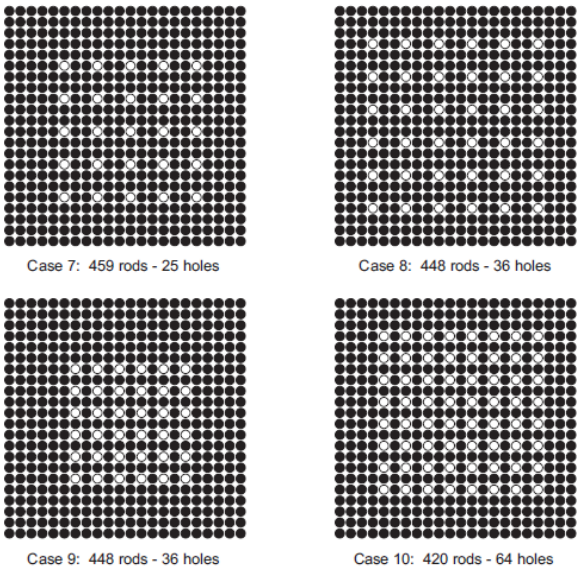

Source: Poullot and Hanlon, 2015b.

Figure 4.5. Cases 11-17 from LCT-039

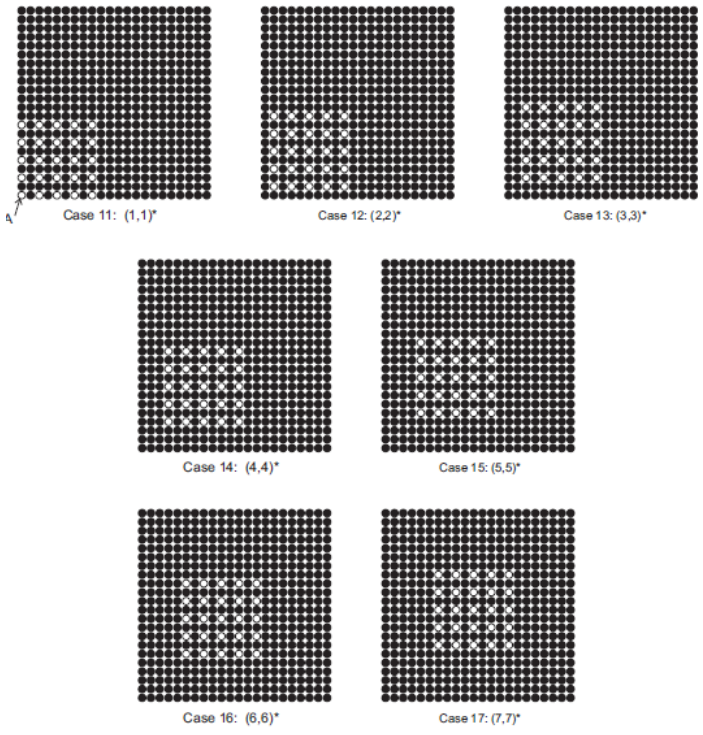

Source: Poullot and Hanlon, 2015b.

According to the description in the ICSBEP Handbook (NEA, 2015), all 21 experiments made use of the same experimental equipment and the same fuel rods. The material uncertainties and geometric uncertainties of the experimental set-up are specified in Section 2 of LCT-007 (Poullot and Hanlon, 2015a) and Section 2 of LCT-039 in (Poullot and Hanlon, 2015b).

The fuel rods had been produced especially for experiments conducted in the "Apparatus B" facility. Obviously, the dependencies of the uncertainties in the fuel rod parameters of different fuel rods (like the fuel rod outer diameter) are determined by the fuel rod production process. However, since details about the production process are not available it is challenging to estimate these dependencies.

The fuel pellet parameter uncertainties are treated in a bounding manner: a complete stochastic dependence between the fuel pellet parameters of different fuel rods is assumed. This means that all fuel rods are assumed to be characterised by a single parameter for the fuel pellet diameter, a single parameter for the fuel density, a single parameter for the ^{235}U enrichment, etc.

Figure 4.6. Positioning of fuel rod within its grid hole

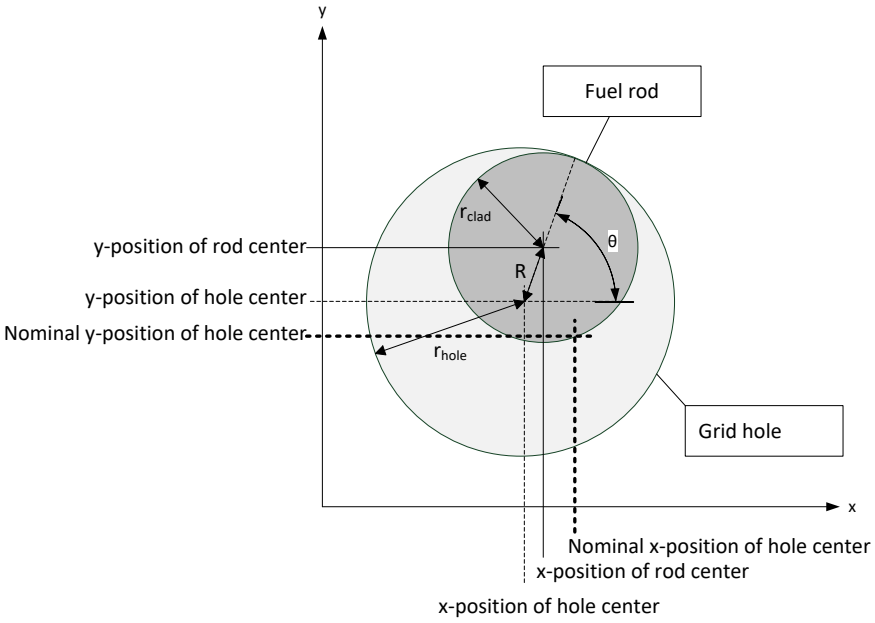

Source: NEA, 2020.

Next, the remaining rod parameters will be addressed, foremost the fuel rod positioning, the clad inner diameter, and the clad thickness.

The figure above displays a fuel rod within its grid hole. The displacement of its centre position from the nominal grid position can be described by two contributions: displacement of the centre of its grid hole from its nominal position, and displacement of the rod centre from the grid hole centre.

According to LCT-007/039, Section 2.2 in the ICSBEP Handbook (NEA, 2015), the pitch of two grid holes has an uncertainty of $\sigma_p = 0.0105$ cm. For two grid holes with co-ordinates (x_1, y_1) and (x_2, y_2), which are aligned along the x-axis we obtain for the variance of their pitch:

$$\mathrm{Var}(\mathrm{Pitch}) \cong \mathrm{Var}(x_1) + \mathrm{Var}(x_1) - 2\mathrm{Cov}(x_1, x_2)\,. \tag{4.1}$$

Assuming the positioning of one single grid hole is independent from the positioning of the remaining holes leads to:

$$\mathrm{Var}(x_1) + \mathrm{Var}(x_1) = \frac{\mathrm{Var}(\mathrm{Pitch})}{2} = \frac{\sigma_p^2}{2}. \tag{4.2}$$

And the same holds true for the y-direction:

$$\mathrm{Var}(y_2) + \mathrm{Var}(y_2) = \frac{\mathrm{Var}(\mathrm{Pitch})}{2} = \frac{\sigma_p^2}{2}. \tag{4.3}$$

Thus, the first uncertainty contribution to the rod centre position is fixed. Next, let us address the position of the rod within its grid hole. In the following, all fuel rods are assumed to lean on their grid hole wall, which will lead to larger uncertainties than assuming the grid centres are equiprobably distributed within their holes. Thus, the radial displacement R from the hole centre is fixed by the grid hole radius r_{hole} and the clad outer radius r_{clad}, which is a function of its inner radius r_{gap} and the clad thickness t_{clad}:

$$R = r_{\mathrm{hole}} - r_{\mathrm{clad}} = r_{\mathrm{hole}} - r_{\mathrm{gap}} - t_{\mathrm{clad}}\,. \tag{4.4}$$

The angular distributions of the rod centres are assumed to be independent for each rod and uniform for all angles[6].

The correlations of the parameters r_{hole}, r_{gap}, and t_{clad} of different fuel rods are unknown. To study parameter correlation effects, the scenarios given in Table 4.1 will be considered.

Scenario A assumes all rods to be positioned at their nominal grid position, i.e. the positioning uncertainty is neglected. Additionally, it assumes that all other parameters are fully correlated over the grid, i.e. there is just one value r_{hole}, r_{gap}, and t_{clad} which describes all rods.

Scenario B is identical to Scenario A, but the rods are leaning on the walls of their grid holes and the grid holes are assumed to be randomly and independently distributed. Scenarios C and D are mixed scenarios intended to study single effects.

Scenario E assumes in contrast to Scenario B that the distributions for the values r_{hole}, r_{gap}, and t_{clad} are independent for all rods.

System parameter uncertainties, which shall be taken into account for this benchmark exercise, are listed in the table below. As can be seen from this table, the parameter uncertainties are expressed either by uniform distribution models $U(a, b)$, where a denotes the minimum possible value and b denotes the maximum possible value, or by normal

6. Note that it is conceivable that all rods might lean towards one side of the grid due some external shock, i.e. that the angular distributions are positively correlated. However, this would lead to a reduction of the overall uncertainty whereas the goal of the approach described here is to maximise the effect in case of missing information.

distribution models $N(\mu, \sigma^2)$, where μ denotes the mean and σ^2 denotes the variance. Uniform distribution models are applied only to the fuel rod inner diameter and the fuel rod thickness, since for these two parameters only the respective upper and lower tolerance limits are given, and to the angle θ, which describes the position of a fuel rod within its hole.

Table 4.1. Options for correlations of benchmark uncertainties and for modelling of the rod position uncertainty

Scenario	Displacement of grid hole position	Radial displacement of rod centre from the hole centre	Grid hole diameters	Fuel rod cladding inner diameters	Fuel rod cladding thicknesses
A	None	$R = 0$	Correlated	Correlated	Correlated
B	Uncorrelated	$R = r_{\text{hole}} - r_{\text{gap}} - t_{\text{clad}}$	Correlated	Correlated	Correlated
C	Uncorrelated	$R = r_{\text{hole}} - r_{\text{gap}} - t_{\text{clad}}$	Uncorrelated	Correlated	Correlated
D	Uncorrelated	$R = r_{\text{hole}} - r_{\text{gap}} - t_{\text{clad}}$	Uncorrelated	Uncorrelated	Correlated
E	Uncorrelated	$R = r_{\text{hole}} - r_{\text{gap}} - t_{\text{clad}}$	Uncorrelated	Uncorrelated	Uncorrelated

Source: NEA, 2020.

Table 4.2. System parameters and their uncertainties

Parameter	Distribution Model	Model Parameters
Fuel rod cladding inner diameter	*U(a,b)*	*a* = 0.81 cm, *b* = 0.83 cm
Fuel rod cladding thickness	*U(a,b)*	*a* = 0.055 cm, *b* =0.065 cm
Fuel pellet diameter	$N(\mu,\sigma^2)$	μ = 0.7892 cm, σ = 0.0017 cm
x-displacement of hole position relative to nominal hole position (see Eq. (4.2))	$N(\mu,\sigma^2)$	μ = 0 cm, $\sigma = 0.0105/\sqrt{2}$ cm $\cong 0.00742$ cm
y- displacement of hole position relative to nominal hole position (see Eq. (4.3))	$N(\mu,\sigma^2)$	μ = 0 cm, $\sigma = 0.00742$ cm
Angle θ fixing position of rod centre within its grid hole	*U(a,b)*	*a* =0, *b* =2π.
Hole diameter	$N(\mu,\sigma^2)$	μ = 1.0105 cm, σ = 0.0085 cm
Height of fissile column	$N(\mu,\sigma^2)$	μ = 89.7 cm, σ = 0.3 cm
Fuel density	$N(\mu,\sigma^2)$	μ = 10.38 g/cm^3, σ = 0.0133 g/cm^3
Fuel impurity (atomic density of ^{10}B)	$N(\mu,\sigma^2)$	μ = 6.9037E-08 atom/(barn·cm), σ = 8.0000E-09 atom/(barn·cm)
^{234}U content in U	$N(\mu,\sigma^2)$	μ = 0.0307 At.-%, σ = 0.0005 At.-%
^{235}U content in U	$N(\mu,\sigma^2)$	μ = 4.79525 At.-%, σ = 0.002 At.-%
^{236}U content in U	$N(\mu,\sigma^2)$	μ = 0.1373 At.-%, σ = 0.0005 At.-%
^{238}U content in U	$N(\mu,\sigma^2)$	μ = 95.03675 At.-%, σ = 0.01 At.-%
Critical water height LCT-07-01	$N(\mu,\sigma^2)$	μ = 90.69 cm, σ = 0.1 cm
Critical water height LCT-07-02	$N(\mu,\sigma^2)$	μ = 73.53 cm, σ = 0.1 cm
Critical water height LCT-07-03	$N(\mu,\sigma^2)$	μ = 77.98 cm, σ = 0.06 cm
Critical water height LCT-07-04	$N(\mu,\sigma^2)$	μ = 79.85 cm, σ = 0.1 cm
Critical water height LCT-39-01	$N(\mu,\sigma^2)$	μ = 81.36 cm, σ = 0.07 cm
Critical water height LCT-39-02	$N(\mu,\sigma^2)$	μ = 77.69 cm, σ = 0.06 cm
Critical water height LCT-39-03	$N(\mu,\sigma^2)$	μ = 73.05 cm, σ = 0.06 cm
Critical water height LCT-39-04	$N(\mu,\sigma^2)$	μ = 89.07 cm, σ = 0.06 cm
Critical water height LCT-39-05	$N(\mu,\sigma^2)$	μ = 84.37 cm, σ = 0.06 cm
Critical water height LCT-39-06	$N(\mu,\sigma^2)$	μ = 58.77 cm, σ = 0.06 cm
Critical water height LCT-39-07	$N(\mu,\sigma^2)$	μ = 69.71 cm, σ = 0.06 cm
Critical water height LCT-39-08	$N(\mu,\sigma^2)$	μ = 66.79 cm, σ = 0.06 cm
Critical water height LCT-39-09	$N(\mu,\sigma^2)$	μ = 64.47 cm, σ = 0.07 cm
Critical water height LCT-39-10	$N(\mu,\sigma^2)$	μ = 58.37 cm, σ = 0.07 cm
Critical water height LCT-39-11	$N(\mu,\sigma^2)$	μ = 81.34 cm, σ = 0.06 cm
Critical water height LCT-39-12	$N(\mu,\sigma^2)$	μ = 75.38 cm, σ = 0.07 cm
Critical water height LCT-39-13	$N(\mu,\sigma^2)$	μ = 72.52 cm, σ = 0.06 cm
Critical water height LCT-39-14	$N(\mu,\sigma^2)$	μ = 71.14 cm, σ = 0.06 cm
Critical water height LCT-39-15	$N(\mu,\sigma^2)$	μ = 69.88 cm, σ = 0.06 cm
Critical water height LCT-39-16	$N(\mu,\sigma^2)$	μ = 69.4 cm, σ = 0.06 cm
Critical water height LCT-39-17	$N(\mu,\sigma^2)$	μ = 68.75 cm, σ = 0.06 cm

Source: NEA, 2020.

4.1 Differences to previous benchmark definition

An earlier version of the benchmark description included some different definitions. The positions of the fuel rods were treated differently, leading to Options 1 to 3 instead of Scenarios A to E. Details are shown in the tables here-under.

Table 4.3. Additional parameters, distributions and model parameters defined in an earlier version of the benchmark description

Fuel rod pitch (for pitch 1.26 cm)	$N(\mu,\sigma^2)$	μ =1.26 cm, σ = 0.0351 cm
Fuel rod pitch (for pitch 1.6 cm)	$N(\mu,\sigma^2)$	μ =1.6 cm, σ = 0.0351 cm
Fuel rod pitch (for pitch 2.1cm)	$N(\mu,\sigma^2)$	μ =2.1 cm, σ = 0.0351 cm
Fuel rod pitch (for pitch 2.52cm)	$N(\mu,\sigma^2)$	μ =2.52 cm, σ = 0.0351 cm

Source: NEA, 2020.

Table 4.4. Options for quantification of benchmark uncertainties and correlations taken from an earlier version of benchmark description

Options → Parameter ↓	Option 1 Uncertainty portion [%]		Option 2 Uncertainty portion [%]		Option 3 Uncertainty portion [%]	
	Systematic	Random	Systematic	Random	Systematic	Random
Fuel rod pitch	-	100	-	100	50	50
Fuel rod cladding inner diameter	100	-	50	50	50	50
Fuel rod cladding thickness	100	-	50	50	50	50

Source: NEA, 2020.

4.2 Phase IV-a: Generation of the integral experiment covariance data

4.2.1 Definition of tasks

The tasks of Phase IV-a are as follows:

1. Evaluate the corresponding uncertainties, covariances, and correlations (Pearson coefficients) of the k_{eff} benchmark uncertainties based on assumptions provided in Table 4.1.
    a. assuming Scenario A for all 21 experiments:
    b. assuming Scenario E for experiments LCT-07 1 to 4 and LCT-39 1, 6, 7 and 8.
    c. results assuming Scenarios B, C and D are optional.

The original benchmark specification also included the following task, which is not included in this evaluation report:

2. Evaluate k_{eff} sensitivities to variation of parameters for each of the 21 configurations assuming Scenario A.

4.2.2 Overview of received results

For Task 1a, ten results were received from seven different participants. The higher calculational and numerical effort for Task 1b resulted in a decrease from eight to five participants. Two participants sent the results for the optional Task 1c.

4.2.2.1 Task 1a: Scenario A

Figure 4.7. Overview of received results for Scenario A

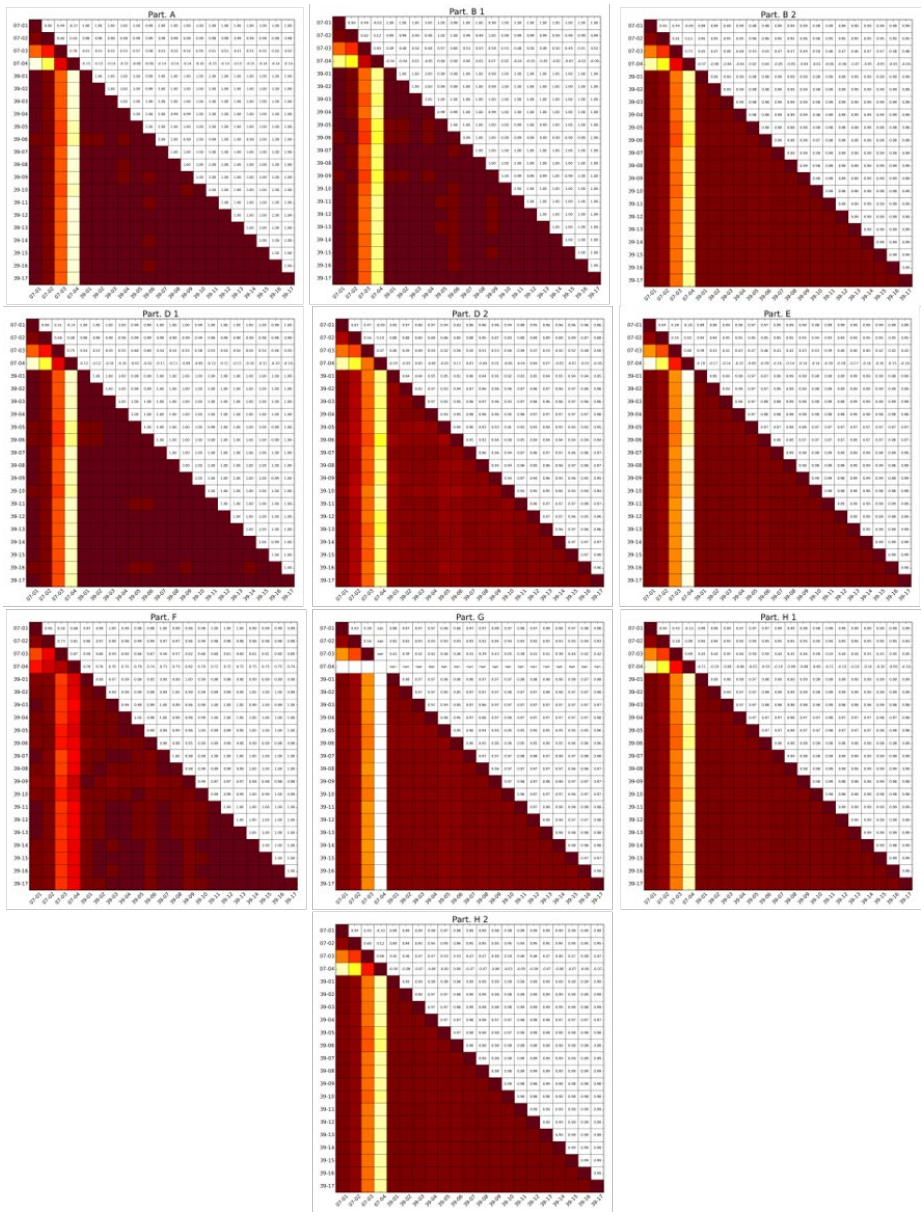

Source: NEA, 2020.

Note: A more detailed individual representation can be found in the corresponding Appendices.

4.2.2.2 Task 1b: Scenario E

Figure 4.8. Overview of received results for Scenario E

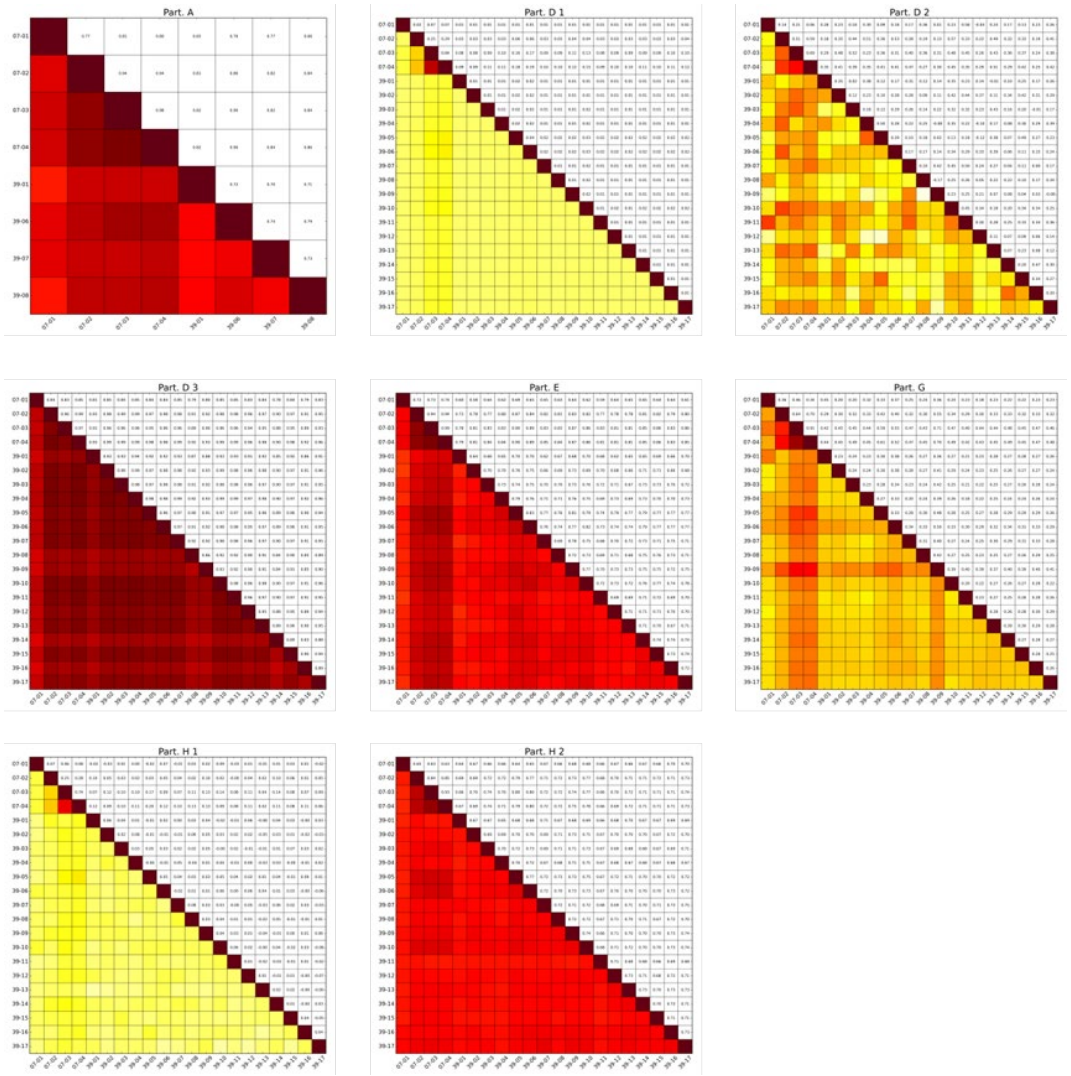

Source: NEA, 2020.

Note: A more detailed individual representation can be found in the corresponding Appendices.

4.2.2.3 Task 1c: Optional and further results for Scenarios B, C and D

Figure 4.9. Received results for Scenarios B, C, and D (from left to right)

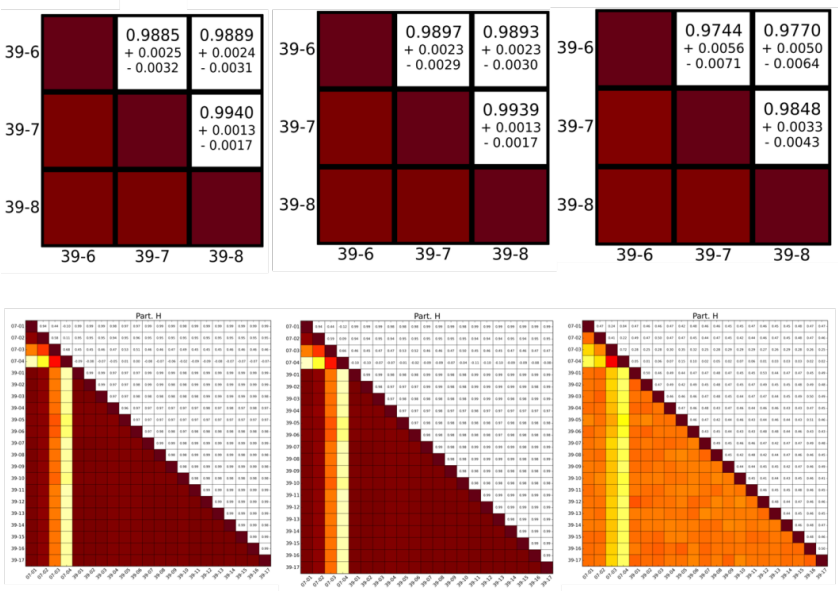

Source: NEA, 2020.
Note: The top row shows results from Participant E, the lower row shows results from Participant H.

4.2.2.4 Results for earlier benchmark definition

Figure 4.10. Received result for Option 1

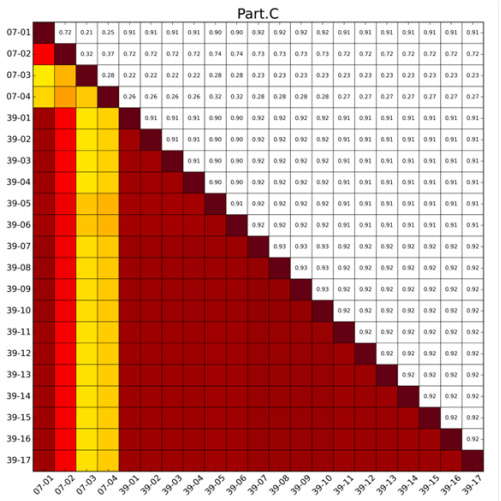

Source: NEA, 2020.

Figure 4.11. Received result for Option 2

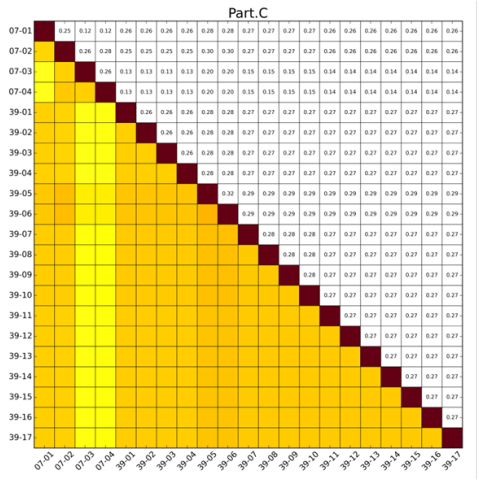

Source: NEA, 2020.

Figure 4.12. Received result for Option 3

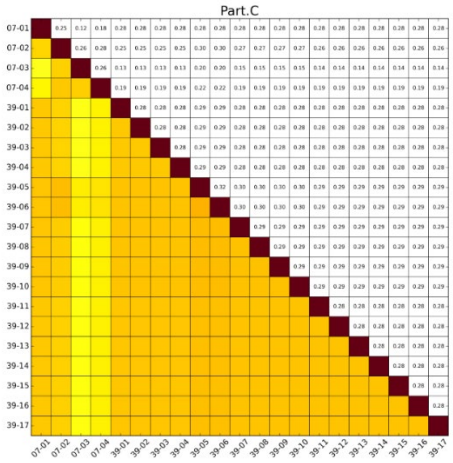

Source: NEA, 2020.

4.3 Phase IV-b: Study on importance of accounting for the integral experiment correlations in the criticality safety validation

The aim of Phase IV-b is to quantify the impact of the correlations established in Phase IV-a, Exercise 1 on the prediction of the bias-corrected k_{eff} value and its related uncertainty for the two application cases specified in this section.

4.3.1 Application Case 1: Water-moderated and water-reflected 16x16 fuel assembly

The first application case is a simplified 16×16 PWR fuel assembly fully reflected by water. The positions of the 236 fuel rods and 20 guide thimbles are shown in Figure 4.13. In Table 4.5, the system parameters and their corresponding uncertainties are specified. All additional materials like the assembly foot, assembly head and spacer grids are neglected.

As appears from Table 4.5, only the uncertainties in the fuel rod and guide thimble dimensions and in the height of the fuel column will be considered.

Figure 4.13. Geometry for 16x16 fuel rod lattice of Application Case 1

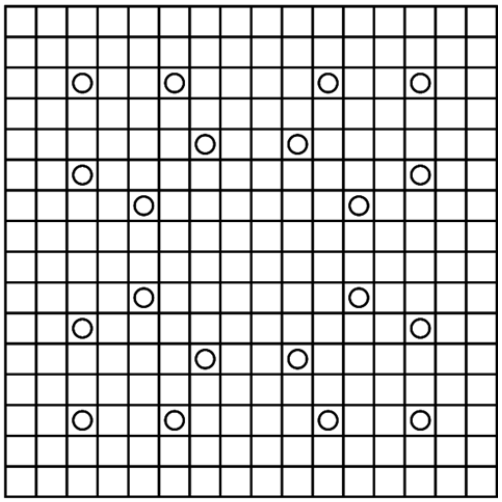

Source: NEA, 2020.

Note: The squares symbolise the fuel rod positions, while the circles mark the guide thimble positions.

Table 4.5. Parameters defining Application Case 1

Parameter	Specification	Distribution Model
Fuel Assembly		
• Square lattice	16×16	-
• Fuel rod pitch	1.43 cm	-
• Number of fuel rods	236	-
• Number of guide thimbles	20	-
Fuel Rod:		
• Pellet diameter	μ = 9.11 mm, σ = 0.013 mm	$N(\mu,\sigma^2)$
• Cladding inner diameter	μ = 9.30 mm, σ = 0.04 mm	$N(\mu,\sigma^2)$
• Cladding outer diameter	μ = 10.75 mm, σ = 0.05 mm	$N(\mu,\sigma^2)$
• Cladding material	Zircaloy-2	-
• Active length	μ = 390 cm, σ = 1.5 cm	$N(\mu,\sigma^2)$
Guide Thimble:		
• Inner diameter	μ = 12.4 mm, σ = 0.05 mm	$N(\mu,\sigma^2)$
• Outer diameter	μ = 13.8 mm, σ = 0.05 mm	$N(\mu,\sigma^2)$
• Material	Zircaloy-2	-
Fuel (UO_2):		
• ^{235}U enrichment	5 wt.-%	-
• ^{238}U content	95 wt.-%	-
• UO_2 density	10.96 g/cm^3	-
• Dishing of fuel pellets	no dishing	
Moderator/reflector (pure water)		
• Temperature	293 K	-
• Density	1 g/cm^3	-

Source: NEA, 2020.

4.3.2 Application Case 2: LEU-COMP-THERM-079 Configurations

The LEU-COMP-THERM-079 series of experiments (Harms, 2015) implement 4.31 wt.% UO_2 fuel rods in a hexagonally pitched array with two different fuel rod pitches of 2.0 and 2.8 cm, as shown in Figure 4.14 and Figure 4.15, correspondingly.

Figure 4.14. LEU-COMP-THERM-079 Case 1 with 2.0-cm pitch

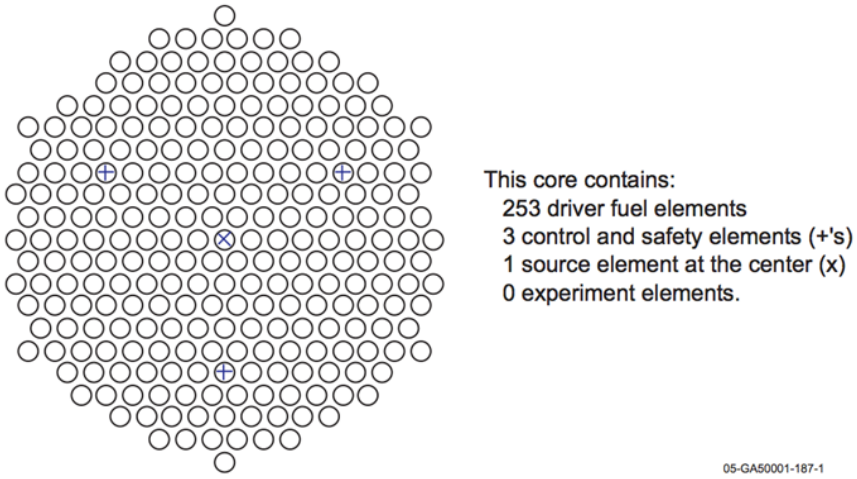

Source: Harms, 2015.

Figure 4.15. LEU-COMP-THERM-079 Case 6 with 2.8-cm pitch

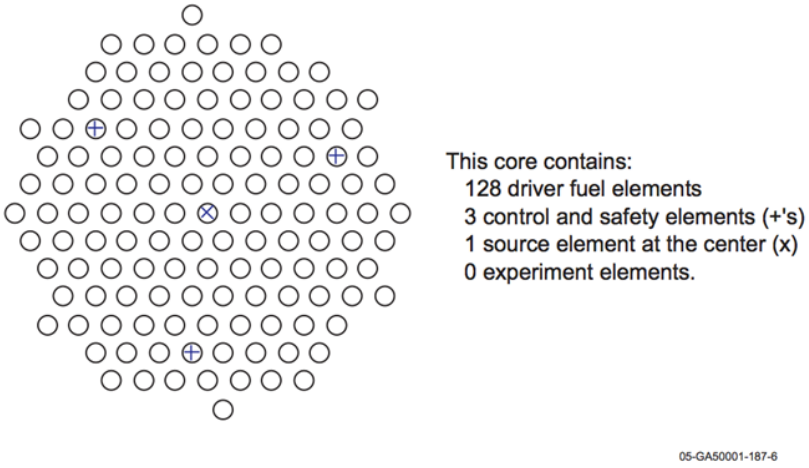

Source: Harms, 2015.

Although the intent of the benchmark is to examine ^{103}Rh for fission product burn-up credit, Cases 1 and 6 from this evaluation are reference cores that contain only UO_2 driver rods with no additional poison. The full specification of the benchmarks and their uncertainties is provided in the ICSBEP Handbook (Harms, 2015).

4.3.3 Tasks of Phase IV-b exercises

The tasks of Phase IV-b are as follows:

For the Application Cases 1 and/or 2, calculate the k_{eff} values, bias-corrected k_{eff} values and quantify the bias uncertainties based on the results of Phase IV-a (covariances generated for the benchmark configurations).

a) neglecting the dependencies (correlations) between the system parameters of different benchmark experiments due to common components; and

b) taking into account the dependencies (correlations) between the system parameters of different benchmark experiments due to common components.

4.3.4 Overview of received results

In total, nine different sets of results were received for the bias-corrected k_{eff} values of Application Case 1. Six results were sent for the bias-corrected k_{eff} value neglecting correlations, seven results accounting for correlations following Scenario A (and one assuming Option 2), and five results accounting for correlations assuming Scenario E (and one assuming Option 3).

Table 4.6. Received results for Application Case 1

Part.	Prior	Posterior neglecting correlations	Posterior accounting for correlation (Scenario A)	Posterior accounting for correlation (Scenario E)
A1	0.97653 ± 0.002337	0.97995 ± 0.00101	0.97995 ± 0.00433	
A2	0.97653 ± 0.002337	0.97926 ± 0.00177	0.97926 ± 0.00420	0.97926 ± 0.00050
B1	0.96921 ± 0.005803	0.97322 ± 0.002106	0.972428 ± 0.0020716	
B2	0.96921 ± 0.005803	0.97322 ± 0.0020971	0.972326 ± 0.0022906	
C(*)	0.96930 ± 0.00050	0.97340 ± 0.00064	0.9735 ± 0.00096	0.9733 ± 0.00088
D	0.96915 ± 0.00009		0.97248 ± 0.005	0.97248 ± 0.00225
E	0.96891 ± 0.006983	0.98074 ± 0.002394	0.96946 ± 0.003077	0.97118 ± 2.4153
H1	0.97350		0.97737 ± 0.00364	0.97732 ± 0.00097
H2	0.97383			0.97715 ± 0.00056

Source: NEA, 2020.

Note: The asterisk for Participant C is to highlight that the corresponding solutions are based on the earlier benchmark definition of Options 1, 2 and 3.

Figure 4.16. Results for Application Case 1

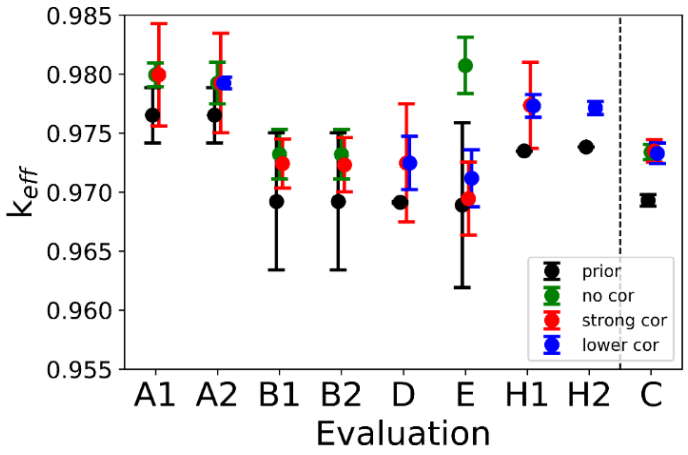

Source: NEA, 2020.
Note: The results for Participant C are based on the older benchmark definition.

For the Application Case LCT-079 experiment 1 we received four sets of results.

Table 4.7. Received results for Application Case LCT-079-001

Part.	Prior	Posterior neglecting correlations	Posterior accounting for correlation (Scenario A)	Posterior accounting for correlation (Scenario E)
B1	0.99785 ± 0.006054	1.0021 ± 0.0016262	1.00160 ± 0.0018384	
B2	0.99785 ± 0.006054	1.0021 ± 0.00160982	1.00141 ± 0.0021496	
D	0.99922 ± 0.00009		1.00252 ± 0.0045	1.00252 ± 0.004
E	0.9913 ± 0.007404	0.99957 ± 0.0017656	0.99184 ± 0.003226	0.99434 ± 0.001766

Source: NEA, 2020.

Figure 4.17. Received results for the Application Case LCT-079 Case 1

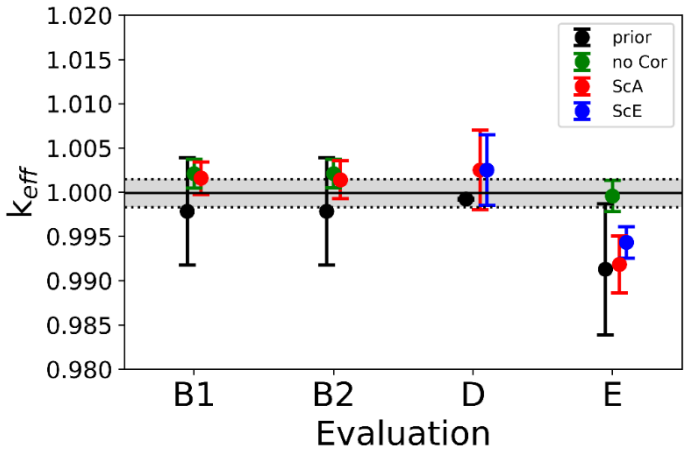

Source: NEA, 2020.
Note: The grey band denotes the 1-σ uncertainty of the literature value of $k_{eff} = 1$.

4.4 Summary and discussion of results

4.4.1 Task IV-a

The received results for the correlation coefficients assuming Scenario A generally show good agreement: All results show coefficients close to one except for cases LCT-007, experiments 3 and 4. The latter differs from the other experiments due to moderation effects leading to significantly lower correlation coefficients with the remaining 19 experiments.

The results for the k_{eff} correlation coefficients assuming Scenario E show a wide variety of solutions among the participants. The correlation coefficients vary from slightly negative values to one. Also, the patterns of the correlation matrices vary significantly between the different participants. The patterns of evaluations A, E and H2 are similar, as well as the patterns of evaluations D1 and H1. The reasons for the discrepancies seem to be the following:

- Different interpretations of the benchmark specification concerning the dependent and independent system parameters led to different modelling assumptions. The different interpretations led to different modelling approaches and thus to different sensitivity profiles of the importance of parameter uncertainties on the k_{eff} uncertainty. If different parameters with different associated uncertainties play the leading role for the k_{eff} uncertainty, the resulting covariance and correlation coefficients differ, too.
- Convergence of results for the correlation coefficients derived by Monte Carlo methods was not always reached. Stating the uncertainty due to the Monte Carlo sampling would allow a more thorough comparison of results.

The optional results show good agreement for Scenarios B and C and some differences for Scenario D due to different interpretations of the specifications.

Only one participant sent results based on the older benchmark definitions of Option 1, 2 and 3 and thus no direct comparison is possible. However, the results for Option 1 can be compared to solutions of Scenario A. Good agreement can be found with all results for Scenario A, except for experiment 2 of LCT-079. The solution of Option 1 found a slightly decreased correlation coefficient with the remaining 20 experiments.

4.4.2 Task IV-b

The calculated prior k_{eff} values for the Application Case 1 can be divided into two groups. Participants A and H calculated higher values than Participants B, D, E and C. All results show an increase for the bias-corrected k_{eff} values and a decrease of the 1-sigma interval, except for the bias-corrected values of Participant A assuming strong correlation. It is notable that the results for the bias-corrected k_{eff} values are comparable for both definitions of the benchmark.

The bias-corrected values of Participants B, D, E and C are all in agreement within the 1-sigma uncertainty. The same is true for the bias-corrected values of A, H and the no-correlation value of Participant E. Except for the latter, the discrepancy can be explained by the different “starting points” of the analysis, aka the a priori value. The bias-corrected values rely on the prior estimations and if these vary, so do the bias-corrected values.

The results for the Application Case LCT-079 are all in agreement. The results of Participants B and D reproduce within 1-sigma the experimental k_{eff} value given in the ICSBEP Handbook (Harms, 2015). Due to the lower prior estimate of Participant E, the experimental k_{eff} values can only be reproduced within 2-sigma assuming Scenarios A and E.

5. Conclusions and outlook

The objective of UACSA Benchmark Phase IV was to test methodologies to express the joint variability between benchmark neutron multiplication factors in terms of covariances and to evaluate the impact of these covariances on the predictions of the bias-corrected neutron multiplication factors. Two different benchmark exercises were included: an analytic toy model exercise and a realistic case involving experiments with water-reflected UO_2 fuel rod arrays.

For the analytic toy model, nine results by six participants were discussed. Including the correlation effects, all results reproduce the true value within 1-σ, except results A1 and A2, which reproduce the true value within less than 2-σ.

For the Application Case 1 the results of five participants following the actual benchmark definition and one result stemming from an older benchmark definition were analysed. Six results include the k_{eff} values for the non-correlated and highly correlated Scenario A (Option 1), and only one result (Participant E) showed a notable difference from the other results (see Figure 4.16).

Comparatively small variations were observed for the k_{eff} predictions of the Application Case LCT-079 Case 1. An exception is again the result obtained for the no-correlation assumption by Participant E showing a notable difference to the other results. For the three sets of solutions including the bias-corrected values assuming no correlation and strong correlation, individual consequences can be observed. Participant A finds a significant increase of the 1-sigma uncertainty of the bias-corrected k_{eff} values assuming strong correlation. Participant B finds almost no difference between assuming strong and no correlation. The reason for the comparatively huge difference between the results corresponding to the two different assumptions by Participant E might lie in an erroneous data file. However, to draw a definite conclusion on the impact of the investigated covariances on the predictions of the bias-corrected neutron multiplication factors, more solutions for the Application Case LCT-079 Case 1 would have been desirable, since for this application case the actual experimental k_{eff} value is known.

Far more solutions for the correlation coefficients calculated in Task 2 (see Figures 4.7 and 4.8) were received than for the bias-corrected k_{eff} values. Also, the results of the updated k_{eff} value and the corresponding uncertainties are the results of a lengthy calculation chain including numerous individual assumptions. This can be seen, for example, in the variety of the correlation coefficients for Scenario E in Figure 4.8. It is notable that the description of the Benchmark Phase IV included additional information compared to the ICSBEP Handbook, but participants still sometimes chose significantly different modelling approaches. As a result, this led to different k_{eff} uncertainties and sensitivity profiles and thus to sometimes significant differences between correlation coefficients. This individuality in the interpretation of experimental data can be referred to as a type of user-dependent bias.

A clear comparison between the methods used by the participants would be beneficial. This seems to be not straightforward, based on the received results. It is recommended to conduct further investigations based on far simpler and unambiguous benchmark definitions for which no user-specific biases hamper the comparisons between the results by different participants.

Based on this report, drawing generalised statements on the methodologies to express the joint variability between benchmark neutron multiplication factors in terms of covariances

and on the evaluation of the impact of these covariances on the predictions of the bias-corrected neutron multiplication factors proves challenging.

From a practical point of view, Benchmark Phase IV required too much time from its first proposal and definition in 2012 until its finalisation. Especially the crucial changes to the benchmark definition made over the years led to several delays in the completion of the benchmark tasks. Furthermore, parts of the benchmark definition were computationally challenging and needed significant computational power. In retrospect, a clearer and unambiguously defined benchmark with fewer tasks could have equally served the purpose and led to clearer comparisons of results. Also, more participants would have been able to take part and the benchmark could have been completed earlier.

However, the benchmark and the accompanying discussions in and outside the WPNCS led to an increased awareness of the challenges and the development of different methodologies to account for shared uncertainties and covariances between benchmark experiments.

References

Barbry, F., P. Grivot, E. Girault, P. Fouillaud, P. Cousinou, G. Poullot, J. Anno, J.M. Bordy and D. Doutriaux (2003), "Criticality experiments performed in Saclay and Valduc Centers, France (1958-2002)", *Nuclear Science and Engineering*, Vol. 145, Number 1, pp. 39-63, https://doi.org/10.13182/NSE03-A2362.

Brandt, S. (1999), *Data Analysis: Statistical and Computational Methods for Scientists and Engineers*, 3rd ed., Springer, New York.

Buss, O., A. Hoefer, J.C. Neuber, and M. Schmid (2010), "Hierarchical Monte Carlo approach to bias estimation for criticality safety calculations", *Proceedings paper and presentation at the International Conference on the Physics of Reactors 2010* (PHYSOR 2010), Pittsburgh, United States.

Harms, G. (2015), "Water-moderated U(4.31)O2 fuel rod lattices containing Rhodium foils, LEU-COMP-THERM-079", *International Handbook of Evaluated Criticality Safety Benchmark Experiments,* OECD Publishing, https://doi.org/10.1787/110ba6fc-en.

Manaranche, J.C., D. Mangin, L. Maubert, G. Colomb and G. Poullot (1979), "Critical experiments with lattices of 4.75-wt-% 235U-enriched UO_2 rods in water", *Nuclear Science and Enginerring*, Vol. 71, Number 2, pp. 154-163, https://doi.org/10.13182/NSE79-4.

NEA (2015), *International Handbook of Evaluated Criticality Safety Benchmark Experiments,* NEA/NSC/DOC(95)03, OECD Publishing, Paris, https://doi.org/10.1787/110ba6fc-en.

Poullot, G. and D. Hanlon (2015a), "Water-reflected 4.738-wt% enriched Uranium dioxide fuel-rod arrays, LEU-COMP-THERM-007", *International Handbook of Evaluated Criticality Safety Benchmark Experiments*, OECD Publishing, https://doi.org/10.1787/110ba6fc-en.

Poullot, G. and D. Hanlon (2015b), "Incomplete arrays of water-reflected 4.738wt% enriched Uranium dioxide fuel-rod arrays, LEU-COMP-THERM-039", *International Handbook of Evaluated Criticality Safety Benchmark Experiments,* OECD Publishing, https://doi.org/10.1787/110ba6fc-en.

Appendix A. List of participants

This benchmark has a long history to which numerous colleagues contributed with remarks, discussions and support. The participants of the WPNCS UACSA and then WPNCS Subgroup 1 meetings where the Phase IV Benchmark was discussed were (in alphabetical order):

Matthias BEHLER	Alexis JINAPHANH
John BESS	Anatoly KOCHETKOV
François BIDAULT	George KOMPANIETS
Joseph Blair BRIGGS	Lukasz KOSZUK
Victor BOYARINOV	Nicolas LECLAIRE
Forrest BROWN	Eric LETANG
Oliver BUSS	Margaret MARSHALL
Coralie CARMOUZE	William MARSHALL
Maksym CHERNYK	Dennis MENNERDAHL
Carlos DIEZ	Franco MICHEL-SENDIS
Anatoly A. DUDNIKOV	Joachim MISS
Isabelle DUHAMEL	Yoshinori MIYOSHI
Michael DUNN	Jens-Christian NEUBER
James DYRDA	Alberto OTTONELLO
Oscar CABELLOS DE FRANCISCO	Marco PECCHIA
Stéphane EVO	Christopher PERFETTI
Ivan FAST	Elisabeth PETERS
Peter FOMICHENKO	Laura PICARD
Frederic FERNEX	Dmitry POLIAKOV
Ian C. GAULD	Bastien QUAGHEBEUR
Yury GOLOVKO	Meraj RAHIMI
Sedat GOLUOGLU	Anssu RANTA-AHO
Dirk SCHULZE GRACHTRUP	Bradley T. REARDEN
Milan GREN	Ingo REICHE
Mikhail GUREVICH	Yann RICHET
Maik HENNEBACH	Michael RISING
Ian Hill	Evgeny ROZHIKHIN
Axel HOEFER	Benjamin RUPRECHT
Gabor HORDOSY	Alain SANTAMARINA
Germina ILAS	John SCORBY
Evgeny IVANOV	Alyse Marie SCURLOCK
Tatiana IVANOVA	Shigeki SHIBA
Daiki IWAHASHI	Pavel TEPLOV
Valentin SINITSA	Sven TITTELBACH
Paul N. SMITH	Anatoly TSIBOULYA
Fabian SOMMER	Guillaume TRUCHET
Gil Soo LEE	Alexander VASILIEV
Maik STUKE	Radim VOCKA
Kenya SUYAMA	Toshihisa YAMAMOTO
Marcel TARDY	Yuichi YAMANE
Travis TATE	Kent WOOD
Vladimir TEBIN	Gennady ZHERDEV

Appendix B. Correlation matrices

B.1 Toy model

B.1.1 Task 1a

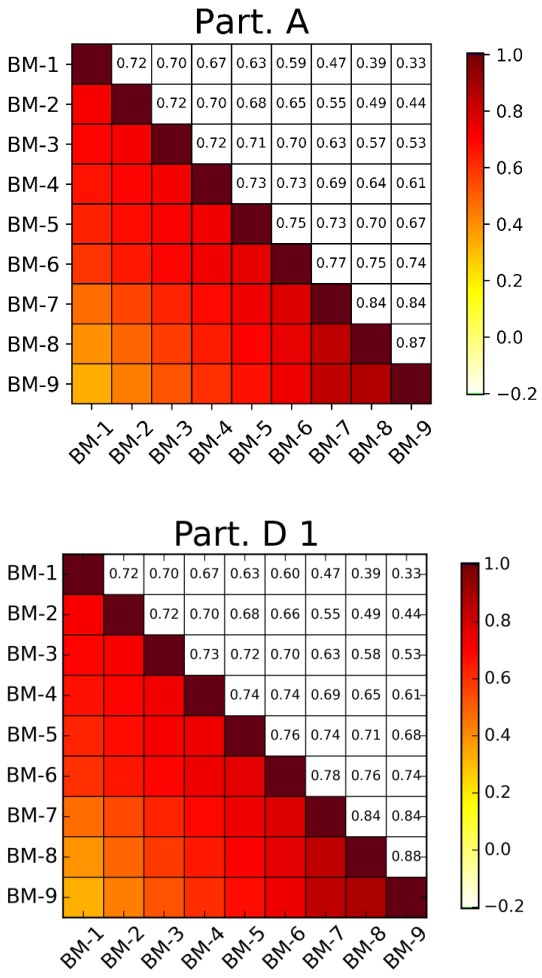

Source: NEA, 2020.

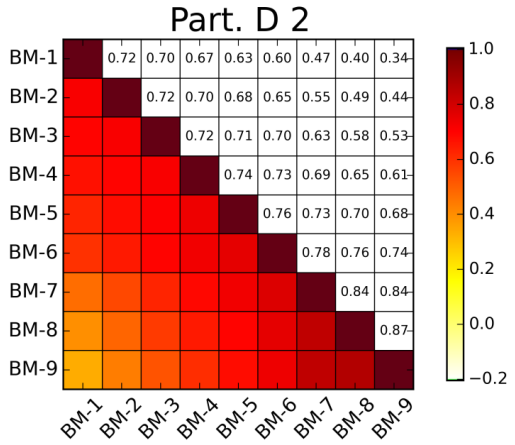
Part. D 2
BM-1 0.72 0.70 0.67 0.63 0.60 0.47 0.40 0.34
BM-2 0.72 0.70 0.68 0.65 0.55 0.49 0.44
BM-3 0.72 0.71 0.70 0.63 0.58 0.53
BM-4 0.74 0.73 0.69 0.65 0.61
BM-5 0.76 0.73 0.70 0.68
BM-6 0.78 0.76 0.74
BM-7 0.84 0.84
BM-8 0.87
BM-9
1.0 0.8 0.6 0.4 0.2 0.0 −0.2
BM-1 BM-2 BM-3 BM-4 BM-5 BM-6 BM-7 BM-8 BM-9

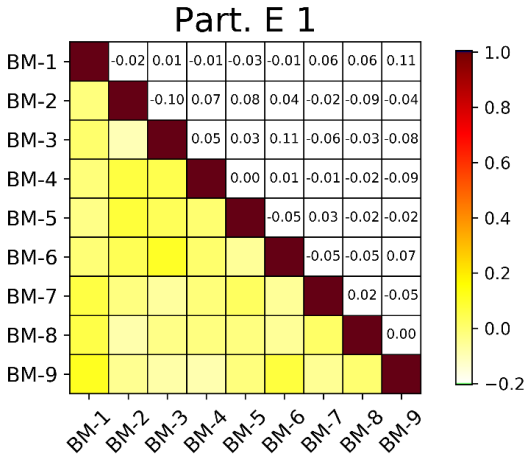
Part. E 1
BM-1 -0.02 0.01 -0.01 -0.03 -0.01 0.06 0.06 0.11
BM-2 -0.10 0.07 0.08 0.04 -0.02 -0.09 -0.04
BM-3 0.05 0.03 0.11 -0.06 -0.03 -0.08
BM-4 0.00 0.01 -0.01 -0.02 -0.09
BM-5 -0.05 0.03 -0.02 -0.02
BM-6 -0.05 -0.05 0.07
BM-7 0.02 -0.05
BM-8 0.00
BM-9
1.0 0.8 0.6 0.4 0.2 0.0 −0.2
BM-1 BM-2 BM-3 BM-4 BM-5 BM-6 BM-7 BM-8 BM-9

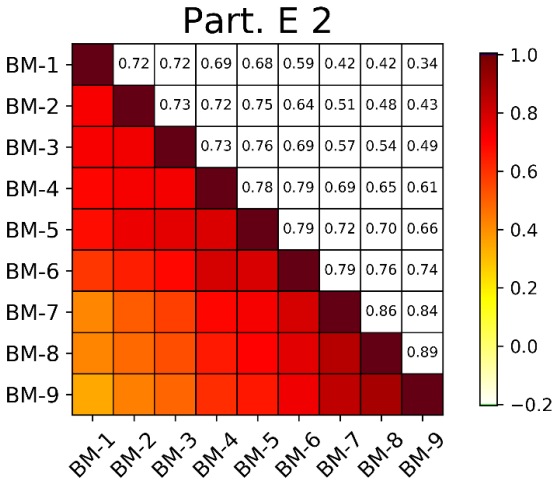
Part. E 2
BM-1 0.72 0.72 0.69 0.68 0.59 0.42 0.42 0.34
BM-2 0.73 0.72 0.75 0.64 0.51 0.48 0.43
BM-3 0.73 0.76 0.69 0.57 0.54 0.49
BM-4 0.78 0.79 0.69 0.65 0.61
BM-5 0.79 0.72 0.70 0.66
BM-6 0.79 0.76 0.74
BM-7 0.86 0.84
BM-8 0.89
BM-9
1.0 0.8 0.6 0.4 0.2 0.0 −0.2
BM-1 BM-2 BM-3 BM-4 BM-5 BM-6 BM-7 BM-8 BM-9

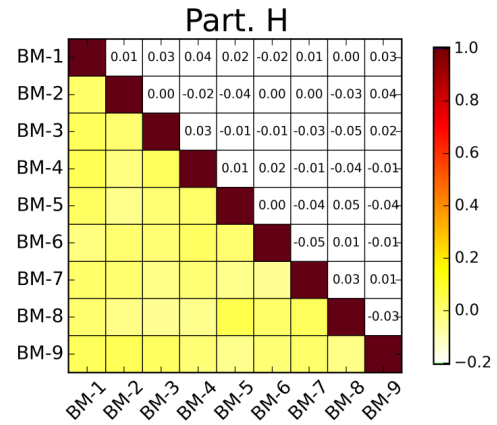

Source: NEA, 2020.

B.1.2 Task 1b

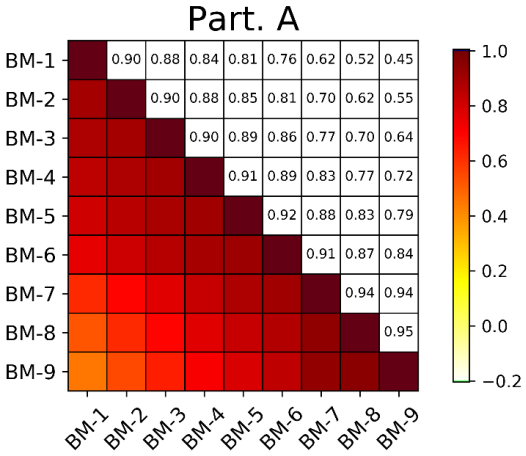

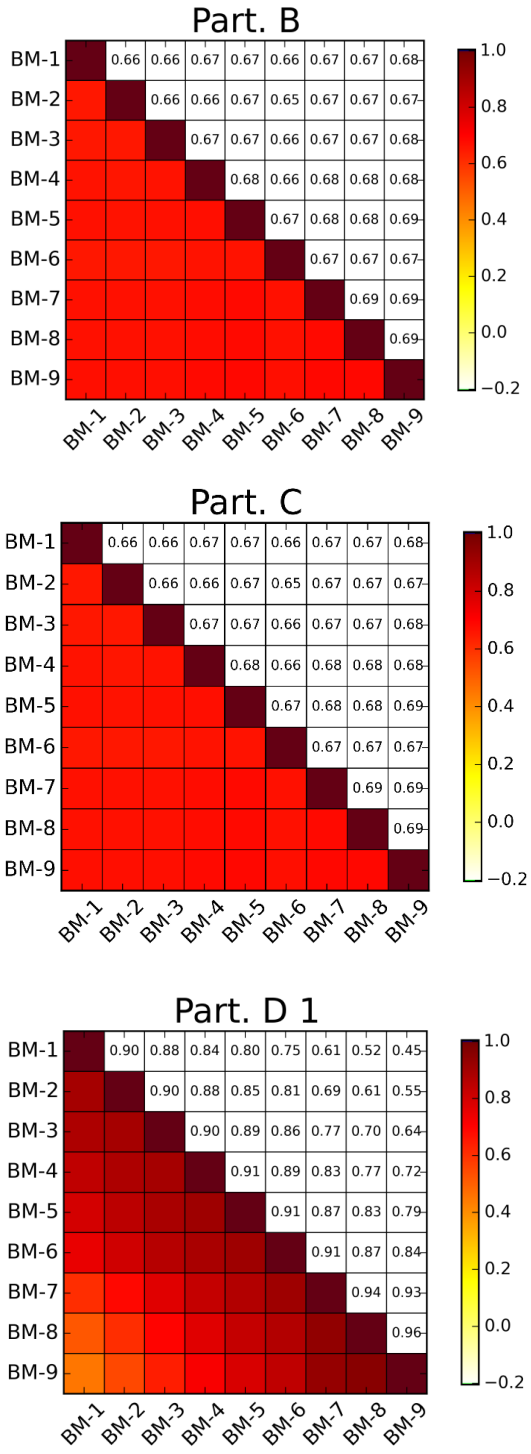
Part. B
BM-1 0.66 0.66 0.67 0.67 0.66 0.67 0.67 0.68
BM-2 0.66 0.66 0.67 0.67 0.65 0.67 0.67 0.67
BM-3 0.67 0.67 0.67 0.66 0.67 0.67 0.68
BM-4 0.68 0.66 0.68 0.68 0.68
BM-5 0.67 0.68 0.68 0.69
BM-6 0.67 0.67 0.67
BM-7 0.69 0.69
BM-8 0.69
BM-9
BM-1 BM-2 BM-3 BM-4 BM-5 BM-6 BM-7 BM-8 BM-9
1.0 0.8 0.6 0.4 0.2 0.0 −0.2
Part. C
BM-1 0.66 0.66 0.67 0.67 0.66 0.67 0.67 0.68
BM-2 0.66 0.66 0.67 0.67 0.65 0.67 0.67 0.67
BM-3 0.67 0.67 0.67 0.66 0.67 0.67 0.68
BM-4 0.68 0.66 0.68 0.68 0.68
BM-5 0.67 0.68 0.68 0.69
BM-6 0.67 0.67 0.67
BM-7 0.69 0.69
BM-8 0.69
BM-9
BM-1 BM-2 BM-3 BM-4 BM-5 BM-6 BM-7 BM-8 BM-9
1.0 0.8 0.6 0.4 0.2 0.0 −0.2
Part. D 1
BM-1 0.90 0.88 0.84 0.80 0.75 0.61 0.52 0.45
BM-2 0.90 0.88 0.85 0.81 0.69 0.61 0.55
BM-3 0.90 0.89 0.86 0.77 0.70 0.64
BM-4 0.91 0.89 0.83 0.77 0.72
BM-5 0.91 0.87 0.83 0.79
BM-6 0.91 0.87 0.84
BM-7 0.94 0.93
BM-8 0.96
BM-9
BM-1 BM-2 BM-3 BM-4 BM-5 BM-6 BM-7 BM-8 BM-9
1.0 0.8 0.6 0.4 0.2 0.0 −0.2

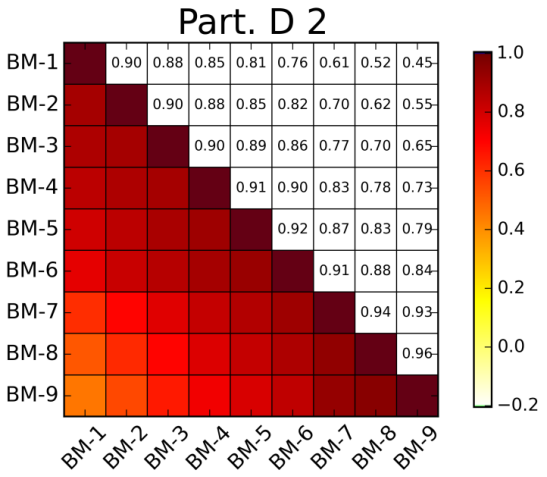
Part. D 2
BM-1 0.90 0.88 0.85 0.81 0.76 0.61 0.52 0.45
BM-2 0.90 0.88 0.85 0.82 0.70 0.62 0.55
BM-3 0.90 0.89 0.86 0.77 0.70 0.65
BM-4 0.91 0.90 0.83 0.78 0.73
BM-5 0.92 0.87 0.83 0.79
BM-6 0.91 0.88 0.84
BM-7 0.94 0.93
BM-8 0.96
BM-9
BM-1 BM-2 BM-3 BM-4 BM-5 BM-6 BM-7 BM-8 BM-9
1.0 0.8 0.6 0.4 0.2 0.0 −0.2

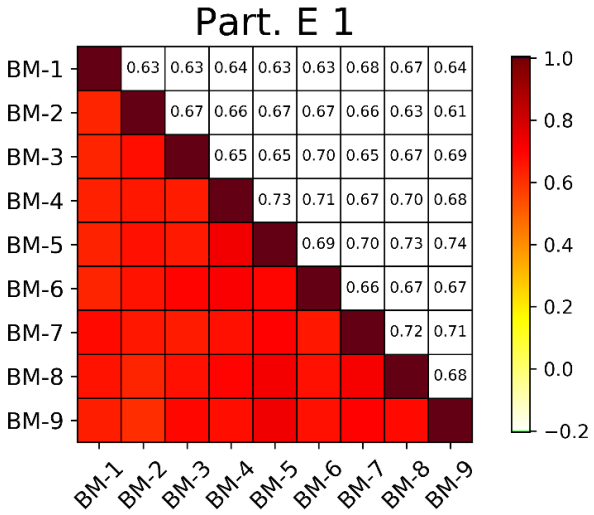
Part. E 1
BM-1 0.63 0.63 0.64 0.63 0.63 0.68 0.67 0.64
BM-2 0.67 0.66 0.67 0.67 0.66 0.63 0.61
BM-3 0.65 0.65 0.70 0.65 0.67 0.69
BM-4 0.73 0.71 0.67 0.70 0.68
BM-5 0.69 0.70 0.73 0.74
BM-6 0.66 0.67 0.67
BM-7 0.72 0.71
BM-8 0.68
BM-9
BM-1 BM-2 BM-3 BM-4 BM-5 BM-6 BM-7 BM-8 BM-9
1.0 0.8 0.6 0.4 0.2 0.0 −0.2

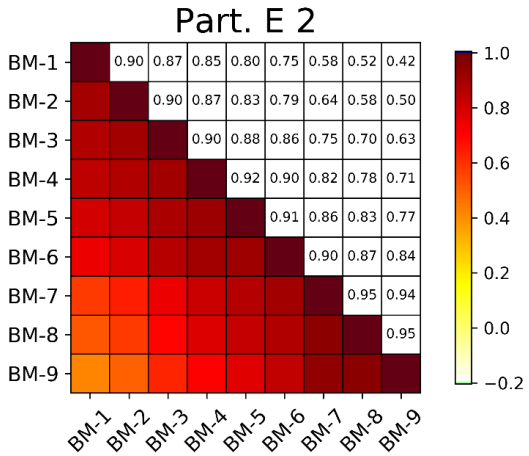
Part. E 2
BM-1 0.90 0.87 0.85 0.80 0.75 0.58 0.52 0.42
BM-2 0.90 0.87 0.83 0.79 0.64 0.58 0.50
BM-3 0.90 0.88 0.86 0.75 0.70 0.63
BM-4 0.92 0.90 0.82 0.78 0.71
BM-5 0.91 0.86 0.83 0.77
BM-6 0.90 0.87 0.84
BM-7 0.95 0.94
BM-8 0.95
BM-9
BM-1 BM-2 BM-3 BM-4 BM-5 BM-6 BM-7 BM-8 BM-9
1.0 0.8 0.6 0.4 0.2 0.0 −0.2

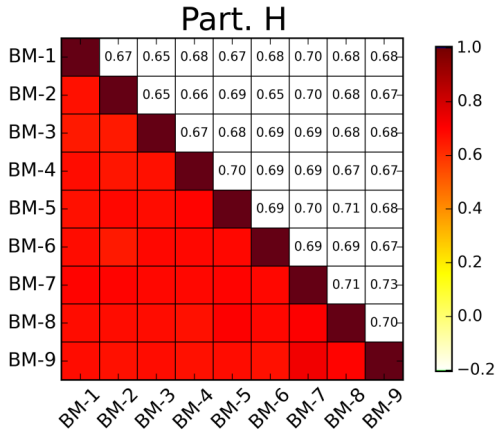

Source: NEA, 2020.

B.2 Scenario A

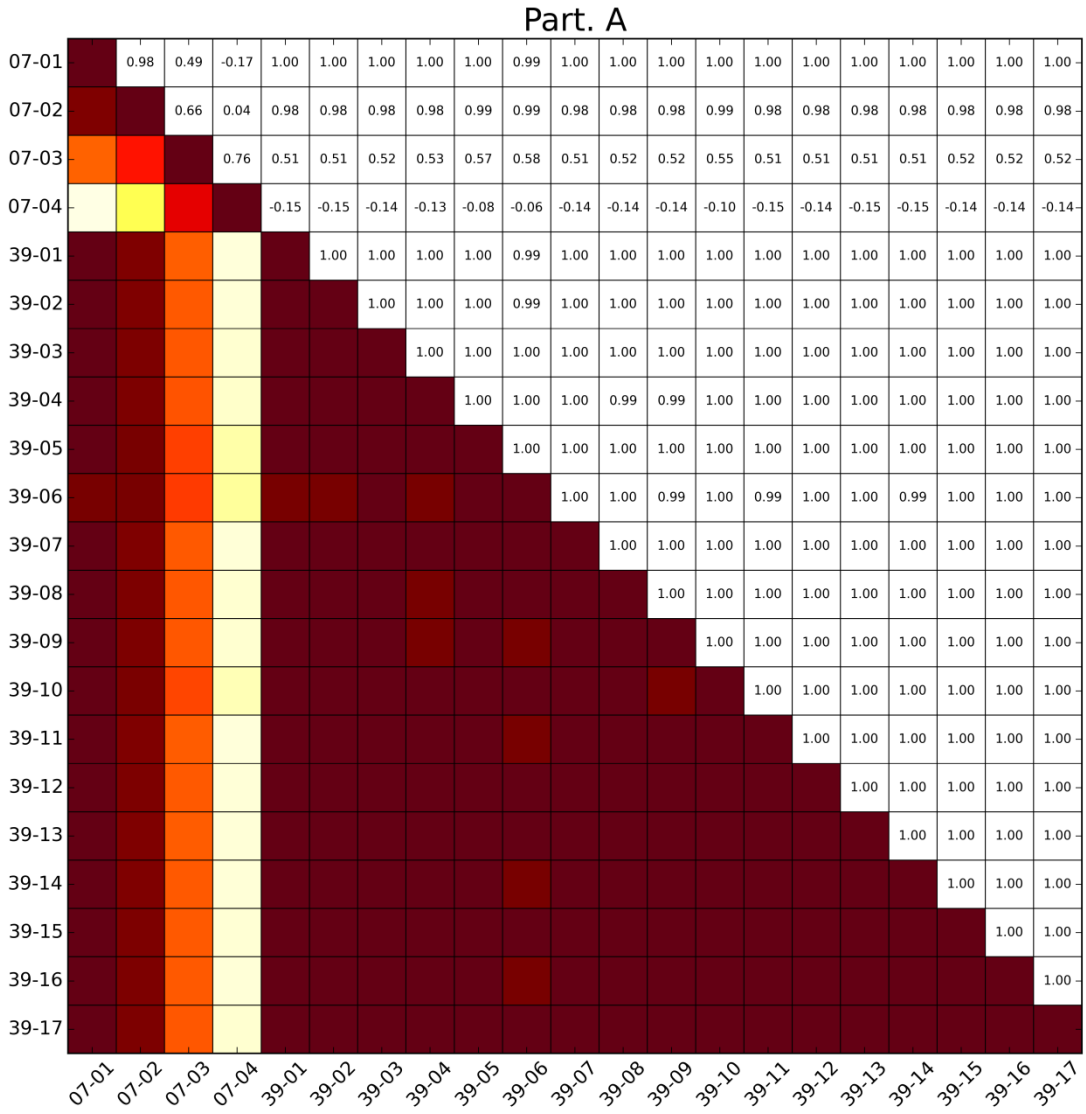

Source: NEA, 2020.

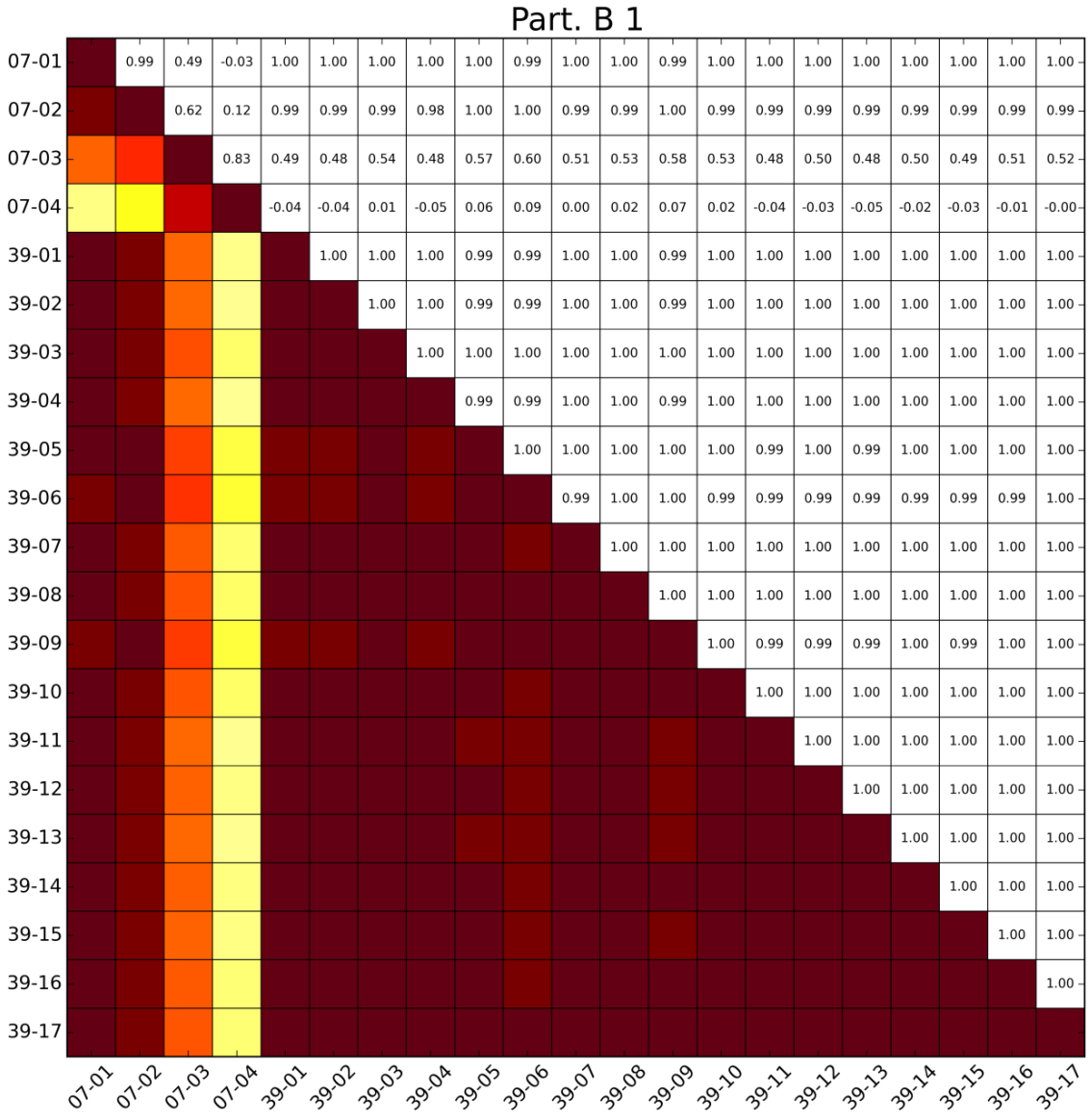

Source: NEA, 2020.

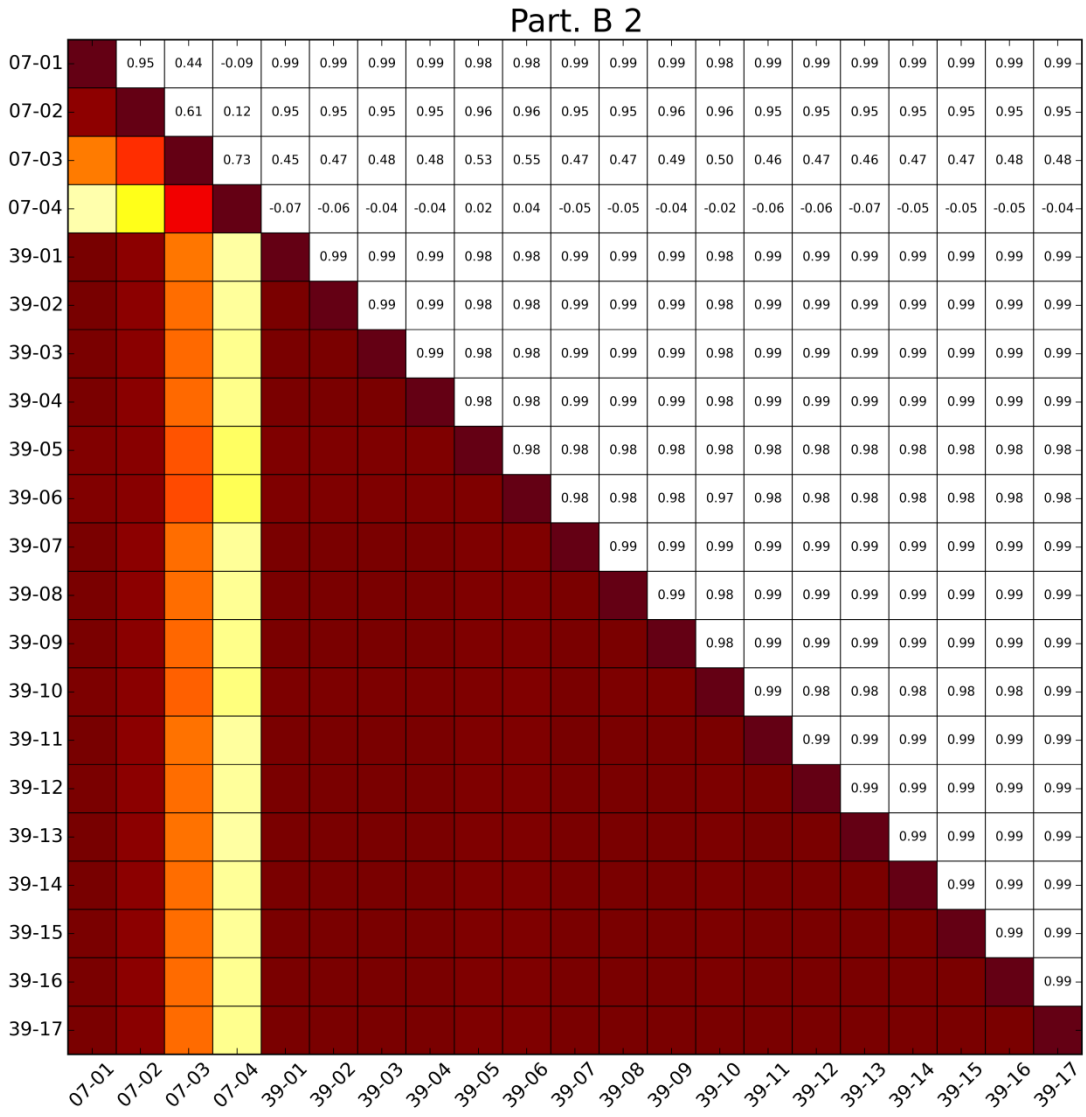

Source: NEA, 2020.

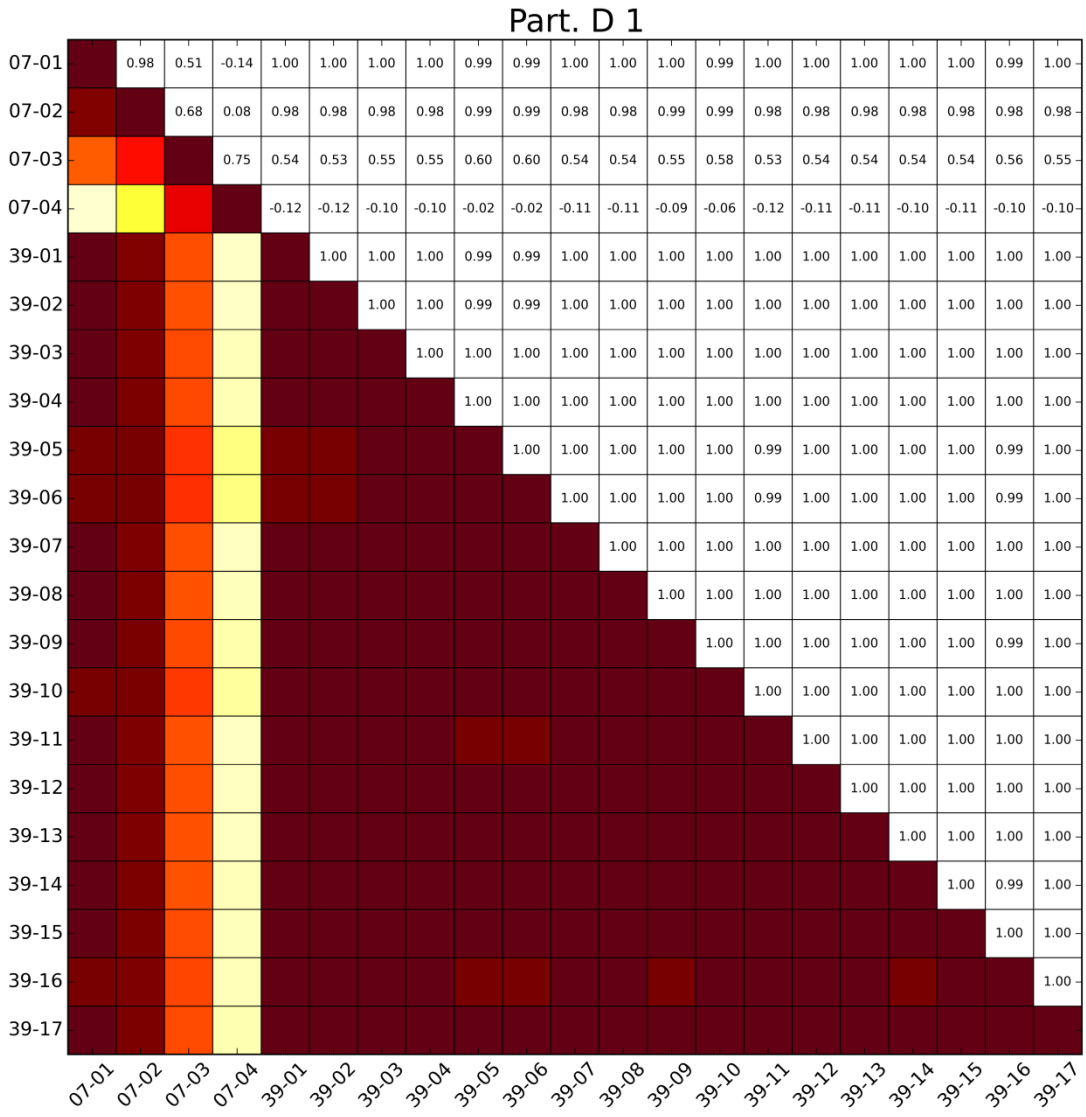

Source: NEA, 2020.

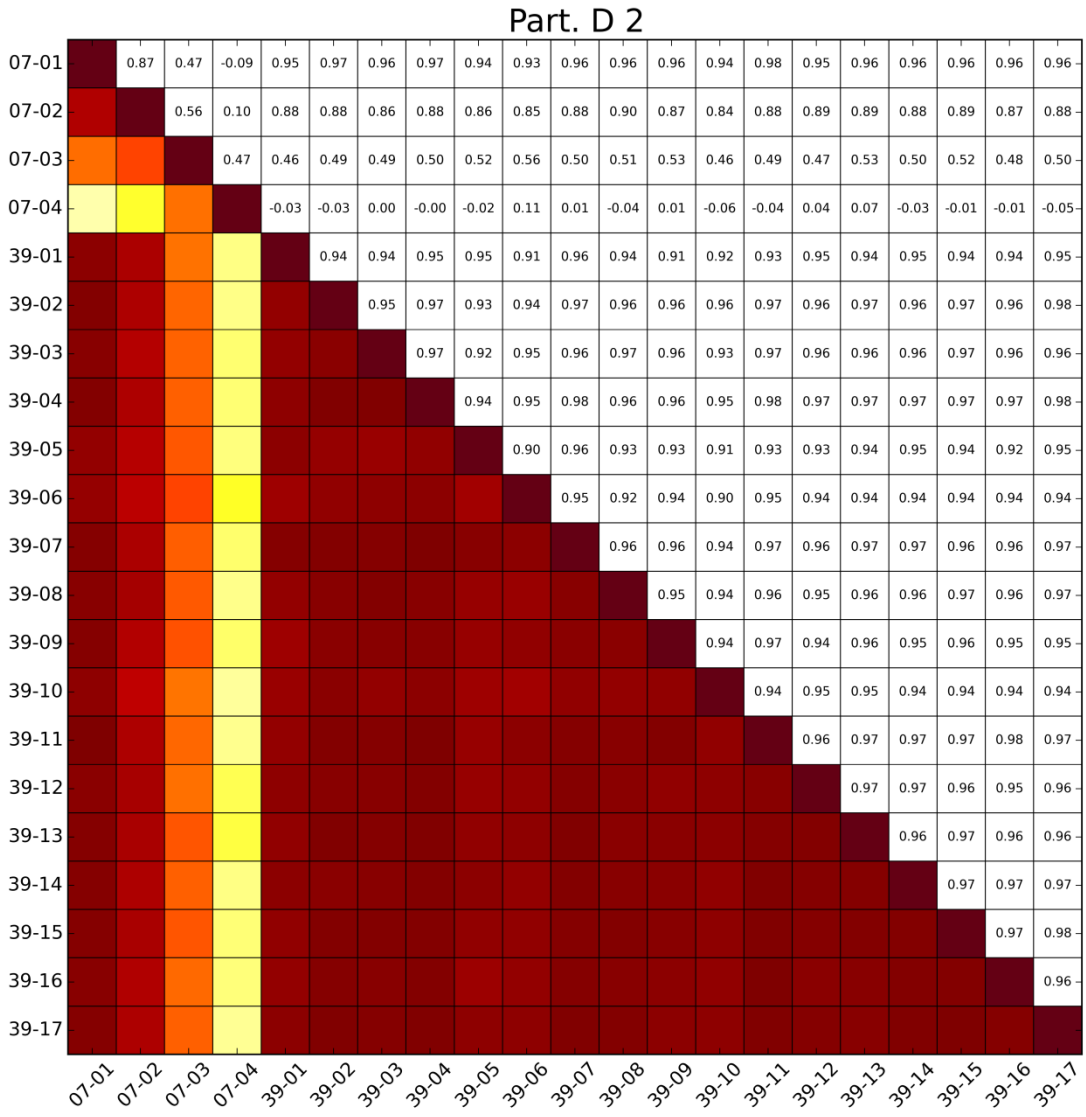

Source: NEA, 2020.

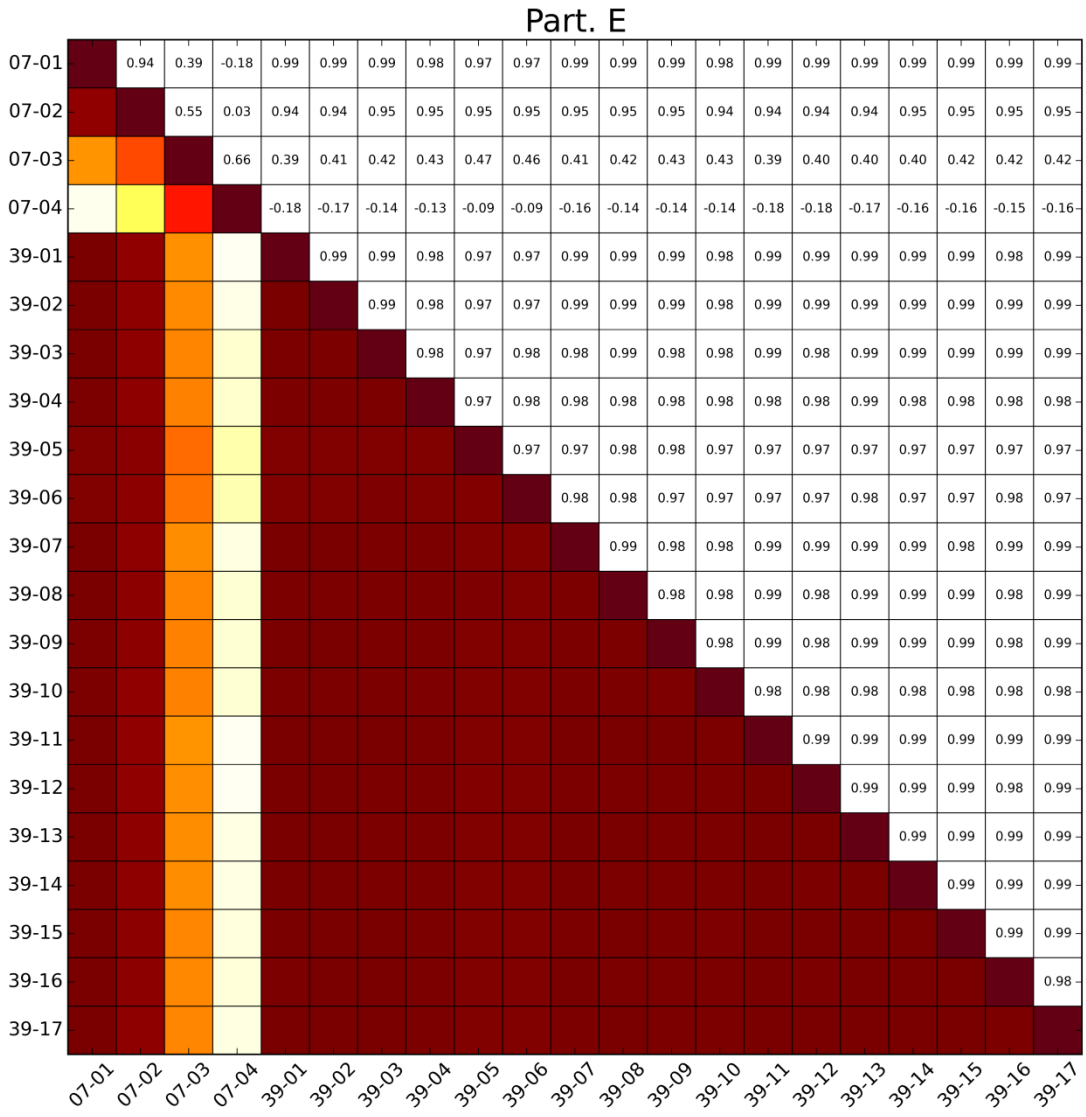

Source: NEA, 2020.

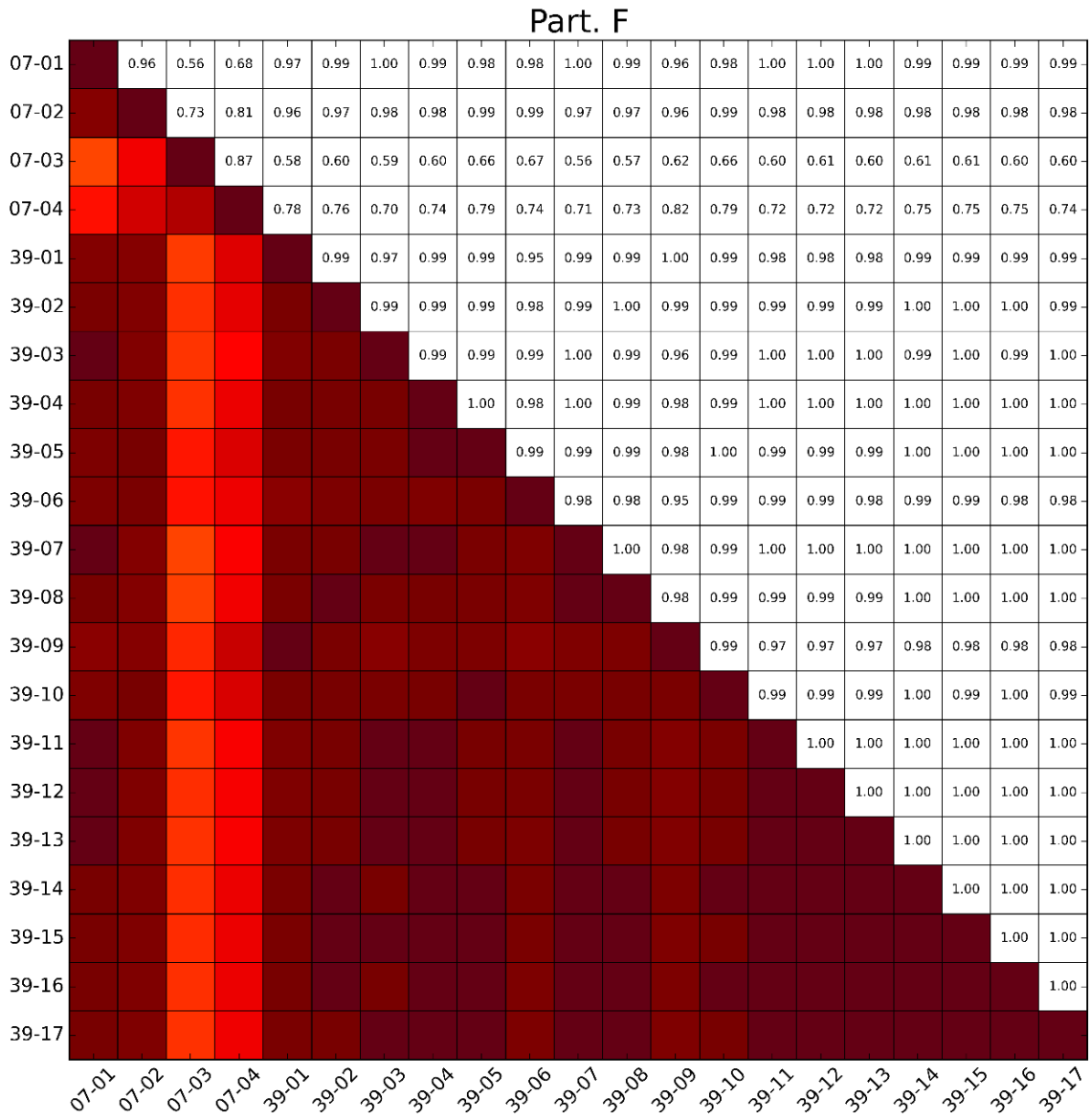

Source: NEA, 2020.

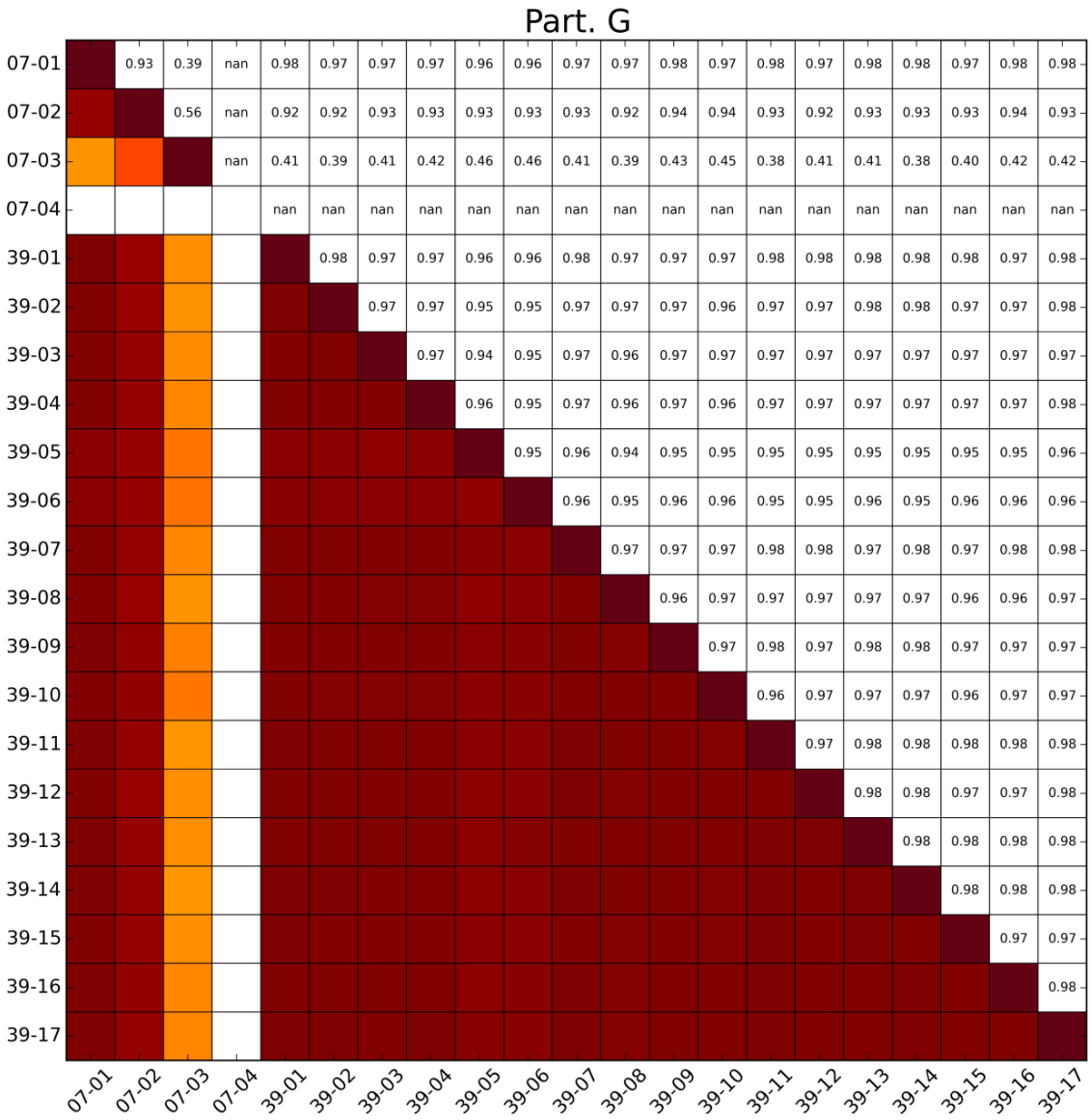

Source: NEA, 2020.

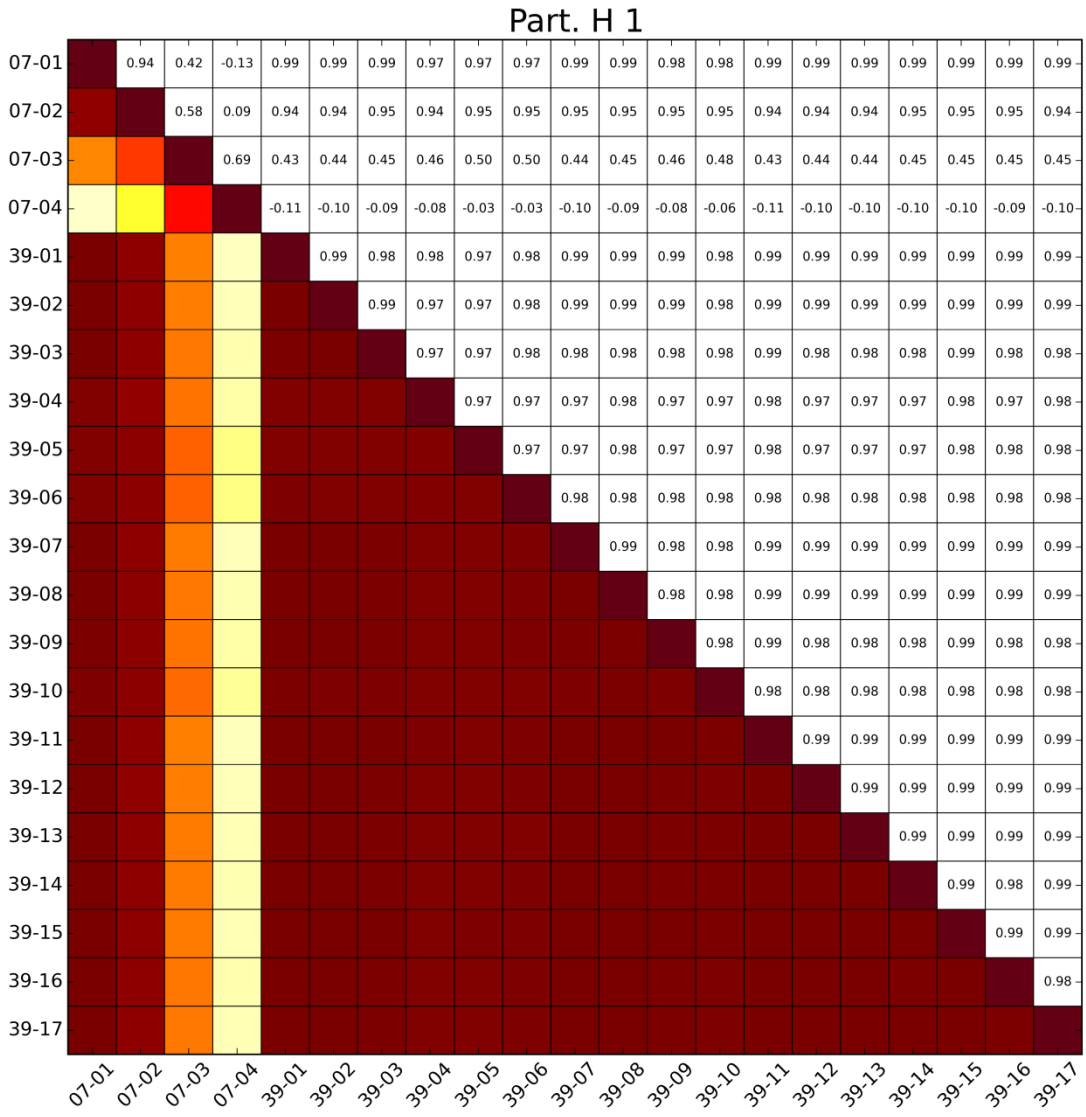

Source: NEA, 2020.

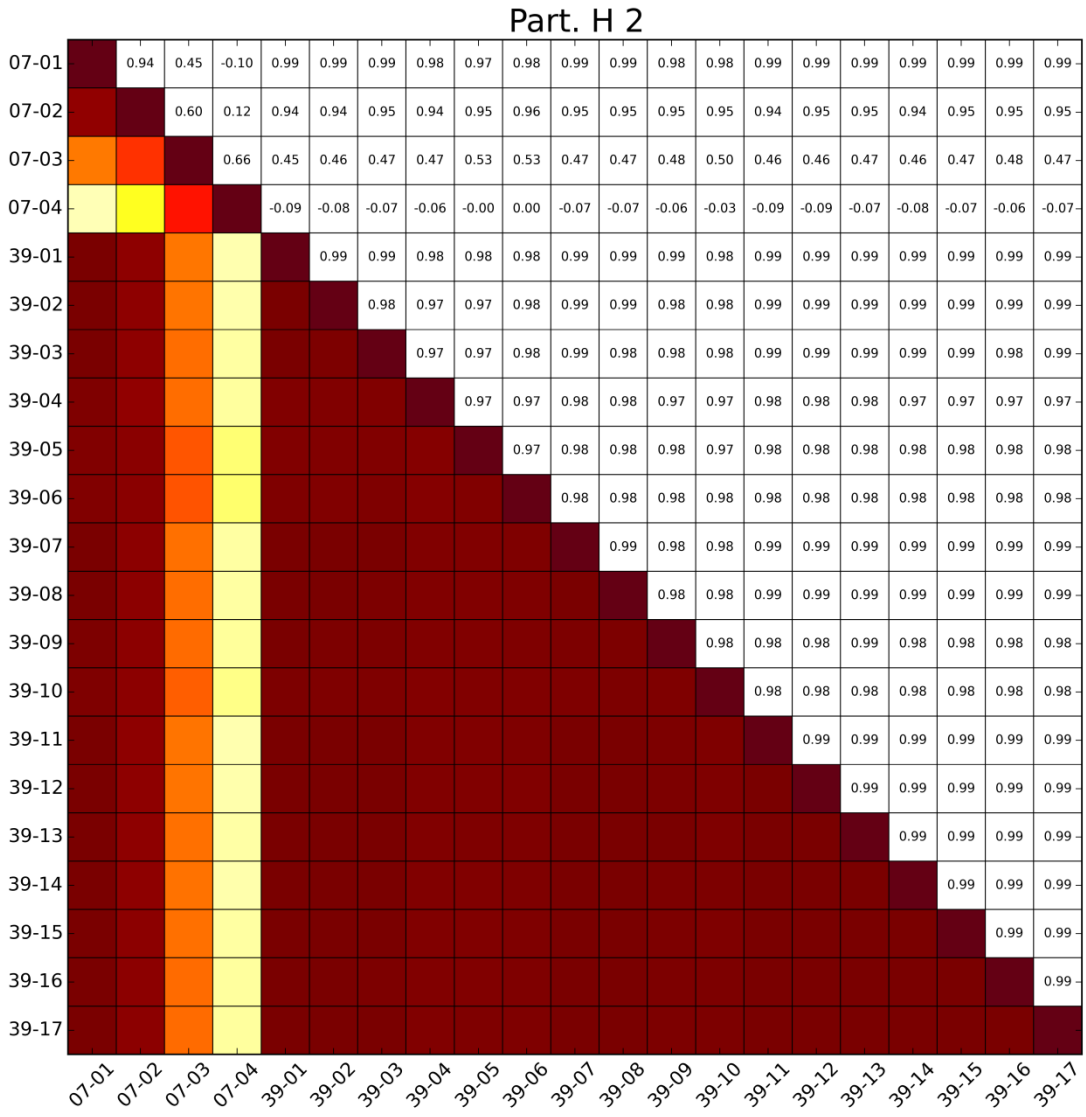

Source: NEA, 2020.

B.3 Scenario E

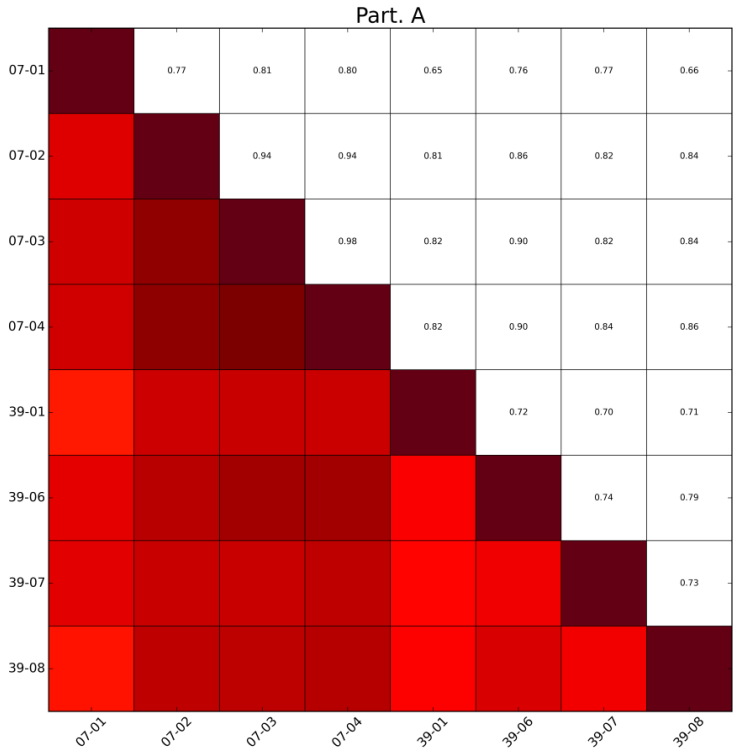

Source: NEA, 2020.

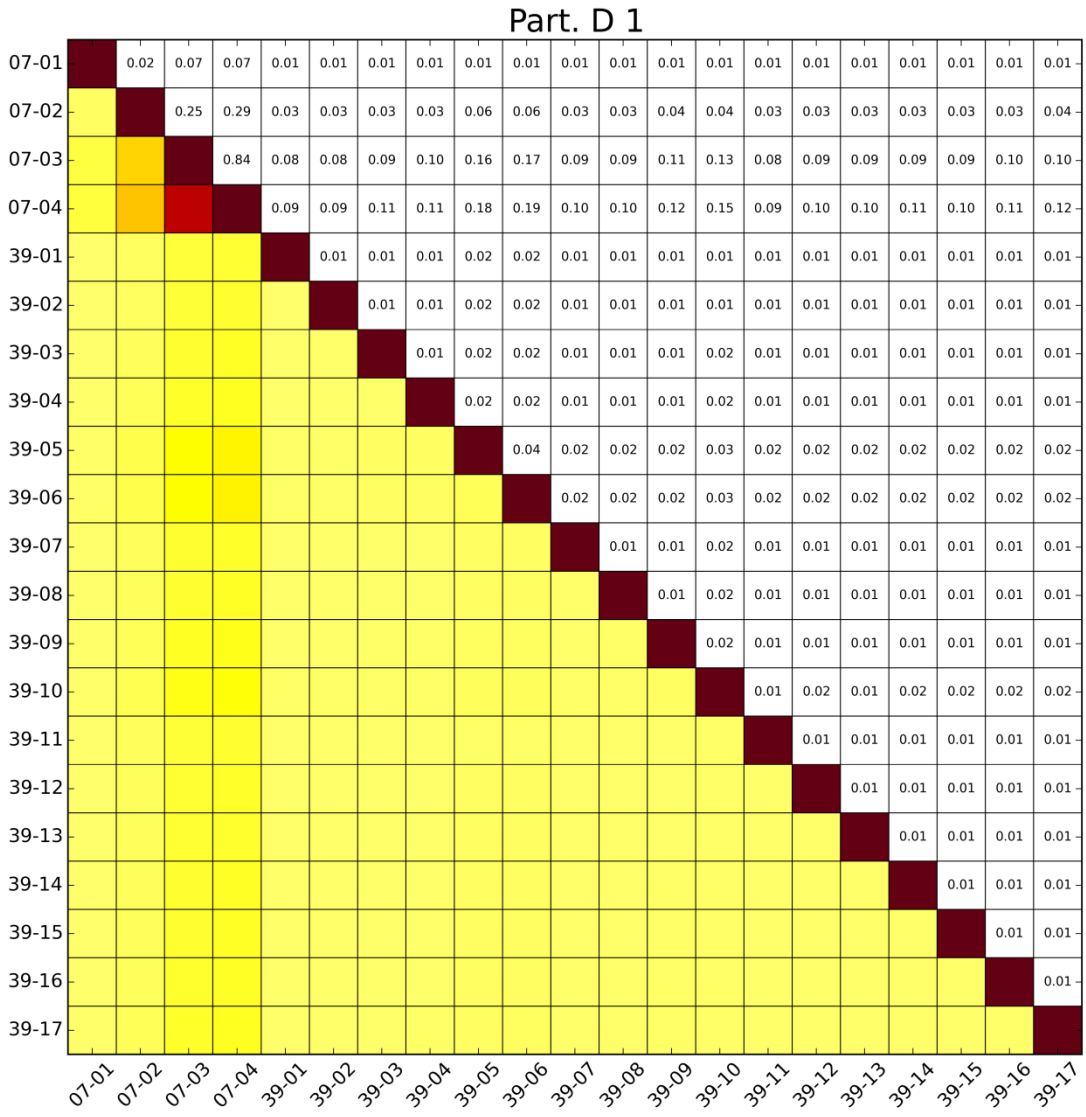

Source: NEA, 2020.

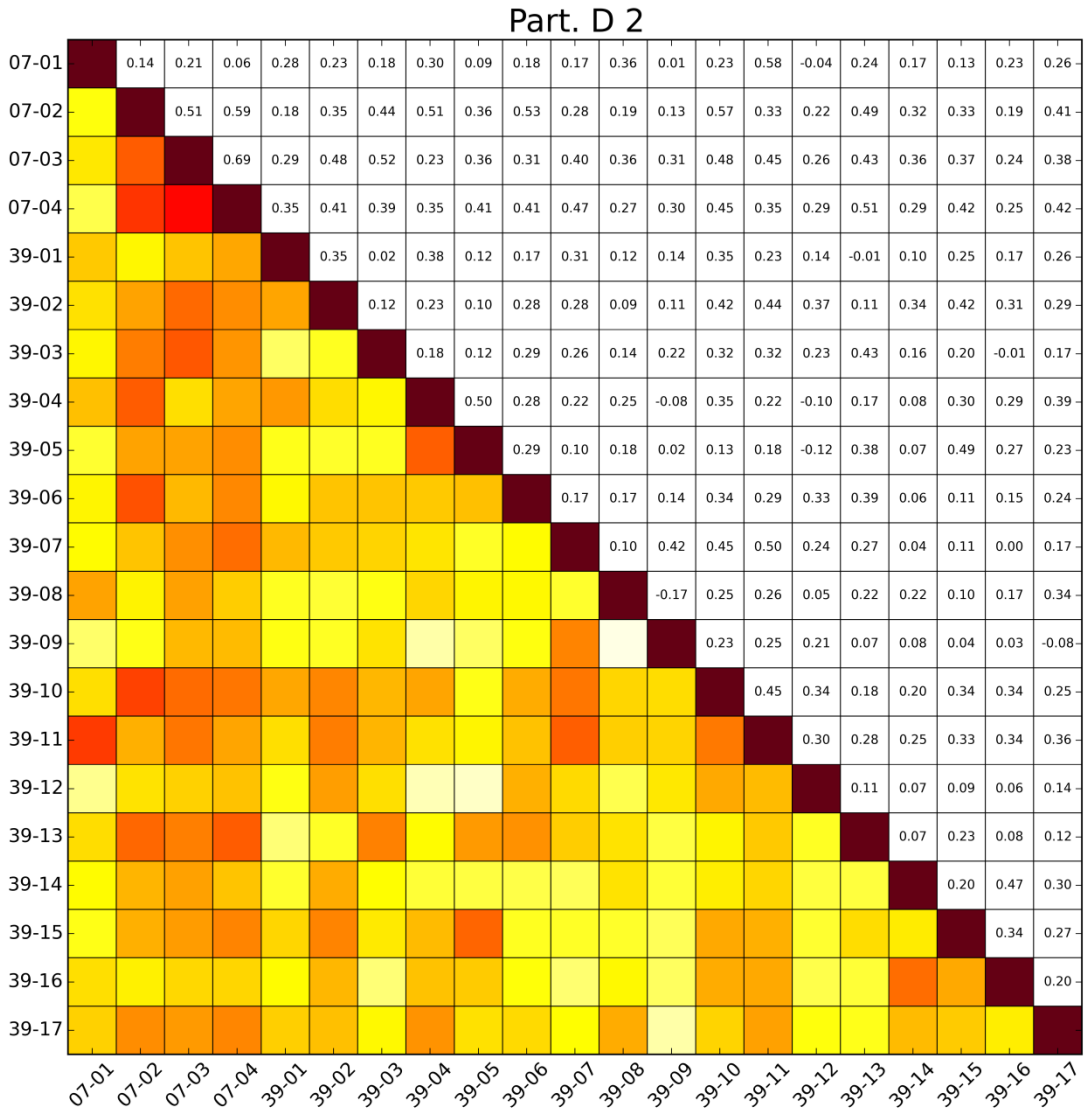

Source: NEA, 2020.

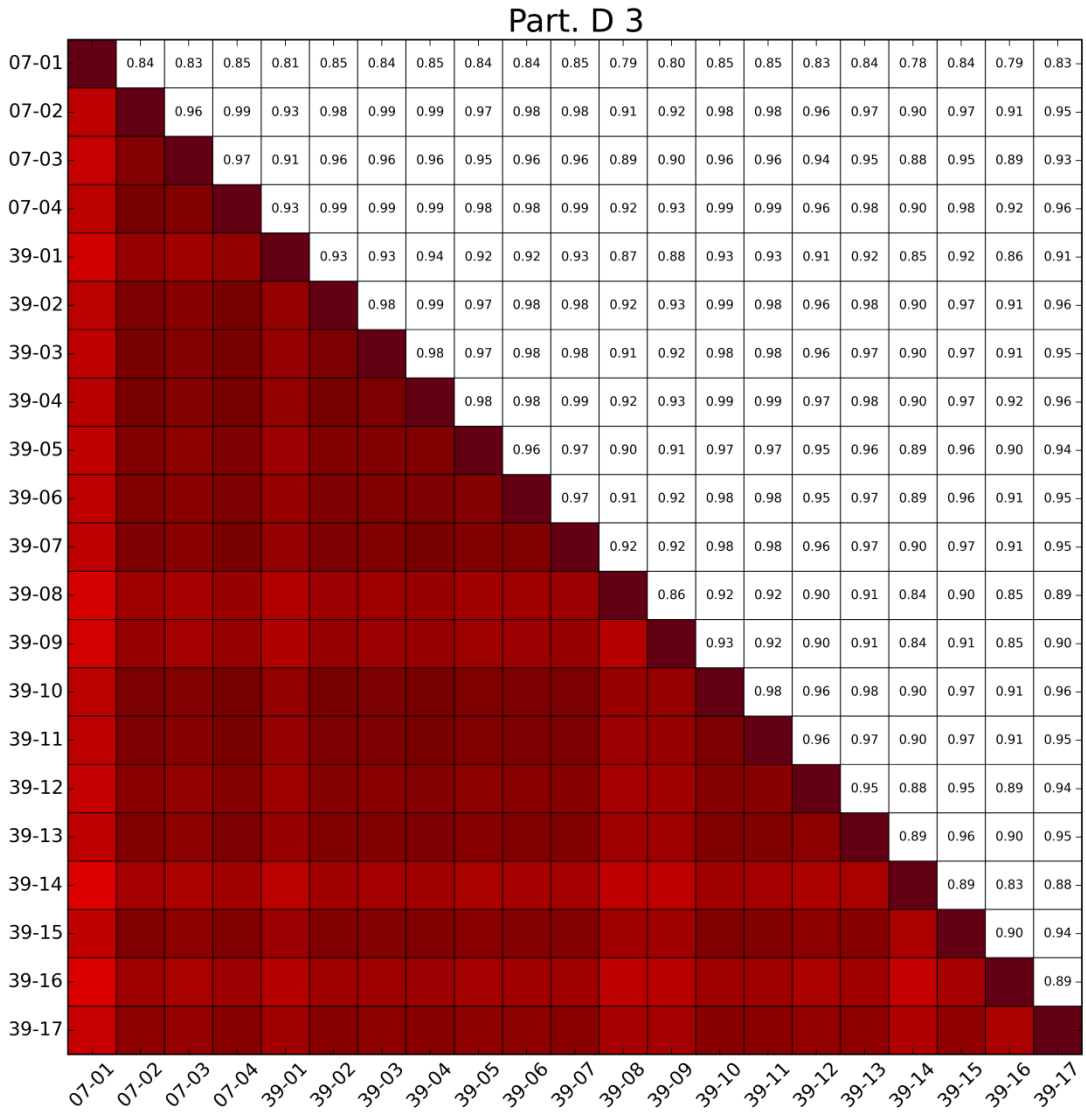

Source: NEA, 2020.

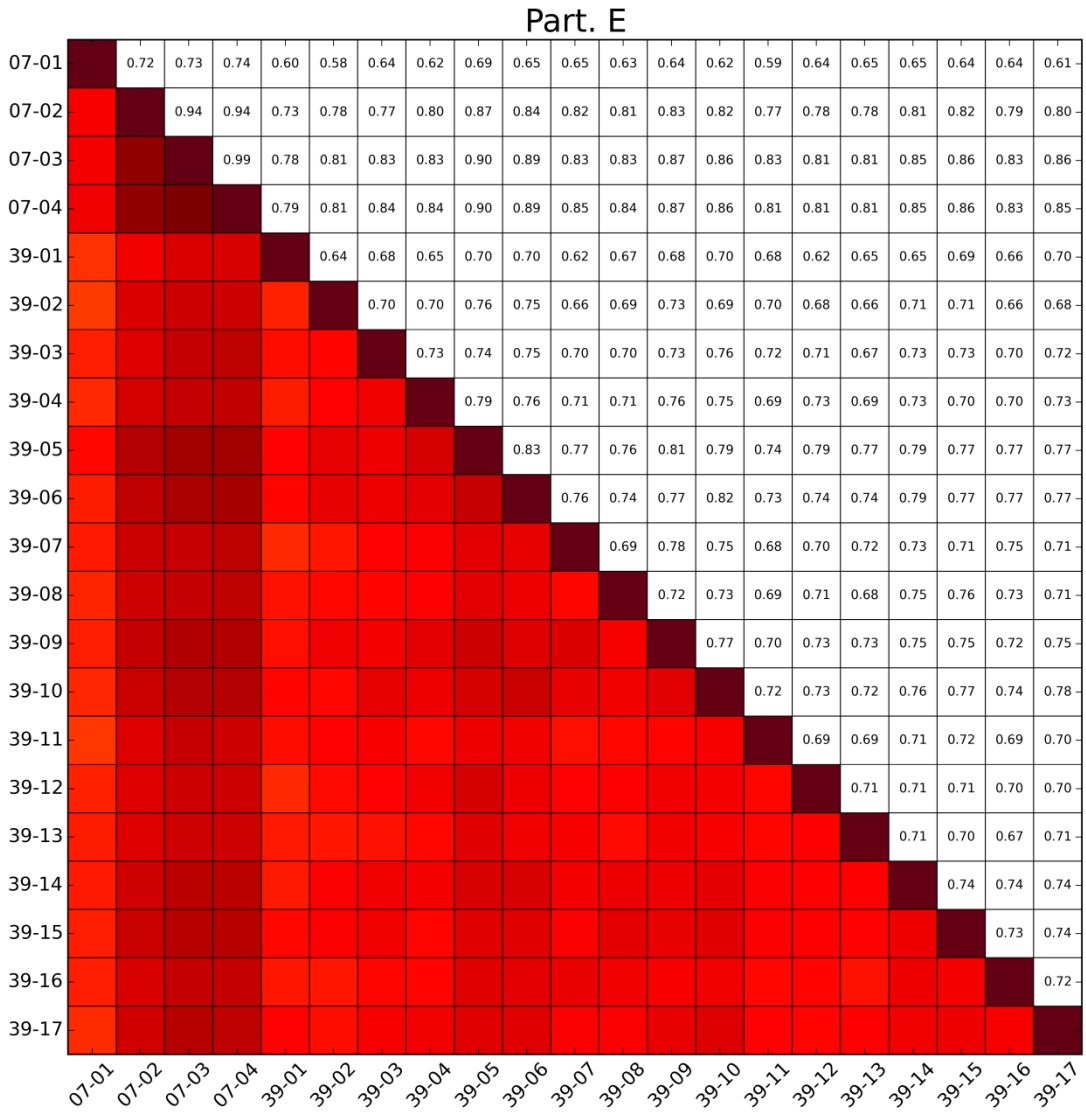

Source: NEA, 2020.

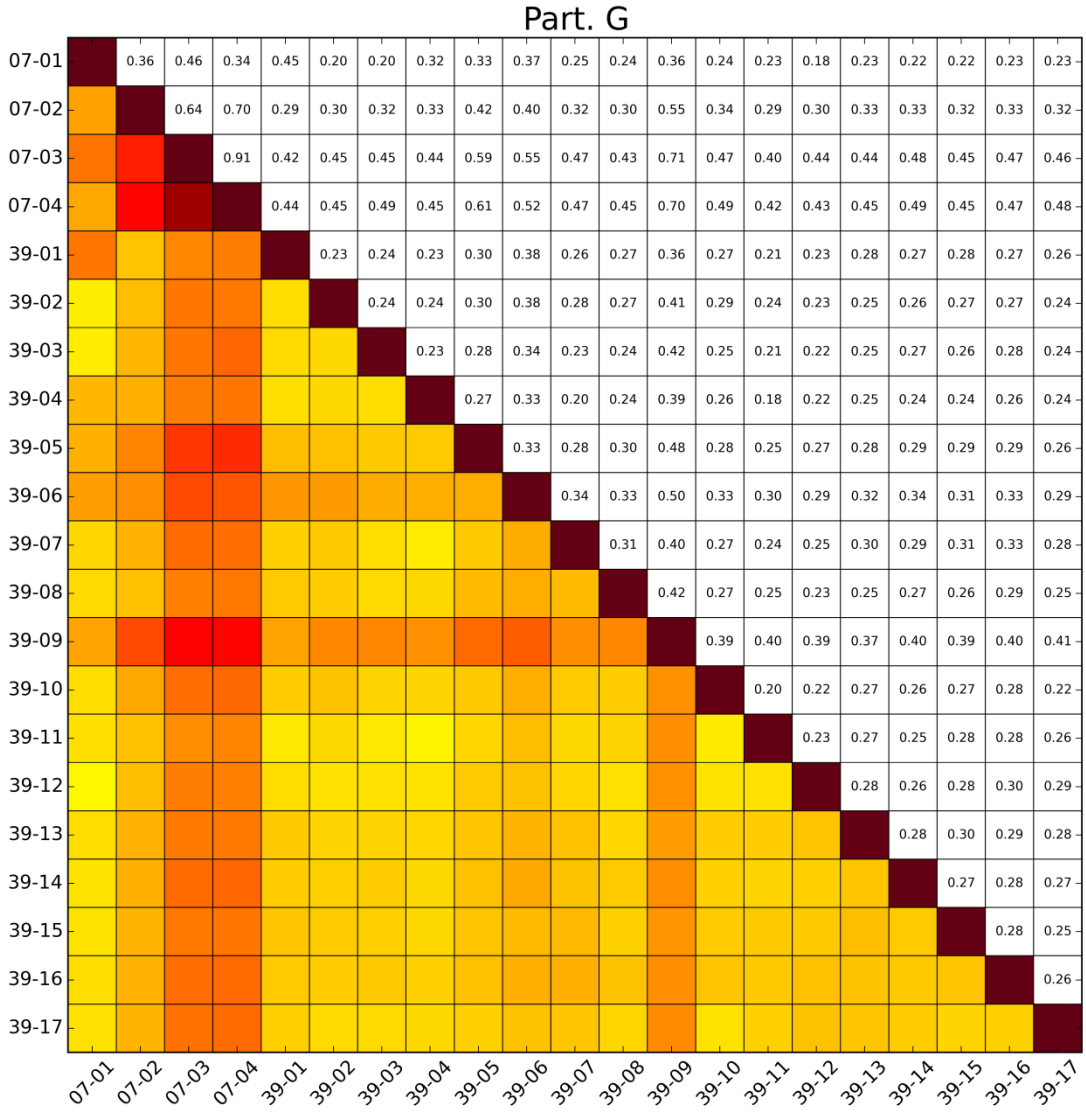

Source: NEA, 2020.

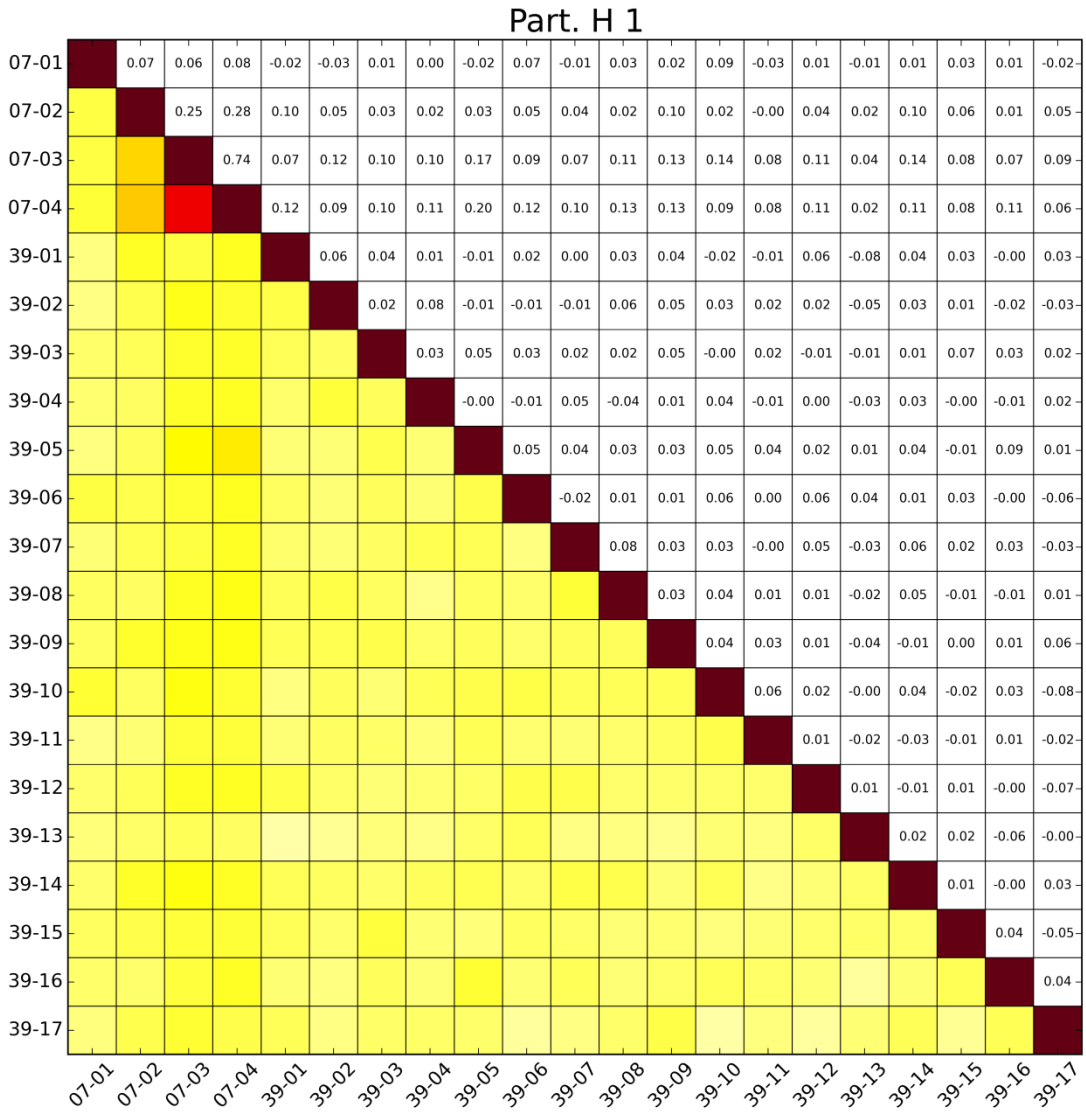

Source: NEA, 2020.

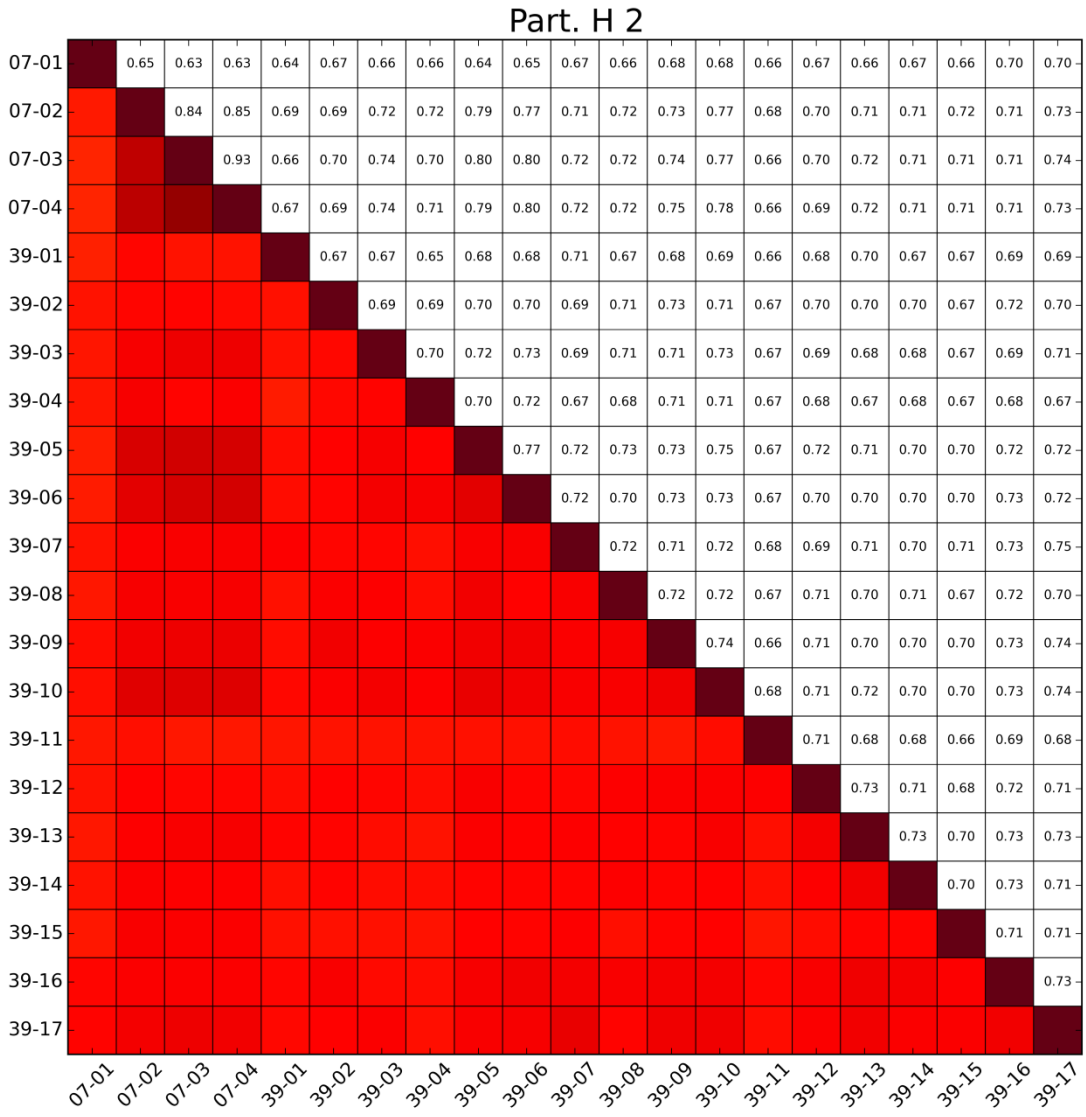

Source: NEA, 2020.

B.4 Optional and further results for Scenarios B, C and D

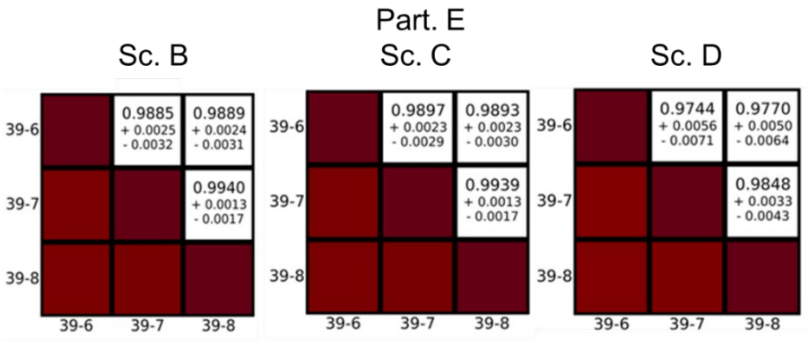

Source: NEA, 2020.

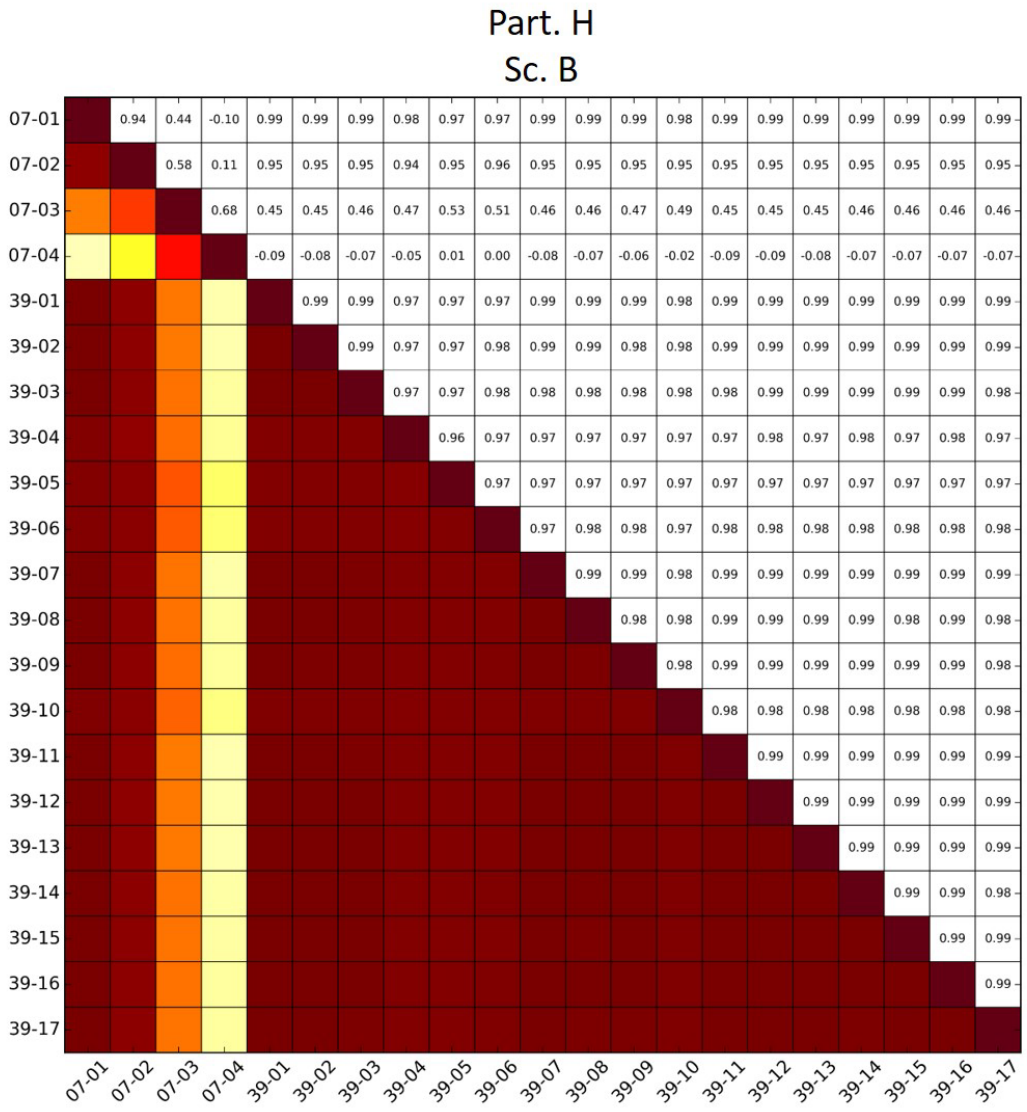

Source: NEA, 2020.

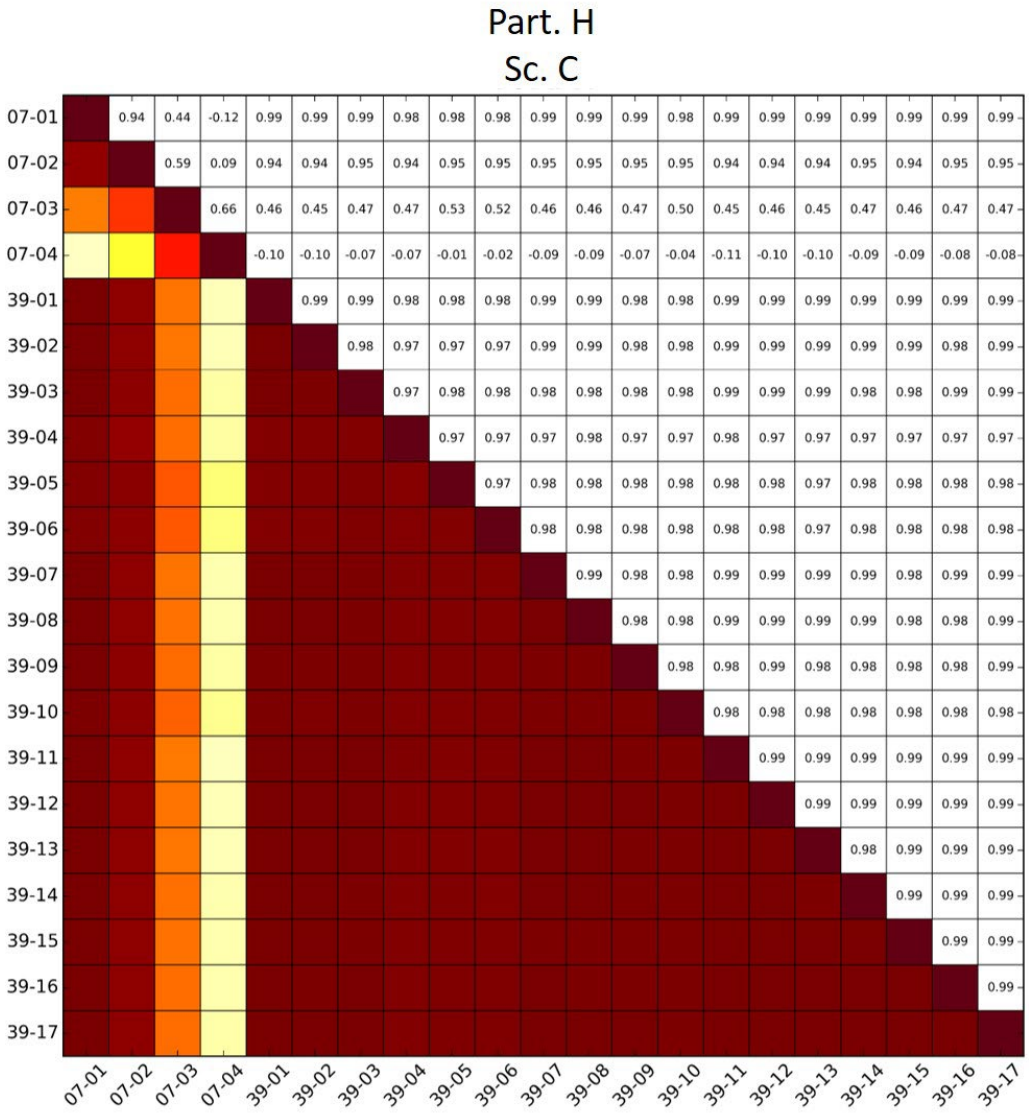

Source: NEA, 2020.

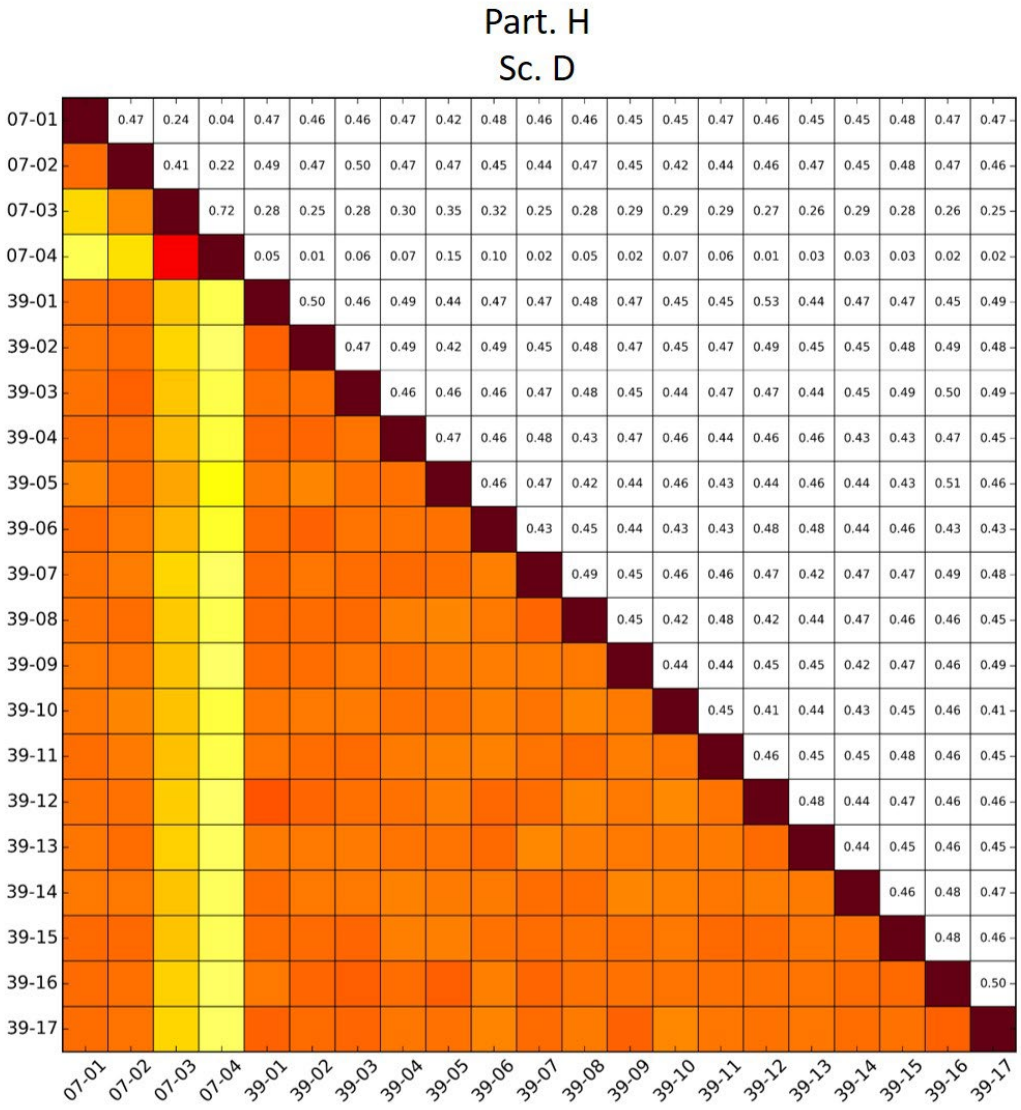

Source: NEA, 2020.

B.5 Option 1

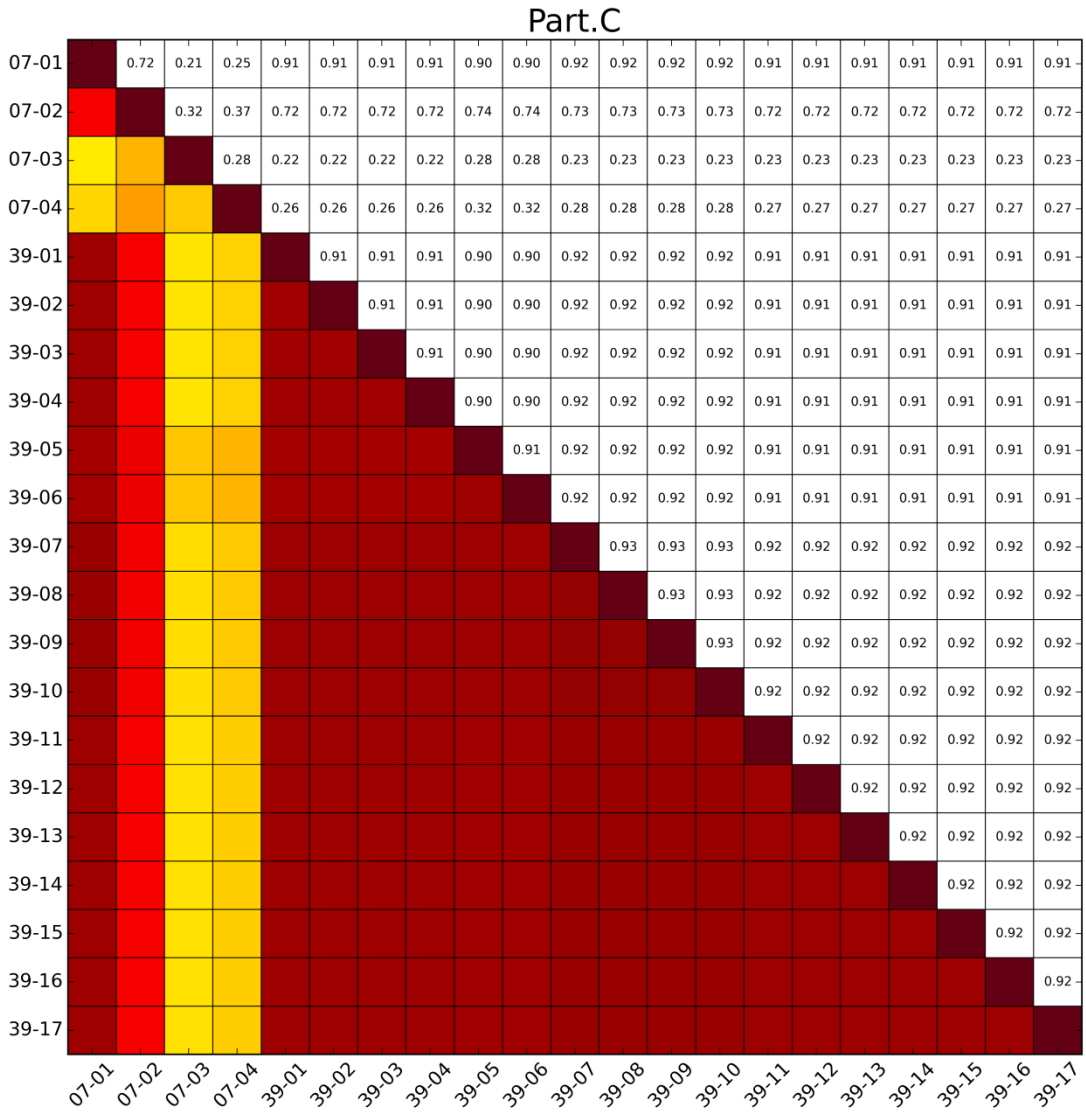

Source: NEA, 2020.

B.6 Option 2

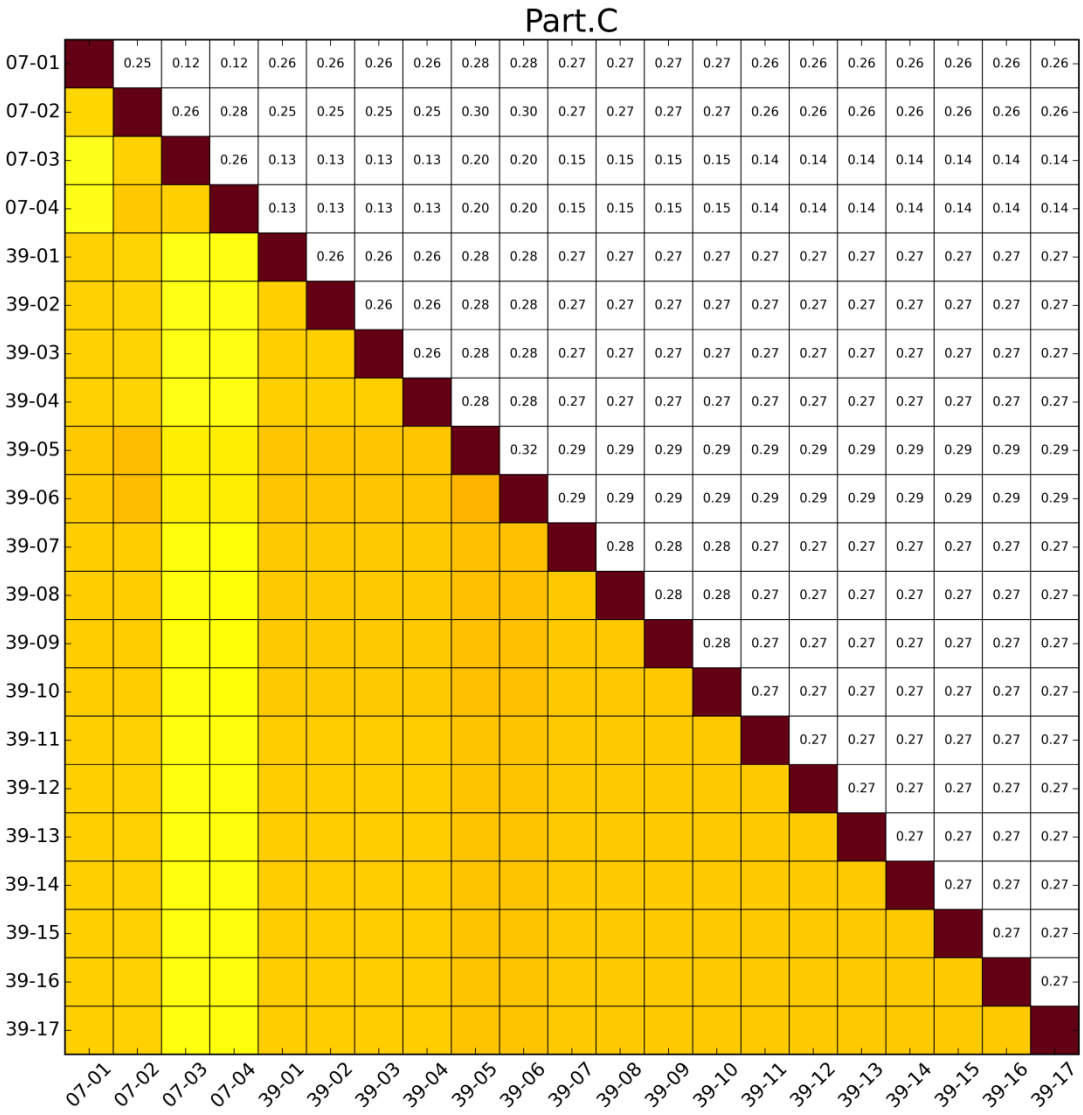

Source: NEA, 2020.

B.7 Option 3

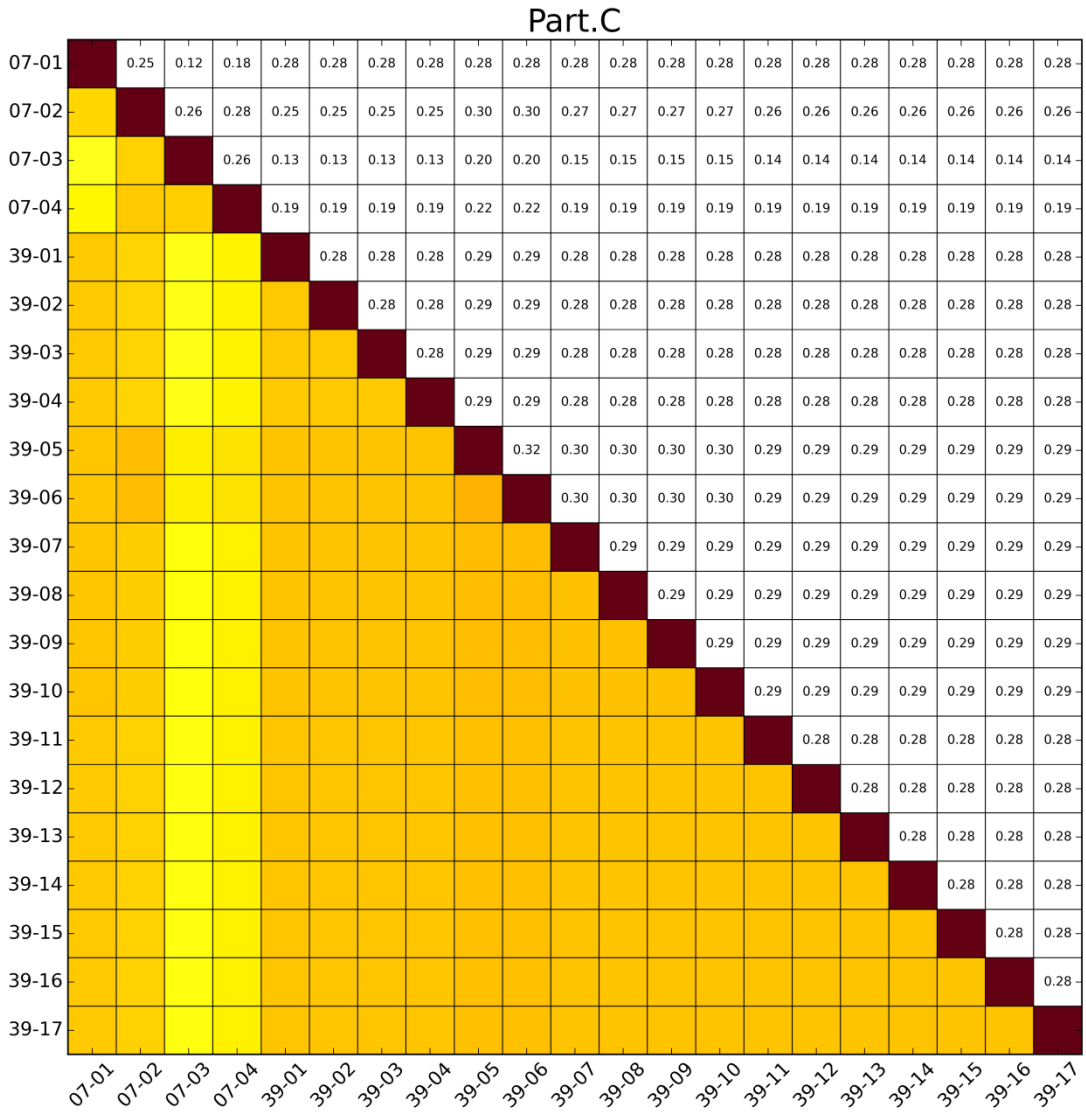

Source: NEA, 2020.